

**TREATMENT OF TEXTILE EFFLUENT USING  
MOVING BED BIOFILM REACTOR (MBBR) COUPLED  
WITH ADVANCED OXIDATION PROCESSES**

*Thesis Submitted to*

**UNIVERSITY OF CALICUT**

*In fulfillment for the award of the degree of*

**DOCTOR OF PHILOSOPHY**

**UNDER THE FACULTY OF ENGINEERING**



*By*

**SOSAMONY K. J.**

**(Reg.No: 7298/RESEARCH-B-SO/2014/CU)**

*Under the supervision of*

**Dr. SOLOMAN P. A.**

**DEPARTMENT OF CHEMICAL ENGINEERING  
GOVERNMENT ENGINEERING COLLEGE THRISSUR**

**UNIVERSITY OF CALICUT,**

**KERALA**

**December 2020**

## **DECLARATION**

I hereby declare that this thesis “TREATMENT OF TEXTILE EFFLUENT USING MOVING BED BIOFILM REACTOR (MBBR) COUPLED WITH ADVANCED OXIDATION PROCESSES” submitted to the University of Calicut, for the award of the Degree of Doctor of Philosophy under the Faculty of Engineering is an independent work done by me under the supervision and guidance of Dr. P. A. SOLOMAN, Professor in Chemical Engineering, Chemical Engineering Department, Government Engineering College, Thrissur, University of Calicut.

I also declare that this thesis contains no material which has been accepted for the award of any other degree or diploma of any University or Institution and to the best of my knowledge and belief, it contains no material previously published by any other person, except where due references are made in the text of the thesis.

Place: Thrissur

**SOSAMONY K. J.**

Date : 06-01-2021

(Reg.No: 7298/RESEARCH-B-SO/2014/CU)

The suggestions / corrections from the adjudicators as per Ref. No. 4782/RESEARCH-E-ASST-3/2021/Admn dated 07-08-2021 from the Director of Research, University of Calicut, has been incorporated in this thesis.

Place: Thrissur

**SOSAMONY K. J.**

Date : 31-08-2021

(Reg.No: 7298/RESEARCH-B-SO/2014/CU)

**DEPARTMENT OF CHEMICAL ENGINEERING  
GOVERNMENT ENGINEERING COLLEGE THRISSUR  
UNIVERSITY OF CALICUT, KERALA**

**CERTIFICATE**

This is to certify that the work reported in this thesis entitled **TREATMENT OF TEXTILE EFFLUENT USING MOVING BED BIOFILM REACTOR (MBBR) COUPLED WITH ADVANCED OXIDATION PROCESSES** that is being submitted by **Ms. SOSAMONY K. J.** for the award of the Degree of Doctor of Philosophy, to the University of Calicut, is based on the bonafide research work carried out by her under my supervision and guidance in the Department of Chemical Engineering, Government Engineering College, Thrissur, University of Calicut. The results embodied in this thesis have not been included in any other thesis submitted previously for the award of any degree or diploma of any other University or Institution.

Place: Thrissur

Date : 06-01-2021

**Dr. SOLOMAN P. A.**

Professor in Chemical Engineering

Department of Chemical Engineering

Government Engineering College Thrissur.

The suggestions / corrections from the adjudicators as per Ref. No. 4782/RESEARCH-E-ASST-3/2021/Admn dated 07-08-2021 from the Director of Research, University of Calicut, has been incorporated in this thesis.

Place: Thrissur

Date : 31-08-2021

**Dr. SOLOMAN P. A.**

Professor in Chemical Engineering

Department of Chemical Engineering

Government Engineering College Thrissur.

# ACKNOWLEDGEMENT

First and foremost, praises and prayers to the supreme power, **Almighty God**, for the showers of blessings throughout my research work to complete the research successfully.

I would like to express my gratitude to my guide and supervisor **Dr. P. A. Soloman**, Professor in Chemical Engineering, Department of Chemical Engineering, Government Engineering College, Thrissur, University of Calicut for giving me a chance for doing research under his guidance and providing valuable suggestions throughout the research. Without his continuous support, patience, motivation and immense knowledge, this work would not have been materialized.

I am immensely grateful to my doctoral committee members **Dr. N. E. Jaffer**, **Dr. B. Ranjanadevi** and **Dr. Shalij P. R.** for their suggestions, support and for providing all the facilities to carry out the research work. I am deeply indebted to **Dr. Manju M. S.**, Chairman, Head of the Department, Chemical Engineering Department, Government Engineering College, Thrissur and **Dr. C. V. Lal**, Head of the Department, Civil Engineering Department, Government Engineering College, Thrissur, for their full cooperation in this endeavor.

I would like to thank **Dr. Renjini Bhattathiripad T.**, Principal, and **Dr. Sheeba V. S.**, **Dr. K. Vijayakumar**, **Dr. Indiradevi K. P.** and **Dr. B. Jayanand**, former Principals, Government Engineering College, Thrissur, for extending the facilities in the research centre. I am also thankful to **Dr. K. Meenakshy**, Dean, (Research), **Dr. N. Sajikumar** and **Dr. P. Vijayan**, (Former Deans, Research) for providing all the facilities to carry out the research works.

I am also grateful to Director of Technical Education (DTE), for giving me permission to carry out part-time research at Government Engineering College, Thrissur. I extend my gratitude to the Registrar, Directorate of Research, University of Calicut for his guidance. I place on record my sincere thanks to all ministerial staff members in Government Engineering College, Thrissur, Directorate of Research, and University of Calicut, for the help and support extended to me.

I wish to express my sincere thanks to **Dr. Satish K. P., Prof. Meena John M. and Prof. Anand Lali Neera** for helping me in the subjects of my course work. Also, I acknowledge the support given by the Department of Microbiology, Kerala Agriculture University, Vellanikkara.

I am thankful to my fellow research scholars **Dr. Minimol Pieus T., Dr. Manilal A., Dr. Divya A.H., Dr. Miji Cherian R. and Prof. Francis John V.** for their technical and moral support. Also, my heartfelt thanks to **Dr. Sreelekha M.G.** for her technical help extended.

My fondest gratitude goes to all teaching and non-teaching staff of Civil Engineering Department and Chemical Engineering Department, Government Engineering College, Thrissur for their encouragement and support during the long journey of deliberating this thesis.

The advices and prayers of my loving parents are always a source of constant encouragement to me. Finally, I must express my very profound gratitude to my husband **Javahar V. S.**, my dearest children **Amal V. Javahar** and **Alma V. Javahar**, for providing me unfailing support and continuous encouragement throughout the years of research. This accomplishment would not have been possible without them. Thank you all.

**Sosamony K. J.**

# ABSTRACT

The global textile and clothing industry is bound to be huge, as it fulfills the second basic requirement of man. The textile industry plays an important role in several countries' economic development; however, it consumes large amounts of water and generates huge amounts of wastewater. Effluents from textile processes are highly variable in composition and contain a complex mixture of toxic substances such as dyes and pigments, salts, metals, biocides, surfactants and many other organic and inorganic components. Due to their complex chemical content, these effluents are recalcitrant in nature and of great environmental concerns. Textile effluents have low biodegradability and high COD. In most cases, the BOD<sub>5</sub>-to-COD ratio is around 0.25, which means that it includes large amounts of barely biodegradable organic matter. It is not feasible to use a single physico-chemical or biological method in treating textile effluent. As the efficacy of such traditional methods are limited, other advanced, eco-friendly and cost-effective alternatives have to be developed. This will enable the industry to meet stringent environmental protocols. The suggested method is an integrated chemical-biological system of treatment in which the biodegradability to be enhanced by some chemical method before biological treatment.

The viability of various photo Fenton processes, namely Homogeneous Photo Fenton (HPF), Homogeneous Solar Photo Fenton (HSPF), Advanced Photo Fenton (APF), and Advanced Solar Photo Fenton (ASPF), has been studied to propose the best alternative for improving the biodegradability of the effluent. The toxicity reduction ability of these processes has been analyzed using static bioassay test engaging *Poecilia Libestes Reticulate* (Guppy fish) as the test organism and found that all these processes were effective in reducing toxicity. The physical state of the sludge reduced after these processes in terms of sludge volume index has also been investigated. The solar based photo Fenton processes (HSPF and ASPF) have been suggested as the most suitable pretreatments for the textile effluent as they are efficient and cost-effective. The Response Surface Methodology with Box-Behnken Design has been used for the analysis and optimization of all the processes conducted in the study.

Use of biosynthesized nano zero valent iron in photo Fenton processes has been attempted and its reusability and iron leachability have been checked. It is found that the

biosynthesized nZVI can be effectively used upto third cycle with very small percentage of iron leaching.

The performance of modified MBBR in the treatment of pretreated effluent has been investigated. The carrier materials used in MBBR are made of PVC attached with inoculated bacteria which are predominant in textile sludge, isolated and identified by 16S rRNA method. In order to upgrade the effluent quality, treatment through magnetic field induced MBBR has also been tried. It has been observed that the pretreated textile effluent after treatment through magnetic field induced MBBR can be disposed either into irrigation water or into surface water bodies. The cost of the processes alternatives has been compared to propose an optimal integral treatment scheme minimizing the treatment cost and found that the integrated ASPF-MBBR treatment incurred slightly less expensive than HSPF-MBBR treatment system.

# CONTENTS

## Chapter 1 GENERAL INTRODUCTION

1.1	Textile industry – Global and Indian scenario -----	1
1.2	Need of textile effluent treatment -----	2
1.3	Conventional methods of treatment -----	3
1.4	New trends in treatment -----	3
1.5	Photo Fenton process -----	4
1.6	Application of nano zero valent iron in photo Fenton process -----	5
1.7	Biodegradability and toxicity of textile effluent -----	6
1.8	Moving bed biofilm reactor (MBBR) -----	7
1.9	MBBR induced with magnetic field -----	8
1.10	Design of experiments -----	8
1.11	Problem definition -----	9
1.12	Scope of the present research -----	9
1.13	Objectives of the study -----	10

## Chapter 2 LITERATURE REVIEW

2.1	Background information -----	12
2.2	Textile industry and manufacturing process -----	13
2.3	Chemicals used in the textile industry -----	15
2.3.1	Dyes -----	16
2.3.2	Classification of dyes -----	17
2.4	Environmental concerns of textile effluents -----	22
2.5	General characteristics of textile effluents and standards for discharge of effluents -----	23

2.6	Biodegradability of textile waste -----	24
2.7	Emerging techniques for textile effluent treatment -----	25
2.7.1	Physical and chemical treatment -----	26
2.7.1.1	Coagulation and sedimentation -----	26
2.7.1.2	Adsorption -----	27
2.7.1.3	Ion exchange method -----	27
2.7.1.4	Electro-chemical treatment -----	27
2.7.1.5	Electro-coagulation -----	28
2.7.1.6	Reverse osmosis -----	28
2.7.1.7	Nano-filtration -----	28
2.7.1.8	Ozonation -----	28
2.7.2	Biological treatment -----	29
2.7.2.1	Rotating Biological Contactor (RBC) -----	29
2.7.2.2	Biologically Aerated Filter (BAF) -----	30
2.7.2.3	Anaerobic Filter (AF) -----	30
2.7.2.4	Trickling Filter (TF) -----	30
2.7.2.5	Activated Sludge Process (ASP) -----	30
2.7.2.6	Sequencing Batch Reactor (SBR) -----	31
2.7.2.7	Upflow Anaerobic Sludge Blanket (UASB) -----	31
2.8	Advanced Oxidation Processes (AOPs) -----	33
2.8.1	Fenton reaction -----	33
2.9	Photo Fenton process -----	36
2.10	Nano Zero Valent Iron (nZVI) -----	38

2.10.1	nZVI synthesis -----	38
2.10.2	Biological synthesis of nZVI from plant leaf extracts -	39
2.10.3	Characterization of nano particles -----	40
2.11	Biodegradability Index (BI) -----	40
2.12	Toxicity assessment -----	41
2.13	Kinetic coefficients -----	41
2.14	Sludge Volume Index (SVI) -----	42
2.15	Moving Bed Biofilm Reactor (MBBR) -----	42
2.15.1	Advantages of moving bed biofilm process -----	43
2.16	Isolation, identification and inoculation of microorganisms in MBBR	44
2.16.1	Serial plate dilution method -----	44
2.16.2	16S rRNA method -----	44
2.17	Magnetic field effect in wastewater treatment -----	45
2.18	Optimization of factors influencing the removal process -----	46
2.18.1	Response Surface Methodology (RSM) -----	46
2.18.2	Experimental design -----	47
2.18.3	Selection of model -----	48
2.18.4	Checking the model adequacy -----	48
2.18.5	Graphical representation of the model -----	49
2.18.6	Response surface optimization -----	50
2.19	Previous studies on textile effluent treatment -----	50
2.19.1	Physico-chemical conventional methods -----	50
2.19.2	Biological conventional methods -----	55

2.19.2.1	Dye degradation by fungus -----	55
2.19.2.2	Dye degradation by yeasts -----	55
2.19.2.3	Dye degradation by algae and plants -----	55
2.19.2.4	Dye degradation by bacteria -----	56
2.19.3	Fenton treatment on textile effluent -----	56
2.19.4	Photo Fenton treatment on textile effluent -----	57
2.19.5	nZVI biological synthesis -----	58
2.19.6	Use of nZVI in textile effluent treatment -----	58
2.19.7	MBBR process for textile effluent -----	59
2.19.8	Integrated process for textile wastewater treatment -----	60
2.19.9	Use of magnetic field in wastewater treatment -----	62
2.19.10	Response surface methodology in research -----	65

### **Chapter 3 METHODOLOGY**

3.1	Sampling of original textile wastewater -----	66
3.2	Analytical methods -----	66
3.3	Treatment of effluent using MBBR with textile sludge -----	67
3.3.1	Experimental setup of MBBR -----	67
3.3.2	Carrier materials -----	68
3.3.3	Seeding and attachment of microorganisms -----	68
3.4	Treatment of textile effluent using MBBR with bacteria inoculated Carriers -----	69
3.4.1	Isolation, identification and inoculation of bacteria -----	69
3.4.1.1	Isolation -----	69

3.4.1.2	Identification -----	69
3.4.1.3	Inoculation -----	70
3.5	Pretreatment of textile effluent before biological treatment -----	70
3.6	Homogeneous Photo Fenton process (HPF) -----	71
3.6.1	Chemicals -----	71
3.6.2	Experimental procedure -----	71
3.6.3	Design of experiments -----	72
3.7	Homogeneous Solar Photo Fenton process (HSPF) -----	72
3.7.1	Chemicals -----	72
3.7.2	Experimental procedure -----	72
3.8	Synthesis of nano zero valent iron (nZVI) -----	73
3.8.1	Preparation of leaf extract -----	73
3.8.2	Synthesis of nano zero valent iron -----	73
3.8.3	Characterization techniques -----	74
3.9	Advanced Photo Fenton process (APF) -----	74
3.9.1	Chemicals -----	74
3.9.2	Experimental procedure -----	74
3.10	Advanced Solar Photo Fenton process (ASPF) -----	74
3.10.1	Chemicals -----	74
3.10.2	Experimental procedure -----	74
3.11	Reusability of nZVI and iron leachability -----	74
3.12	Determination of kinetic coefficients k and K <sub>s</sub> -----	75
3.13	Calculation of sludge volume index (SVI) -----	75

3.14	Bioassay experiment for toxicity assessment -----	76
3.15	Pretreatments selected -----	76
3.16	Variation of BI with time -----	77
3.17	Experimental design of MBBR -----	77
3.18	MBBR under magnetic field -----	77
3.19	Cost estimation and economic valuation -----	78

## **Chapter 4 RESULTS AND DISCUSSIONS**

4.1	Sample characterization -----	80
4.2	Treatment of textile effluent using MBBR with carrier materials	
	Inoculated with textile sludge -----	80
4.2.1	Effect of contact time on COD removal -----	81
4.2.2	Effect of pH on COD removal -----	81
4.2.3	Effect of filling ratio of carrier materials on COD	
	Removal -----	82
4.3	Treatment of textile effluent using MBBR with bacteria inoculated	
	Carriers -----	83
4.3.1	Effect of contact time on COD removal -----	84
4.3.2	Effect of pH on COD removal -----	85
4.3.3	Effect of filling ratio of carrier materials on COD	
	Removal -----	85
4.4	Homogeneous Photo Fenton process (HPF) -----	86
4.4.1	Optimization using BBD for COD reduction in HPF	
	Process -----	87

4.4.2	Regression model for COD reduction in HPF process --	88
4.4.3	Optimization results of COD reduction in HPF process	90
4.4.4	Contour plots for COD reduction in HPF process -----	90
4.4.5	Effect of parameters on COD reduction in HPF process	91
4.5	Homogeneous Solar Photo Fenton process (HSPF) -----	92
4.5.1	Optimization using BBD for COD reduction in HSPF process -----	92
4.5.2	Regression model for COD reduction in HSPF process	93
4.5.3	Optimization results of COD reduction in HSPF process	94
4.5.4	Contour plots for COD reduction in HSPF process -----	95
4.6	Biosynthesis and characterization of nZVI -----	96
4.6.1	UV spectroscopy analysis -----	96
4.6.2	FT-IR analysis -----	97
4.6.3	TEM analysis -----	98
4.6.4	BET surface area analysis -----	98
4.7	Advanced Solar Photo Fenton process (ASPF) -----	99
4.7.1	Optimization using BBD for COD reduction in APF process -----	99
4.7.2	Regression model for COD reduction in APF process --	100
4.7.3	Optimization results of COD reduction in APF process	101
4.7.4	Contour plots & effects of parameters on COD reduction in APF process -----	102
4.8	Advanced Solar Photo Fenton process (ASPF) -----	103

4.8.1	Optimization using BBD for COD reduction in ASPF process -----	103
4.8.2	Regression model for COD reduction in ASPF process	104
4.8.3	Optimization results of COD reduction in ASPF process	106
4.8.4	Contour plots & effects of parameters on COD reduction in ASPF process -----	106
4.9	Comparison of pretreatments -----	107
4.10	Validation of the models -----	108
4.11	Reusability of nZVI & iron leachability -----	109
4.12	Toxicity assessment after AOPs -----	111
4.13	Determination of k, Ks and SVI -----	115
4.14	Gas chromatographic analysis after ASPF process -----	119
4.15	Selection of pretreatments -----	122
4.16	Validation of BI with time -----	122
4.17	MBBR process after HSPF pretreatment -----	124
4.17.1	Design of experiment with analysis -----	124
4.17.2	Optimization of results -----	127
4.17.3	Contour plots & Main effects plots for %removals -----	128
4.18	MBBR induced with magnetic field after HSPF process -----	132
4.19	MBBR process after ASPF pretreatment -----	134
4.19.1	Design of experiment with analysis -----	134
4.19.2	Optimization of results -----	138
4.19.3	Contour plots & Main effects plots for %removals -----	139

4.20	MBBR induced with magnetic field after ASPF process -----	142
4.21	Conductivity measurements -----	144
4.22	Comparison of time, effluent BOD & COD after various Treatment options -----	146
4.23	Cost analysis -----	149
<b>Chapter 5</b>	<b>CONCLUSIONS</b> -----	153
	<b>REFERENCES</b> -----	156
	<b>PUBLICATIONS</b> -----	176
	<b>APPENDIX</b>	

## LIST OF TABLES

Table 2.1 :	Water requirements for cotton textile wet finishing operations	15
Table 2.2 :	Effluent production from different processes of textile industry	15
Table 2.3 :	General characteristics of textile wastewater-----	23
Table 2.4 :	General standards for discharge of effluents-----	23
Table 2.5 :	Textile wastewater treatment- current technologies-----	32
Table 3.1 :	Methods/Instruments used for analysis-----	66
Table 4.1 :	Characteristics of textile effluents-----	80
Table 4.2 :	Levels of varying factors for BBD in HPF-----	87
Table 4.3 :	Design of experimental runs for BBD in HPF-----	87
Table 4.4 :	Estimated regression coefficients for COD removal in HPF-----	88
Table 4.5 :	Design of experimental runs for BBD in HSPF-----	93
Table 4.6 :	Estimated regression coefficients for COD removal in HSPF---	93
Table 4.7 :	Levels of varying parameters for BBD in APF-----	99
Table 4.8 :	Design of experimental runs for BBD in APF process-----	100
Table 4.9 :	Estimated regression coefficients for COD removal in APF process-----	100
Table 4.10:	Design of experimental runs for COD removal in ASPF process-----	104
Table 4.11:	Results of regression analysis of BBD in ASPF process-----	104
Table 4.12:	Comparison of results of AOPs-----	107
Table 4.13:	Validation of the models-----	108

Table 4.14: Reusability of nZVI-----	109
Table 4.15: Percentage of iron leaching-----	110
Table 4.16: LC <sub>50</sub> values of textile effluent-----	114
Table 4.17: Observations at various detention times for k & K <sub>s</sub> -----	115
Table 4.18: Values of k, K <sub>s</sub> & SVI-----	118
Table 4.19: GC results before and after treatment-----	121
Table 4.20: BI Vs Time in HSPF and ASPF process-----	122
Table 4.21: Levels of factors for BBD in MBBR process-----	124
Table 4.22: Experimental runs in BBD for MBBR after HSPF pretreatment-	124
Table 4.23: Results of regression analysis for COD removal in MBBR after HSPF-----	125
Table 4.24: Results of regression analysis for BOD removal in MBBR after HSPF-----	126
Table 4.25: Results of regression analysis for color removal in MBBR after HSPF-----	126
Table 4.26: Variation of COD removal with exposure time for MBBR with magnetic field after HSPF-----	132
Table 4.27: Variation of COD and BOD removal with field intensity for MBBR with magnetic field after HSPF-----	133
Table 4.28: Experimental runs in BBD for MBBR after ASPF pretreatment-	135
Table 4.29: Results of regression analysis for COD removal in MBBR after ASPF-----	135

Table 4.30: Results of regression analysis for BOD removal in MBBR after ASPF-----	136
Table 4.31: Results of regression analysis for color removal in MBBR after ASPF-----	137
Table 4.32: Variation of COD removal with exposure time for magnetic field induced MBBR after ASPF-----	142
Table 4.33: Variation of COD and BOD removal with field intensity for magnetic field induced MBBR after ASPF-----	143
Table 4.34: Conductivity measurements-----	145
Table 4.35: Reaction time required for various treatment options-----	146
Table 4.36: Characteristics of treated effluent from MBBR with magnetic field pretreating by HSPF-----	147
Table 4.37: Characteristics of treated effluent from MBBR with magnetic field pretreating by ASPF-----	148
Table 4.38: Capital cost of the Integrated system (HSPF+MBBR)-----	149
Table 4.39: Operating cost of the Integrated system (HSPF+MBBR)-----	150
Table 4.40: Capital cost of the Integrated system (ASPF+MBBR)-----	150
Table 4.41: Operating cost of the Integrated system (ASPF+MBBR)-----	151
Table 4.42: Consolidated cost analysis-----	151

## LIST OF FIGURES

Figure 2.1: Textile manufacturing by wet process-----	14
Figure 3.1: Schematic diagram of experimental setup of MBBR-----	67
Figure 3.2: Carrier elements-----	68
Figure 3.3: Schematic diagram of UV Photo Fenton reactor-----	71
Figure 3.4: nZVI powder-----	73
Figure 3.5: Schematic diagram of experimental setup of MBBR with Magnetic field-----	78
Figure 4.1: Variation of COD removal with contact time-----	81
Figure 4.2: Variation of COD removal with pH-----	82
Figure 4.3: Variation of COD removal with filling ratio-----	82
Figure 4.4: Quadrant streaked culture of azoarcus bacteria-----	84
Figure 4.5: Variation of COD removal with contact time-----	84
Figure 4.6: Variation of COD removal with pH-----	85
Figure 4.7: Variation of COD removal with filling ratio-----	86
Figure 4.8: Optimization plot for %COD removal in HPF process-----	90
Figure 4.9: Contour plots for %COD removal in HPF process-----	91
Figure4.10: Optimization plot for %COD removal in HSPF process-----	95
Figure4.11: Contour plots for %COD removal in HSPF process-----	96
Figure4.12: UV spectra of nZVI-----	96
Figure4.13: FTIR spectrum of nZVI-----	97
Figure4.14: TEM image of nZVI-----	98

Figure4.15: Optimization plot for %COD removal in APF process-----	102
Figure4.16: Contour plots for %COD removal in APF process-----	102
Figure4.17: Optimization plot for %COD removal in ASPF process-----	106
Figure4.18: Contour plots for %COD removal in ASPF process-----	107
Figure4.19: Percentage removal versus process graph-----	108
Figure4.20: Reusability of nZVI-----	110
Figure4.21: Toxicity graph (after 96 hrs) for raw effluent-----	111
Figure4.22: Toxicity graph (after 96 hrs) for effluent after HPF process-----	112
Figure4.23: Toxicity graph (after 96 hrs) for effluent after HSPF process----	112
Figure4.24: Toxicity graph (after 96 hrs) for effluent after APF process-----	113
Figure4.25: Toxicity graph (after 96 hrs) for effluent after ASPF process----	113
Figure4.26: $X\theta/(S_0-S)$ Vs $1/S$ graph for k & $K_s$ of raw effluent-----	116
Figure4.27: $X\theta/(S_0-S)$ Vs $1/S$ graph for effluent after HPF process-----	116
Figure4.28: $X\theta/(S_0-S)$ Vs $1/S$ graph for effluent after HSPF process-----	117
Figure4.29: $X\theta/(S_0-S)$ Vs $1/S$ graph for effluent after APF process-----	117
Figure4.30: $X\theta/(S_0-S)$ Vs $1/S$ graph for effluent after ASPF process-----	118
Figure4.31: Gas chromatogram for untreated textile effluent-----	120
Figure4.32: Gas chromatogram for effluent after ASPF treatment-----	120
Figure4.33: Variation of BI with time-----	123
Figure4.34: Optimization plot for %removals in MBBR after HSPF pretreatment-----	128
Figure4.35: Contour plots for %COD removal in MBBR after HSPF pretreatment-----	128

Figure4.36: Contour plots for %BOD removal in MBBR after HSPF pretreatment-----	129
Figure4.37: Contour plots for %color removal in MBBR after HSPF pretreatment-----	129
Figure4.38: Main effects plots for COD removal in MBBR after HSPF process-----	130
Figure4.39: Main effects plots for BOD removal in MBBR after HSPF process-----	131
Figure4.40: Main effects plots for color removal in MBBR after HSPF process-----	131
Figure4.41: COD removal Vs exposure time in magnetic field induced MBBR after HSPF-----	133
Figure4.42: %removals Vs field intensity in magnetic field induced MBBR after HSPF-----	134
Figure4.43: Optimization plot for %removals in MBBR after ASPF pretreatment-----	138
Figure4.44: Contour plots for %COD removal in MBBR after ASPF pretreatment-----	139
Figure4.45: Contour plots for %BOD removal in MBBR after ASPF pretreatment-----	139
Figure4.46: Contour plots for %color removal in MBBR after ASPF pretreatment-----	140

Figure4.47: Main effects plots for BOD removal in MBBR after ASPF process-----	140
Figure4.48: Main effects plots for COD removal in MBBR after ASPF process-----	141
Figure4.49: Main effects plots for color removal in MBBR after ASPF process-----	141
Figure4.50: COD removal Vs exposure time in magnetic field induced MBBR after ASPF-----	143
Figure4.51: %removals Vs field intensity in magnetic field induced MBBR after ASPF-----	144
Figure4.52: Time versus treatment graph-----	146
Figure4.53: BOD versus treatment graph-----	148
Figure4.54: COD versus treatment graph-----	149
Figure4.55: Cost versus treatment graph-----	152

## ABBREVIATIONS

BOD	:	Biochemical Oxygen Demand
COD	:	Chemical Oxygen Demand
DO	:	Dissolved Oxygen
SVI	:	Sludge Volume Index
BI	:	Biodegradability Index
PVA	:	Poly Vinyl Alcohol
CMC	:	Carboxy Methyl Cellulose
SS	:	Suspended Solids
TDS	:	Total Dissolved Solids
EDTA	:	Ethylene Diamine Tetra Acetate
TOC	:	Total Organic Carbon
RBC	:	Rotating Biological Contactor
BAF	:	Biologically Aerated Filter
AF	:	Anaerobic Filter
SBR	:	Sequencing Batch Reactor
UASB	:	Upflow Anaerobic Sludge Blanket
AOP	:	Advanced Oxidation Process
nZVI	:	Nano Zero Valent Iron
TEM	:	Transmission Electron Microscopy
FTIR	:	Fourier Transform Infrared Spectroscopy
MBBR	:	Moving Bed Biofilm Reactor

S rRNA	:	Svedberg unit ribosomal Ribo Nucleic Acid
RSM	:	Response Surface Methodology
BBD	:	Box Behnken Design
CCD	:	Central Composite Design
PCR	:	Polymerase Chain Reaction
HPF	:	Homogeneous Photo Fenton
HSPF	:	Homogeneous Solar Photo Fenton
APF	:	Advanced Photo Fenton
ASPF	:	Advanced Solar Photo Fenton
DI	:	De-ionized water
CRF	:	Capital Recovery Factor

## NOMENCLATURE

$k$	:	Biodegradation rate constant
$K_s$	:	Half-velocity constant
$Y$	:	Yield coefficient
$k_d$	:	Endogenous decay coefficient
$X$	:	Mixed liquor suspended solids
$\Theta$	:	Hydraulic detention time
$S_o$	:	Influent COD
$S$	:	Effluent COD

# CHAPTER 1

## GENERAL INTRODUCTION

### 1 Introduction

Saving water to save the world and make the humanity's future secure is what we need now. The planet is approaching new high horizons with the growth of civilization, culture, science and technology, but the costs which we are paying or will be paying in near future is certainly be too high. Climate disaster with a major pollution problem is among the implications of this rapid development. Anthropogenic activities have caused considerable harm to the quality of our lifeline, i.e. water. Because of fast depletion of the freshwater resources, there seems to be a crisis of the same. Water pollution is a global concern and, it is the high time that we realize the severity of the situation. The crying need of the hour is to eliminate toxins from water and to establish a cost effective and environmentally sustainable system and to achieve the same is a challenging task for engineers. This is the future of humanity, which is at stake, after all.

#### 1.1 Textile industry - Global and Indian scenario

The global textile industry was estimated to be around USD 920 billion in 2018 and it is projected to witness a CAGR of approximately 4.4% to reach about USD 1230 billion by 2024 (<https://www.mordointelligence.com/industry-reports-global-textile-industry>). The global textile industry is an ever-growing market, with key competition between China, the European Union, the United States and India. It occupies a unique place in our country. One of the earliest to come into existence in India, it accounts for 14% of the total Industrial production, contributes to nearly 30% of the total exports and is the second largest employment generator after agriculture. It is a self-reliant industry, from the production of raw materials to the delivery of finished products, with substantial value-addition at each stage of processing; it is a major contribution to the country's economy. Its vast potential for creation of employment opportunities in the agricultural, industrial, organized and decentralized sectors & rural and urban areas, particularly for women, makes this industry the most important. India's textile and apparel exports stood at

US\$ 38.70 billion in FY 19 and is expected to increase to US\$ 82.00 billion by 2021 from US\$ 22.95 billion in FY 20. India's textiles industry contributed seven per cent of the industry output (in value terms) of India in 2018-19. It contributed two percent to the GDP of India and employs more than 45 million people in 2018-19. The sector contributed 15 percent to the export earnings of India in 2018-19. (<https://www.ibef.org/industry/textiles.aspx>). In short, textiles and clothing industries are important in economic and social terms, in the short-run by providing incomes, jobs, especially for women, and foreign currency receipts and in the long-run by providing countries the opportunity for sustained economic development. The leading production of cotton was achieved by India at around 6200 thousand metric tons (<https://www.mordointelligence.com/industry-reports-global-textile-industry>).

## **1.2 Need of textile effluent treatment**

The textile industry is one of the most complicated industries among manufacturing industry. It is an important industry which consumes more water and produces more wastewater. An important environmental concern relating to textile industry is the production and disposal of vast amounts of highly polluted wastewater, due to the consumption of about 100 to 200 litres of water per kg of textile product and the use of an enormous range of materials and chemicals in the production chain (Adriana et al, 2014, Suresh, 2014). The combination of the processes and products make the wastewater from textile plant produce a number of pollutant forms. The dyeing and finishing operations are such that the dyestuffs, chemicals and textile auxiliaries used will differ from day-to-day and sometimes even within several times a day. It includes numerous waste chemical pollutants such as sizing agents, wetting agents, complexing agents, colouring agents, pigments, softening agents, stiffening agents, fluorocarbon, surfactants, oils, wax and several other additives that are used in the processes. Today there is a great usage of synthetic reactive dyes. The dye effluents generated by textile industry affect the visibility and the photosynthesis in the water bodies and can also be harmful to aquatic life. Throughout the textile industry, manufacturing processes not only use significant quantities of energy and water, but also produce considerable waste products. Such contaminants contribute to high Total Suspended Solids (TSS), Total Dissolved Solid (TDS), Chemical Oxygen Demand (COD), Biochemical Oxygen Demand (BOD), heat, colour, acidity, basicity and other soluble substances (Ramesh et al, 2007; Andleeb et al, 2010).

Price competition, demand for high quality products, fresh and advanced extremely robust materials put more pressure on the industry as they have to use more dosage of chemicals and actively adapt to new chemicals to satisfy consumer demand. This would potentially result in the complication in the wastewater that is being discharged. Stringent discharge regulations as per the requirement of Environmental Quality Act bring the industry more challenges. Thus there is a need for continuous study and research on the effluent treatment to find new methods of treatment in order to sustain this industry (Kim et al, 2004).

### **1.3 Conventional methods of treatment**

Adsorption and chemical coagulation (Patel & Vashi, 2010), precipitation (Sabur et al,2012), photo degradation (Rikta et al,2015), electrochemical treatment (Chatzisyneon et al,2006), biodegradation (Selvakumar et al,2012), etc are the customary treatments used for textile effluent. The sludge formation, sludge disposal, addition of environmentally harmful chemical additives and land area requirements make the physico-chemical processes unfit. Microbial remediation procedures have received a lot of popularity in recent decades, despite the risks of these processes. Microbial decolorization and degradation is an environmentally safe and cost-competitive replacement to different conventional treatment technologies (Wookeun et al., 2014). Biodegradation is a biologically driven dissolution of chemical compounds, termed mineralization i.e. the complete dissolution of organic molecules into water, carbon dioxide and/or any other inorganic end products. These processes have the ability to mineralize dye products to innocuous inorganic compounds such as carbon dioxide, water and the forming small volumes of comparatively negligible quantities of sludge (Palanivelan et al., 2013). Though the biological treatment is inexpensive, dyes are toxic to microorganisms (B.Lellis et al,2019) and affect photosynthetic ability of aquatic life (D. Mazumder,2011). Therefore, effective, economical and apt methods are required.

### **1.4 New trends in treatment**

Textile effluents have low biodegradability and high COD. In most cases, the BOD<sub>5</sub> to COD ratio is around 0.25 which means that large amount of barely biodegradable organic matter are included in the textile wastewater (Wookeun et al., 2014). Using single physico-chemical or biological system in the treatment of concentrated textile wastewater is not feasible (Nawaz &

Ahsan, 2014). The research has been focused on Advanced Oxidation Processes (AOP), which can accomplish two goals by producing hydroxyl radicals that has a high oxidation potential: (i)COD reduction, (ii)detoxification and enhancement of the biodegradability to make subsequent biological treatment possible (Abdul et al, 2012). While AOP takes many advantages of rapid reaction rate and non-selective to contaminants and decaying refractory content, one specific and deadly drawback is high chemical consumption and electrical energy usage for devices such as ozonisers, UV lamps, ultrasounds and heater, resulting in very high treatment costs. However, their usage as a pretreatment stage to improve the biodegradability of wastewater that contains recalcitrant or inhibitory compounds can be justified because microorganisms may readily degrade the intermediates resulting from the reaction. Therefore, integration of AOP as a pretreatment step with biological process for the treatment of wastewater containing recalcitrant or inhibitory compounds appears to be very promising from economical perspective (Vilaseca et al, 2010; Makgato & Chirwa, 2010).

## **1.5 Photo Fenton process**

Fenton's reaction, which consists of non-selective and highly efficient oxidation of organic compounds by means of hydroxyl radicals produced in a chain cycle of hydrogen peroxide decomposition in the presence of bivalent iron salts, is one of the simplest and cheapest methods of AOP which allows for a decrease in pollutant concentrations in wastewater. The process is a radical reaction during which large amounts of hydroxyl radicals are produced which are capable of oxidizing even the most resistant contaminants (Siddique et al, 2017). The basic advantages of this approach include the high oxidation reaction efficiency, low cost, readily available substrates and the simplicity of the technique (Abdul et al., 2012). Although Fenton process has been effective in degrading the organic pollutants present in wastewater, it is considered that the production of ferric hydroxide sludge ( $\text{Fe}(\text{OH})_3$ ) is a downside of this method which needs further separation and disposal (Kim et al., 2004).

Photo-Fenton reagents have experienced the degradation of different organic contaminants for a century. Photo-Fenton reactions are cyclic in nature and the process continues to produce more and more hydroxyl radicals after the addition of  $\text{H}_2\text{O}_2$ . Although the reaction stops when all the  $\text{Fe}^{2+}$  ion have been consumed, in photo-Fenton reactions, two

hydroxyl radicals are produced per ion used and hence, the reaction rate is higher than that in Fenton Reaction (Noopur Ameta et al., 2012).

The photo-Fenton process can be both homogenous and heterogeneous. In the homogenous phase, the chemical changes that take place depend entirely on the existence of interaction between Fenton's reagents with compounds to be degraded by the reacting substances. The downside of this process is sludge formation due to post treatment process, restricted reaction pH range 2.5–3.5 which is also very acidic, H<sub>2</sub>O<sub>2</sub> scavenger, high iron loss to environment, challenge of recovery of iron ions.

The development of a heterogeneous catalyst in Fenton method overcame the demerits caused by homogeneous process for the degradation of wastewater pollutants. In heterogeneous process, in addition to chemical modifications, the physical steps take place on the surface of the catalyst at the active sites where there is minimal adsorption of reactant molecules by mass transfer. At the end of the reaction, the product molecules are desorbed and a new collection of reactant molecules are left open for the active sites to bind to the surface and react. Heterogeneous catalysts are much easier to separate from liquid products; they are non-corrosive and environmentally friendly. After treatment they can decrease the final concentration of iron ions in the bulk. Thus, the formed Fe<sup>3+</sup> complexes can be destroyed, with the aid of UV or solar radiation, allowing Fe<sup>3+</sup> ions to engage in the catalytic process of Fenton (Ai Ni Soon et al, 2011).

## **1.6 Application of nano zero valent iron in photo Fenton process**

Nanotechnology use is growing due to its total performance and cost-reduction capability. Nano-scale materials are used in nanotechnology to convert and detoxify contaminants by means of catalytic processes, chemical reduction etc. Nano zero-valent iron (nZVIs) can be highlighted between such nanoparticles (Machado et al, 2013). Nano zero-valent iron (nZVI) is one of the most intensively researched materials for environmental degradation. These iron nano- particles are able to cause higher reaction rates due to its larger specific surface area (about 30 times more than granular iron or larger sized powders) which in effect allows a greater exposure of these particles to pollutants. They have greater pore penetration potential and reactivity compared with larger particulate zero-valent iron (Taghizadeh et al, 2013).

The most common method for the production of nZVIs is chemical synthesis using sodium borohydride (Sun et al, 2007; Stefanuik et al, 2015). Yet the health concerns related to the sodium boro-hydride toxicity provide opportunities to follow concepts of green chemistry such as the biological synthesis of nZVIs from solvents of natural products (Schrick et al, 2004). A lot of studies have reported using plant extracts in the synthesis. The antioxidant compounds present in plant extracts react with iron(III) in solution to form nZVIs (Nadagouda et al, 2010).

The plant extracts previously reported are Mimosa Pudica (Niraimathee et al, 2016), Green Tea (Shahwan et al, 2011), Henna leaf (Borade et al, 2011), Parthenium hysterophorus (Niyas Ahamed et al, 2016), Murraya Koenigii (Farrukh & Farrukh, 2015), A. Bilimbi (Rosli et al, 2018), Eriobotrya Japonica (Onal et al, 2019), Caricaya Papaya (Alorkpa et al, 2016), Neem (Prashanth & Krishnaiah, 2014), Tulsi (Garg & Sardana, 2016), Guava (Gayathri & Kiruba, 2014; Jeyasundari et al, 2017), Amaranthus Dubius (Harshiny et al, 2015), Spinacia oleracea (Turakhia et al, 2018) etc. Various iron compounds are mixed with different plant extracts at certain volumetric ratio to produce green iron nano particles. Iron compounds used in the synthesis of green iron nano particles are iron (III) chloride (Shahwan et al, 2011), iron (II) sulfate (Onal et al, 2019) and iron (III) nitrate (Turakhia et al, 2018). The main advantages of this method are: i) less toxic reducing agent compared with boro hydride; ii) prolonged reactivity due to the capping ability that the poly phenol extract matrix induces on the nZVIs (Nadagouda et al., 2010); iii) the utilization of natural products which are considered as wastes; and iv) the fact that the extracts can act as a nutrient source which can enhance complementary biodegradation (Hoag et al., 2009, Nadagouda et al. 2010, Machado et al, 2013).

## **1.7 Biodegradability and toxicity of textile effluent**

The textile industries generate effluents that accommodate several types of chemicals such as leveling agents, dispersants, acids, alkalis, various dyes and carriers. Due to the presence of these constituents, the biodegradability of the effluent is very much reduced. In order to enhance the biodegradability, various advanced oxidation processes have been tried as pre-treatment. After pre-treatment, the biodegradability has been ensured by biodegradability index, kinetic coefficients etc. The physical state of the sludge has been assessed by sludge volume index.

The presence of harmful constituents in the textile effluent increases its toxicity, which interfere with the action of microorganisms, reducing the efficiency of biological treatment. Hence, toxicity assessment is a must before biological treatment. Toxicity bioassay test has been done for evaluating the toxicity after pretreatments.

## **1.8 Moving bed bio-film reactor (MBBR)**

Bio-film methods have demonstrated effectiveness for the recovery of organic carbon and nutrients removal from wastewater. Several specific bio-film technologies are currently in use, such as activated sludge process, trickling filters, rotating biological contactors (RBCs), fixed media submerged bio filters, granular media bio filters, fluidized bed reactors, etc. They have both the benefits and inconveniences. The trickling filter requires large land area. Mechanical failures are often experienced with the rotating biological contactors. In fixed media submerged bio filters, it is difficult to get even distribution of the load on the entire carrier surface. The granular media bio filters have to be operated discontinuously because of the need of backwashing and the fluidized bed reactors display hydraulic instability. For these reasons the moving bed biofilm reactor process was developed in Norway in the late 1980s and early 1990s (Ravichandran et al, 2012).

The Moving Bed Bio-film Reactor (MBBR) is a highly efficient biological treatment method for wastewater treatment, both commercial and urban. This simple and effective biological treatment process is suited to unique wastewater treatment systems such as reduction of nitrogen, high BOD or COD elimination, etc. (Kermani et al, 2009). MBBR process is based on the concepts of biofilm and incorporates the advantages of activated sludge process and other biofilm structures. MBBRs are run with the inclusion of freely moving carrier media similar to the activated sludge process. Instead of being suspended in the liquid, biofilm is attached to a surface that is submerged in the liquid. Therefore, there is no need for settling and sludge recirculation. The biomass is grown on small carrier elements that have a little lighter density than water and are kept in motion along with a water stream inside the reactor.

Aeration in an aerobic reactor and a mechanical stirrer in an anaerobic or anoxic reactor may induce motion within the reactor. This action produces a scrubbing effect that prevents clogging. The reactor volume is totally mixed and consequently there is no empty or idle space

in the reactor. As air passes through the water and past the media, the wastes in the water act as food for the microbes growing on the moving media (Kermani et al, 2009).

The advantages of MBBR possesses are high biomass, high COD loading, strong tolerance to loading impact, comparatively smaller size, no periodic backwashing, reduced sludge production, no sludge bulking and use of the whole volume of tank for biomass (Wookeun et al, 2014).

## **1.9 MBBR induced with magnetic field**

Magnetic water treatment (MWT) is a fairly modern method in environmental management. Magnetic field was used for the removal of organic compounds (Tomska & Wolny, 2008), phosphate (Zhao et al, 2012), treatment of coking wastewater (Cheng et al, 2014), pulp and paper wastewater (Liu et al, 2011), palm oil mill effluent (Mohammed et al, 2014) etc. The application of magnetic field has the ability to affect the biological properties through the improvement of bacterial activity (Cheng et al, 2014). Magnetic application also enhances the physical properties of wastewater in terms of solid-liquid separation mainly through aggregation of colloidal particles (Liu et al, 2011). When MBBR is induced with magnetic field, the reactor performance has been boosted up.

## **1.10 Design of experiments**

The software Minitab version 16 was used to design the number of experiments to be performed, calculate the experimental data and evaluate the experimental results. In order to investigate the effects of significant factors and to obtain the optimum condition in this study, the Response Surface Methodology with Box-Behnken statistical design was used. Box-Behnken design is a powerful mathematical tool capable to find significant parameters of an ideal process through multiple qualitative aspects. It requires fewer runs when compared to Central Composite Design making its application more economical. The optimization procedure involves studying the response of statistically designed combination, estimating the coefficients by fitting experimental data to the response functions and predicting the response of fit model (Oliveira et al, 2006). The visualization of the regression model can be presented by two-dimensional contour plots in RSM. These graphical plots are useful to recognize the nature of

the response at different factor levels. The shapes of contour plots may be circle, ellipse, hyperbolic, straight lines etc.

### **1.11 Problem Definition**

- To study the viability of Photo Fenton processes, namely Homogeneous Photo Fenton (HPF), Homogeneous Solar Photo Fenton (HSPF), Advanced Photo Fenton (APF) and Advanced Solar Photo Fenton (ASPF) process to improve the biodegradability of textile effluent and to propose the best alternative.
- To investigate the performance of Moving Bed Biofilm Reactor (MBBR) in the treatment of pretreated textile effluent.
- To test the influence of magnetic field on MBBR in the treatment of textile effluent.

### **1.12 Scope of the present research**

The textile industry uses a large amount of chemical compounds and water during its different production processes. Since large amount of water is consumed, large volume of wastewater is produced in different steps. The wastewater often characterized by high color, high value of COD, BOD, TDS etc. The conventional physicochemical and biological treatment methods are inefficient and have several drawbacks like production of large quantity of sludge, problems related to disposal, formation of toxic by-products etc. Also, biological methods are not much effective as most of the commercial dyes are non-biodegradable pertaining to its complex chemical structure. Hence an efficient treatment method for textile waste effluent is essentially needed.

Advanced Oxidation Processes like Fenton process is preferred as a promising option for degrading dye and to remove persistent pollutants from contaminated water. Here, photo Fenton process is employed which uses UV light or solar light as the energy source of reaction. The photo Fenton process involving the uses of biologically synthesized nano-scale zero-valent iron (nZVI) in the place of ferrous iron can improve the efficiency and also can make it environment friendly and economically efficient.

At present, most nZVI materials are prepared by reducing agents like sodium borohydride or potassium borohydride in liquid phase. This physicochemical method has some disadvantages as borohydride is classified as a toxic substance and the resulting nZVI could induce environment pollution. Therefore, the biological synthesis of nZVI can be proposed as a novel alternative. Ferric or ferrous iron is reduced to  $\text{Fe}^0$  using biologically-active substances called poly-phenols from plant extracts. Compared to classical methods, this approach is both low-cost and environmentally friendly.

The complex oxidation chemistry of AOP transforms the pollutants into a very large number of degradation intermediates which may be even more toxic than original compounds. Hence AOP is used only for enhancing the biodegradability. After the enhancement of biodegradability by specific photo Fenton process, final degradation stage can be attained biologically, i.e. by using MBBR. Exposure of MBBR to a weak magnetic field improves its performance and makes the textile effluent meet the effluent standards capable of disposing into inland waters.

### **1.13 Objectives of the study**

For the development of a coupled chemical-biological system, the following scientific and technological objectives are foreseen.

- To evaluate the performance of MBBR with textile sludge as inoculum for the treatment of textile effluent without any pretreatment
- To evaluate the performance of MBBR without any pretreatment, in which carrier materials are inoculated with the predominant bacteria present in the textile sludge isolated, and identified by 16S rRNA method, for the treatment of textile effluent
- To study the viability of biosynthesized nZVI from *Amaranthus Dubius* leaf extract in AOP and assess its reusability and leaching
- To study the improvement of biodegradability and assess the toxicity of the textile effluent after various photo Fenton based AOPs, namely HPF, HSPF, APF and ASPF process in order to select suitable pretreatment process

- To study the performance of pretreated effluent using MBBR with bacteria inoculated carriers
- To study the enhancement of the performance of MBBR by inducing magnetic field
- To compare the cost of the processes alternatives and propose an optimal integral treatment scheme minimizing the total treatment cost

# CHAPTER 2

## LITERATURE REVIEW

### 2.1 Background information

A cost-effective treatment technology would definitely save a huge quantity of water by reusing the treated water (Gautam et al,2017). Available statistics reveal that India habitats 1/6<sup>th</sup> of the total world's population on 1/50<sup>th</sup> portion of the land and just with 1/25<sup>th</sup> of the total water resource (Avlon Global Research, Mumbai, 2011). This depicts the need to treat and reuse wastewater by taking effective measures for sustainable development. The annual per-capita utilizable surface water has gone down from 1911m<sup>3</sup> in the year 1951 to 575m<sup>3</sup> in the year 2011, mainly because of the ever-rising population (Kumar et al, 2015). Sewage generation is growing with rapid urbanization. India currently has the facility to treat only 33% of the total sewage generated. It is estimated that by 2050, sewage generation quantity would be 132BLD that can meet around 10% of the total irrigation water demand (Bhatnagar & Minocha, 2008; Gautam et al, 2015). The challenge for the next decade is not only to bridge this huge gap in treatment capacity but also to develop suitable cost-effective treatment facilities for wastewater treatment and its recycling.

Water pollution is a state of deviation from pure conditions wholly, partially, or largely as a by-product of human activity. Major industrial contributors to the pollution are the pulp and paper, petrochemical, chemical, refining, metal working, textile and food processing industries. The textile industrial sector is one of the important and largest industrial sectors. It is one of the most complicated industries in the manufacturing industry. The textile industry has a major influence not only on the nation's economy but also on the environmental quality of life in many communities. This industry uses huge amounts of water and creates large volumes of wastewater in the finishing and dyeing processes (Adriana et al, 2014, Ghaly et al, 2014). Hence, the main environmental impact is a huge quantity of water intake (80–100 m<sup>3</sup>/ton of finished textile) and wastewater disposal (115–175 kg COD/ton of finished textile). Reuse of the wastewaters thus poses an ecological and economic problem for the industry as a whole. Depending on the quality of raw materials and goods, textile manufacturing needs a lot of

chemical compounds. Because of the differences in methods, equipment, and used materials, the effluents arising from these methods vary considerably in characteristics. The main pollutants in textile effluent release from processes of dyeing and finishing. Such processes involve the input of a broad variety of chemicals and dyes, which are usually complex organic compounds. As they are not contained in the finished product, it becomes waste and produces problems in disposal (Irina-Isabella Savin et al., 2008). Considering the quantity produced and the composition of the effluent, wastewater in the textile industry is listed as the most polluting of all industrial sectors (Jahid et al, 2013).

## **2.2 Textile industry and manufacturing processes**

Throughout the years, the world textile industry's development has followed an unusual trend. The centre of clothing development, based in the United Kingdom, moved first to the USA, then to Japan and eventually to the Asian countries. The textile industries can be divided into two categories depending on the waste production, which is dry and wet fabric industry. Solid waste is produced in dry fabric industries, and liquid wastes are created in wet fabric industries.

Wet fabric processing includes stages of sizing, scouring, bleaching, mercerization, dyeing, printing and finishing. During each point various types of chemicals such as alkalis, strong acids, inorganic chlorinated compounds, sodium hypochlorite, lubricants, levelling agents, organic compounds such as dye-stuffs, bleaching agents, starch, finishing chemicals, thickening agents, surface active chemicals, wetting agents, dispersing agents and salts are used. Various types of dyes are used for coloring purposes. More than one type of dyes is used to improve the beauty of products (Paul et al, 2012).

The various phases in the textile manufacturing by wet process are given in the Fig.2.1.

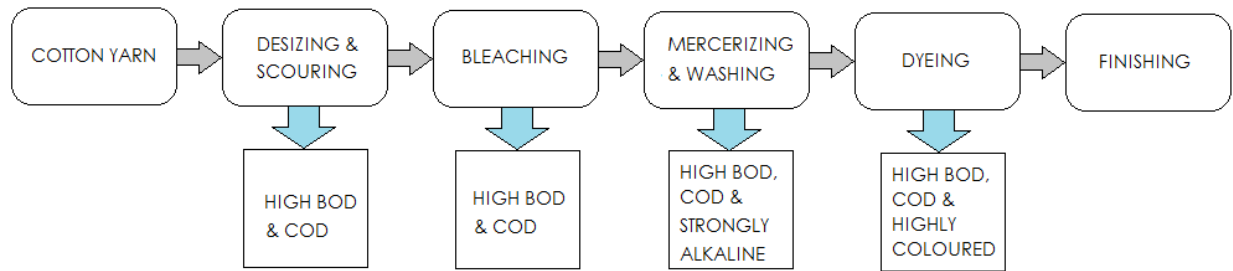


**Fig.2.1 Textile manufacturing by wet process**

a) Sizing : First step in the preparation is sizing, in which sizing agents such as polyvinyl alcohol (PVA), starch and carboxy-methyl cellulose (CMC) are added to provide fibre strength and reduce breakage.

b) De-sizing : It is used before weaving to avoid sizing materials.

c) Scouring : Removes impurities from the fabrics by using acid or alkali, to decompose natural oils, fats, waxes and surfactants, and to emulsify and detain impurities in the scouring bath (Bisschops & Spanjers,2003).

d) Bleaching : This process is done using chemicals such as  $H_2O_2$  and sodium hypochlorite to extract excessive colour from the fibres.

e) Mercerization : This is a chemical process used to transmit lustre, increase strength and enhance the absorption of dye. A concentrated alkaline solution is added in this step, and the fibres are washed by an acid solution before dyeing (Suresh, 2014).

f) Dyeing : Dyeing is the process of adding colour to the fibres which typically involves large amounts of water not only in the dye bath but also during the rinsing phase. Based on the dyeing technique, certain chemicals such as metals, salts, surfactants, sulphide, and formaldehyde can be applied to boost the adsorption of dye on fibres (Paul et al., 2012).

g) Printing : Here, wastewater production is continuous, and can include dye residuals or reactive dyes and chemicals used as fixers, binders, thickeners, etc.

Range of water requirements in various processes are given in Table 2.1.

**Table 2.1 Water requirements for cotton textile wet finishing operations (Shaikh, 2009)**

Process	Requirements in litres per 1000 kg of product
Sizing	500-8200
De-sizing	2500-21000
Scouring	20000-45000
Bleaching	2500-25000
Mercerizing	17000-32000
Dyeing	10000-300000
Printing	8000-16000

### **2.3 Chemicals used in the textile industry**

Printing and dyeing are two essential processes which produce color containing wastewater. Nowadays, synthetic dyes are used to stain the fabrics that were available pre-packaged in any color, while in the past, organic dyes were developed individually by processing natural fruits, vegetables and other goods. Table 2.2 (Mazumder, 2011) explains the various pollutants used in different processes and nature of wastewater generated.

**Table 2.2 Effluent Production from different processes of textile industry**

Process	Effluent composition	Nature
sizing	Starch, carboxy methyl cellulose (CMC), waxes, Poly vinyl alcohol(PVA), wetting agents	High in BOD, COD
De-sizing	Starch, PVA, CMC, fats, waxes, pectins	High in BOD, COD, SS, DS
Bleaching	Cl <sub>2</sub> , NaOH, H <sub>2</sub> O <sub>2</sub> , sodium hypochlorite, surfactants, NaSiO <sub>3</sub> , acids, sodium phosphate	High alkalinity, high SS

Mercerizing	NaOH, cotton wax	High pH, Low BOD, high DS
Dyeing	urea, reducing agents, dye stuff, detergents, oxidizing agents, acetic acid, wetting agents	high BOD, DS, low SS, heavy metals, highly colored
Printing	Pastes, starch, urea, gums, binders, oils, acids, thickeners, alkali, cross linkers, reducing agents	Highly colored, high BOD, SS, slightly alkaline, low BOD, oily appearance
Finishing	Resins, formaldehyde, waxes, hydrocarbons	Low alkalinity, low BOD, high toxicity

### 2.3.1 Dyes

From an ecological point of view, dyes are unfavorable because the effluents generated are heavily colored, contain high concentrations of salts and exhibit low biological oxygen demand/chemical oxygen demand (BOD/COD) values. First of all, nature and origin are considered as general classification criteria of natural and synthetic textile dyes (Carmen et al., 2014). Until 1856, the natural textile dyes derived from vegetable and animal products were used primarily in textile production. The first discovered organic dye was in 1856. Such dyes are aromatic compounds formed by chemical synthesis and have aromatic rings in their structures containing displaced electrons and often separate functional groups. The textile dyes used are complex organic aromatic compounds designed to resist fading when exposed to sweat, sun, water, other chemicals, and microbial attack. Their uses in textile industries vary depending on the type of fabrics that are produced (cotton, silk, rayon, wool etc.). It has been estimated that the worldwide dyes demand is around  $7 \times 10^5$  tons per year (Arun Prasad & Bhaskara Rao, 2010; Ogugbue and Sawidis, 2011).

Color in dyes and their intensity is a result of chromophoric and auxochromic groups being present. Structural chromophores are aryl groups that include delocalized ( $\pi$ ) electrons in the conjugated ring structure and are responsible for the absorption of differing wavelengths of electromagnetic radiation, based on the energy needed by the electron cloud. In addition to the primary chromophore, dye molecules also include auxochromes that include removal of electron or substituent electron donation groups that modify the total energy content of the electron

network. The term auxochrome originates from two roots. The auxo prefix is derived from auxein, meaning, "increased". The second "chrome" part applies to color. The sense of the term auxochrome is enhancer of color strength. Dye molecules can contain either positive or negative charged auxochromes, or their combinations. Forms of functional ionizable groups that can be joined to auxochromes are: (a)-NH<sub>2</sub> (amino) (b)-COOH (carboxyl) (c)-OH (hydroxyl) and (d)-SO<sub>3</sub>H (sulphonic) (Ghaly et al,2014).

### **2.3.2 Classification of dyes**

The textile dyes are mainly classified in two different ways:

- i. Based on its application characteristics: acid, basic, direct, disperse, mordant, reactive, sulphur dye, pigment, vat, azo insoluble dyes.
- ii. Based on its chemical structure: nitro, azo, carotenoid, diphenyl methane, xanthene, acridine, quinoline, indamine, sulphur, amino and hydroxy ketone, anthraquinone, indigoid, phthalocyanine, inorganic pigment etc. (Francisco et al, 2014).

Considering only the general structure, the textile dyes are often classified as anionic, nonionic, and cationic colors. The major anionic dyes are the direct, acid and reactive dyes, and the most troublesome are the brightly colored, water-soluble reactive and acid dyes, because they cannot be eliminated by traditional treatment schemes. The major non-ionic dyes are dispersing dyes that do not ionise in the aqueous environment. The major cationic dyes are the azo, basic, anthraquinone disperse, reactive dyes etc. The most dangerous dyes are those which are made from known carcinogens such as benzidine and other aromatic compounds. Owing to their dynamic composition, organic origin and recalcitrant nature, dyes are difficult to decolourise, which makes it necessary to eliminate them from industrial effluents before they are disposed into water bodies (Carmen et al, 2014). The dyes' chemical composition was resistant to fading when exposed to sun, water and a lot of chemicals. Highest toxicity levels were examined for basic, azo, and direct dyes. Some algae and higher plants exposed to effluent rich in disperse dyes at higher concentration have a tendency to bio-accumulate the heavy metal ions from textile effluents. They contaminate not only the environment but also transform the toxicity through the entire food chain, leading to bio-magnifications (Hosseini et al, 2011).

A brief description of various classes of dyes is presented in the following sub-sections.

**a. Acid dyes**

These dyes are called acid dyes as they applied to the fabrics in inorganic or organic acid solutions. Due to the presence of sulphonate or carboxyl group in the molecular structure, acid dyes are negatively charged (anionic) compounds and are widely used for protein fibres that denature under alkaline pH. They mainly bind to positive group (such as  $\text{NH}^{4+}$ ) of fabrics such as wool, nylon, nylon/cotton blends, acrylics and silk. Azo, anthraquinone, and tri-aryl-methane are commercially important acid dyes. These dyes' molecular weights range from 200 to 1000 and the higher the molecular weight, the worse the leveling property (Uday et al, i2016).

**b. Basic dyes**

Basic dyes are cationic compounds (positively charged) that bind to anionic surfaces or fibre groups. Crystal violet, safranin, basic fuchsin, and methylene blue are some examples of basic dyes. Mostly these dyes are added to wool, silk, cotton and modified acrylic fibers (Suresh, 2014).

**c. Direct dyes**

Direct dyes are cationic or anionic, highly soluble in water and added in solutions containing ionic salts and electrolytes to the fibers. These are mostly azo, phthalocyanine, stilbene, or oxazine compounds (one or more azo bonds). They are used on cotton, other cellulosic fabrics, paper, leather, wool, silk, and nylon. They also act as indicators of pH and as biological stains. The wash-quality of direct dyes is very poor because with every washing the dye molecules are slowly leached out. Therefore special treatment is done with cationic bulking agents to bind the dye onto fibers. Few of the direct dyes have outstanding luminosity (Suresh, 2014).

**d. Reactive dyes**

Reactive dyes were introduced in 1956, and its use has since increased, especially in developing countries. Total reactive dyes production in 2011 was estimated to be 350,000 tons. These dyes have a special function of forming a covalent bond with the dyed fibers. The

cellulosic, silk, cotton, and wool are the most commonly dyed fibers. However, under alkaline (dyeing) conditions, these dyes are particularly prone to hydrolysis and are considered to show the lowest fixation rate. In contrast with direct dyes, reactive dyes are more costlier. However, they have outstanding shade reproducibility with excellent wet fastness (Chintha & Vijaykumar, 2013).

Reactive dyes have four components listed below:

- The chromogen (azo, carbonyl, anthraquinone or phthalocyanine class). The number of azo group is variable and depending on the number, dyes can be classified as mono azo, diazo or polyazo.
- The fibre-reactive group is often a heterocyclic substituted aromatic ring and is the part of the dye molecule that is able to react with the fiber.
- The water solubilizing group improves the solubility of reactive dyes for application to fibers (ionic groups, often sulphonate salts). Water solubilizing group is linked to the chromogen as well as to the fiber-reactive group.
- The bridging group (commonly an amino group) links the chromogen and the fiber-reactive group.

There are three types of reactive fiber-based dyes: vinyl sulphone (example C.I. Reactive Black 5), chloro/fluoro triazine (C.I. Reactive Red 3) and chloro/fluoro pyrimidine. Reactive dyes can be homo-bi-functional (including two groups of mono chloro-triazine) or hetero-bi-functional (including one group of mono chloro-triazine and one group of vinyl sulfone). The major attractive features of reactive dyes are permanency and resistance to washing due to strong chemical bonding with the fabric.

#### **e. Disperse dyes**

Disperse dyes are colloidal in nature and have poor water solubility. They are used to dye synthetic fabrics, such as acetate cellulose, polyester, nylon, triacetate, and acrylic. Fine disperse solutions of these dyes are added directly to fabrics for colloidal absorption. Dye bath conditions such as temperature and pH can differ based on the uniformity of the fabric and the degree of

fiber penetration of the dyes (Sala & Gutierrez-Bouzan, 2012).

#### **f. Mordant dyes**

Mordant dyes use a chemical called mordant which improves the color holding properties of the dye molecules inside the fiber. The mordants include tannic acid, sumac, gall nuts, bark extracts, oleic and stearic acids and various mixtures of soluble metal salts such as chromium, titanium, iron, copper, and nickel. Metallic mordants are often used than acid mordants. Most natural dyes, such as hematein (true black 1), eriochrome cyanine R (mordant blue 3) and celestine blue B (mordant blue 14), are mordant dyes.

#### **g. Vat dyes**

These dyes are basically insoluble in water and cannot be directly added to the fibers. Hence they are applied to the substrate in a reduced, soluble state and eventually oxidized to the insoluble form. Vat dyes can be transformed into water soluble form called leuco dye by reduction with a strong reducing agent, hydrosulphite and solubilising agent, sodium hydroxide. The reduced dye-stuff penetrates into the fiber and it is reoxidized on the fiber back to the insoluble form, which remains fixed in the fabric (Smelcerovic et al, 2010). Common vat dyes are quinones, anthraquinones and indigoids dyes. Application of vat dyes is achieved with sodium dithionite, caustic soda and hypo-sulphite in alkaline conditions. Upon ensuring oxidation, the dye is absorbed into the fiber. Vat dyeing is used to stain cotton, wool, and other fibers. Vat dyes include the natural dye, indigo (used for denim jeans) and artificial dyes known by their brand names, indanthrene, and flavanthrene. Among traditional dyes, vat dyes are eco-friendly, while resistance to light and wash (i.e. fastness) are the highest (Choudhury, 2018).

#### **h. Sulphur dyes**

Sulphur dyes are like vat dyes, water insoluble and function as reduced water soluble form or oxidized water insoluble type. They are complex aromatic polymers with heterocyclic rings containing sulphur. They are often used for low cost fabrics and garments such as working clothes. Environmentally speaking, sulphur dye is free from heavy metals and other toxic materials, so it is not too bad when compared to reactive dyes. However, 90% of all sulphur dyes make use of sodium sulphide, which makes the effluent more toxic than any others. The

effluent from sulphur dyeing endangers life and possibly alters DNA of waterborne species, corrodes sewage systems, damages treatment plants and possesses high pH and odour (Choudhury, 2018).

#### **i. Pigment dyes**

Pigment dyes are non-ionic, insoluble compounds that maintain their particulate form during their application. Using dispersing agents, they are distributed in aqueous solution. Generally, pigments are used in combination with thickeners to print different fabrics. The bulk of pigment dyes are azo compounds (yellow, orange, and red) or phthalocyanin metal complexes (blue and green). Pigment dyes of anthraquinone and quinacridone are also applied to the fabric (Wang & Yin, 2012).

#### **j. Solvent dyes**

Solvent dyes are non-ionic, used for dyeing objects, and also act as a dissolution phase, for example paints, varnish and wax. They are also named as lyso-chrome, meaning the word "lyso" disappear, and the color "chrome". Their use in garment manufacturing has recently increased. They are mainly diazo compounds that underwent some molecular rearrangement and hence lacked the ability to ionize (Uday et al, 2015).

#### **k. Natural dyes**

Dyes of biological origin are known as natural dyes. Many of the natural dyes have been derived from plant parts, such as roots, leaves, flowers, fruits and bark. Pigments have also been recorded to synthesize from micro-organisms such as fungi. Examples include carotenoids ( $\beta$  – carotene) from caotenogenic fungi, photo-sensitizing pigments such as hypercin, flavinoids compounds, quinones (anthraquinones, naphthoquinones), secondary metabolite water-soluble monascus pigments formed by ascomycetes (Peralta-Zamora et al, 1999). Disastrously, the main problems accompanied with natural dyes are: a) absence of normal procedures for the extraction and processing of dyes, b) incapacity to fix on to fabrics and need for mordants, and c) lack of enough information related to biogenic dyes' toxicity.

## **2.4 Environmental concerns of textile effluents**

The presence of large quantity of non-biodegradable organic matter, especially textile dyes is the problem of greater emphasis in textile industry (Orts et al, 2018). Discharge of untreated textile dyeing effluents creates the following environmental problems: a) imparting colour to the receiving ecosystem and causing an aesthetic problem b) reducing the reoxygenation potential of the receiving water and preventing sunlight transmission, which in effect disturbs the photo-synthetic behavior of benthic plants in the aquatic system and processes of self-purification (Alunaimi et al, 2008), c) chronic and acute toxicity, d) azo cleavage in the dyes under anaerobic conditions leads to the production of carcinogenic and mutagenic aromatic amines and e) adds to the total COD, BOD, SS, TDS etc. in the receiving habitats. This effluent has detrimental effects on the local freshwater sources, surface water sources and soil. Neighborhood ecological system is severely affected (Hassan and Carr, 2018). It has a detrimental effect on fish survival also (Andleeb et al, 2010). The textile dyes also act as carcinogenic, toxic (Sharma et al,2018) and mutagenic agents (Aquino et al, 2014), persist as environmental pollutants and cross entire food chains providing bio-magnification (Sandhya, 2010), such that organisms at higher trophic levels show higher levels of contamination compared to their prey (Newman, 2015). In humans, exposure to colored effluents can lead to immunological, neurological and circulatory diseases, lung edema inflammation, eye and skin infections and problems with allergies (Islam & Mostafa, 2019). The presence of dyes or their contaminated derivatives in water can also induce diseases of human well-being, such as diarrhea, haemorrhage, skin ulceration and mucous membranes. These toxic compounds also cause severe kidney, reproductive system, liver, brain and central nervous system damage (Palanivelan et al, 2013; Khan and Malik, 2018). The workers who produce or handle reactive dyes may have contact dermatitis, allergic conjunctivitis, rhinitis, occupational asthma or other allergic reactions (Hunger, 2003). Hence, ensure environmental sustainability to the future population (Jordao et al, 2018) by treatment of textile effluent through physico-chemical and biological or their combinations is our responsibility.

Government legislation is becoming more stringent in most developed countries regarding the removal of dyes from industrial effluent. This creates problems for the textile

industries. Most textile industries are developing on-site or in-plant facilities to treat their own effluent before discharge (Selcuk, 2005).

## 2.5 General characteristics of textile effluents and standards for discharge of effluents

Textile industry effluents are extremely variable in composition and vary from plant to plant depending upon the processes used in the industry. Characteristics of a typical textile wastewater is shown in Table 2.3 and General standards for discharge of effluents as per Environmental Protection Rules, 1986, Schedule IV, Part A are given in Table 2.4.

**Table 2.3 General characteristics of textile wastewater (Palanivelan et al., 2013)**

Parameters	Unit	Typical range
pH	–	5.5-10.5
BOD	mg/l	100-4000
COD	mg/l	150-10000
TDS	mg/l	1500-6000
Total alkalinity	mg/l	500-800
Sulphides	mg/l	15-20
Chlorides	mg/l	200-6000

**Table 2.4 General standards for discharge of effluents (Environmental Protection Rules, 1986, Schedule IV, Part A)**

Parameters	Max. admissible concentration if discharged directly into	
	Inland surface water	Irrigation water
COD, mg/l	250	-
BOD, mg/l	30	100
pH	5.5-9	5.5-9
TSS, mg/l	100	200

TDS, mg/l	2100	2100
Sulphide, mg/l	2	-
Chloride, mg/l	600	1000

## 2.6 Biodegradability of textile waste

The dyes and auxiliary chemicals used in the textile industry reduce the biodegradability of textile wastes. The effects of chemicals on the biodegradability are as follows.

### a. Dyes

The most important process imparting pollution in textile industry is the dyeing process. Dyeing allows pollutants to be readily recognized through colour. A very small amount of dye is noticeable in water, reducing surface clarity. This contributes to reduction of sunlight penetration into the water bodies and therefore of photo-synthesis. They also hinder the development and growth of microorganisms, contributing to a decrease in the stream's self-purification ability (Palanivelan et al, 2013; Babu et al, 2007).

### b. Surface active agent

Numerous scientific studies have reported the biodegradation of surface active agents. The hydrophobic groups are essential for the biodegradation of surface active agents (surfactants). The hydrophobic ends are more important to the water solubility than to the biodegradation. Surfactant biodegradation is important because it interferes with successful oxygen delivery in biological treatment systems. It is characterized by relatively high aquatic toxicity and contributes to the final BOD or COD of treated effluents (Bisschops & Spanjers, 2003). While literature indicates that surfactants are easier than ever to biodegrade, they are still very difficult to degrade. For example, in activated sludge treatment, the surfactant alkyl phenol ethoxylate is removed, and it was believed to be biodegradable. This surfactant is resistant to attack from bacteria found in activated sludge but is adsorbed easily on the sludge. The adsorption affected both the biodegradability and elimination. Thus most of the surface active agents used today are actually eliminated and not biodegraded by more than 80%.

### **c. Sizes**

The hydrolysis of polyvinyl acetate produces polyvinyl alcohol (PVA) in an attempt to produce water soluble alcohol. PVA prevents biodegradation if small amounts of acetate groups are found in the polymer. The number and position of these residual groups that varies from batch to batch, creating significant variability in the biodegradability. In biological environments, a part of PVA is lost by sedimentation. Starch is easily biodegradable. Sizes of poly-acrylic and polyester are refractory to biodegradation (Robinson et al, 2001).

### **d. Finishing agents**

In the preparation of textile fabric, various chemicals are used to add favourable properties to the final garment. Compared to their COD values, resin finishes have extremely low BOD values. This may be due to the presence of toxic chemicals or metal catalyst used in the preparation of the finish. Many finishing agents are removed in biological treatment plants by adsorption or sedimentation, and not by biodegradation (Robinson et al, 2001).

### **e. Grease and oils**

Oil and grease may present problems at the waste water treatment plant because they adhere to particulate matter, causing it to float. Not all oils are equally troublesome. Vegetable oils and natural grease tend to be fairly readily degradable.

### **f. Complexing agents**

EDTA (ethylene diamine tetra acetate), the most widely used complexing chemical, is very stable against oxidation and is not biodegradable. Because of its low molecular weight, it is not adsorbed into activated sludge and escapes with treatment plant effluent (Robinson et al, 2001).

## **2.7 Emerging techniques for textile effluent treatment**

Treatment of wastewater is aimed at eliminating pollutants and creating a healthy effluent that can be released into water sources without damaging the environment. Treatment of textile wastewater is usually performed in primary, secondary, and tertiary steps (Palanivelan et al,

2013). The treatments can be further divided into chemical, physical, and biological treatment (Babu et al, 2007).

### **2.7.1 Physical and chemical treatment**

Physical procedures were among the first ways of removing solids from wastewater, typically by filtering through screens to eliminate particles and solids. Furthermore, by gravity, solids thicker than water can fall out of fresh-water. Chemicals may be used to produce pollutant modifications that improve functional processes of eliminating these new types. Simple chemicals such as alum, lime or iron salts may be applied to wastewater that allow such contaminants to flocculate or bunch together into large, heavier masses that can be separated more easily through physical methods (Adriana et al., 2014). Physical and chemical processes include coagulation, absorption, activated charcoal adsorption, ozone oxidation, advanced oxidation, ionizing radiation, ultra-filtration, and photo-catalytic treatment are widely used to treat textile effluents. Specific and complex dyes molecular configurations make effluent impossible for traditional physical and chemical methods to handle. At present, the use of such techniques has not been widely adopted, because they are very costly, consume electricity, have many operating challenges and produce waste that is difficult to dispose of (Adriana et al, 2014; Palanivelan et al, 2013). Usually, any traditional treatment system introduced individually is not capable of eliminating all the different contaminants present in textile wastewater and resolving the wide variation in composition, resulting in minimal outcomes in terms of total reduction of organic matter, nutrients and colour (Adriana et al., 2014).

#### **2.7.1.1 Coagulation and sedimentation**

This technique is one of the most used techniques in the past. In this process, some of the chemicals are added in the water that assists the charged particles to make some compound that can be coagulated in water. Usually, the colloids carry negative charges, so the coagulants are normally inorganic or organic cationic coagulants (with positive charge in water). Some of the organic polymers cause coagulation to an extent that these coagulants combine to give groups and form sediments that is easy to extract (Ciardelli and Ranieri, 2001). The most commonly used chemicals are  $\text{FeCl}_3$ ,  $\text{Al}_2(\text{SO}_4)_3$ ,  $\text{FeSO}_4$ , and lime (Verma et al, 2012).

### **2.7.1.2 Adsorption**

Adsorption is one of the cheapest and most effective techniques (Cotoruelo et al, 2007). It is the exchange of material at the interface between two immiscible phases in contact with one another. In this process dissolved molecules are attached to adsorbent surface by physical and chemical forces. Adsorption appears to have considerable potential in the removal of colour from industrial wastewater. This method is acceptable due to the ease of operation and insensitivity to hazardous pollutants. However, its widespread use is limited due to its high cost. Different adsorbents are used for the removal of dyes from aqueous solutions such as activated carbon, alumina, crushed bricks, peat, sand, bentonite, silica, apricot etc (Rahman et al, 2011; Hu et al, 2006).

### **2.7.1.3 Ion exchange method**

Ion exchange method is a treatment process that has been used to treat wastewater excluding dye-containing wastewater. The main reason of avoidance was a misconception, and it was thought that this method is not effective against dye-containing wastewater and its effectiveness slows down further when wastewater is loaded with other additives in consort with dyes. This flaw was removed with an excellent work of Baouab et al, (2001) who proved in his experiment that sulfur-containing dyes and those with acidic nature could better be treated with a combination of anion exchange column that is packed in series and a non-polar resin. This was a great turning point in treatment of textile wastewater because it added another positive option against dye treatment and it could be further explored within time. The ion exchange resins needed to be regenerated after one-time removal, and this task was completed with the help of organic solvents. The organic solvents are not that much cheap, and their use increased the operational cost, that was the major drawback of ion exchange method.

### **2.7.1.4 Electrochemical treatment**

Electrochemical treatment is an attractive, alternative treatment process and has several advantages over conventional treatment methods such as easy automation, maximum removal efficiency, shorter treatment time, low sludge production, and reasonable operating cost. Under electrochemical treatment process, electro-oxidation methods were widely investigated. Electro-oxidation is a process in which the pollutants are destroyed or converted into simpler forms like

carbon dioxide and water. This oxidation process can be either direct or indirect oxidation. In the indirect oxidation process, strong oxidants like hypochlorite, chlorine, hydrogen peroxide, and hydroxyl ions are electrochemically generated at the anode. All the oxidants are produced in-situ and are utilized immediately (Thakur et al, 2009).

#### **2.7.1.5 Electro-coagulation**

In this technique, effluents are treated in a chamber in which metal electrodes are used to treat wastewater. Electrode plates are suspended in effluent solution, and it can remove metal oxide at a specific pH. Metal oxides are coagulated and can be easily removed from the solution. This method is effective and has been reviewed in many articles (Khandegar and Saroha, 2013). This technique uses direct current source between metal electrodes immersed in the effluent, which causes the dissolution of electrode plates into the effluent. The metal ions, at an appropriate pH, can form wide range of coagulated species and metal hydroxides that destabilize and aggregate particles or precipitate and adsorb the dissolved contaminants.

#### **2.7.1.6 Reverse osmosis**

Reverse osmosis membranes have a holding degree of 90% or greater for most kinds of ionic complexes. Decolorization and removal of chemical auxiliaries in dye-house wastewater can be done in a single step by reverse osmosis. Reverse osmosis causes the elimination of all mineral salts, hydrolyzed responsive dyes, and chemical auxiliaries. This process needs a very high energy since a very high pressure is required herein (Babu et al, 2007).

#### **2.7.1.7 Nano-filtration**

Nano-filtration has been used for the management of color discharges from the textile industry. Nano-filtration membranes hold low molecular weight organic complexes, divalent ions, big mono-valent ions, hydrolyzed responsive dyes, and dyeing auxiliaries (Ellouze et al, 2012). Membrane fouling is a major limitation of this method.

#### **2.7.1.8 Ozonation**

Ozone is being used for the wastewater treatment since 1970. It is highly unstable which makes it a strong oxidizer. When compared to chlorine having oxidizing potential of 1.36, it was

found to be a better oxidizing agent with an oxidizing potential of 2.07 (Koch et al, 2002). Ozonation is relatively effective in decolouration of various dye origins and toxic effects of textile effluents; the main environmental concern related textile wastewater effluent discharge. Dissolved in water, ozone reacts with many organic compounds in two different ways: by direct oxidation as molecular ozone or by indirect reaction through formation of secondary oxidant like hydroxyl radical (Metcalf & Eddy, 2003). Use of ozone for wastewater treatment in textile industry to remove colouration and lower toxicity has been documented in several studies; however sufficient effect on BOD/TOC removal was not confirmed (Baban et al, 2003).

### **2.7.2 Biological treatment**

Biological methods for removing dyes are based on microbial biotransformation of dyes. The biodegradation is proposed as the most economical resource for the treatment of textile effluents (Pa'zdziar et al, 2017) when using enzymes secreted extra-cellularly by microorganisms, such as azoreductases, laccases and the peroxidases (Imran et al, 2015) in order to transform or even mineralize textile dyes. In addition, there is the bio-absorption that can act when the dye is very toxic to the growth of the microorganism, through absorption, deposition and ion exchange, using dead bacteria, yeasts and fungi. Biological management of chemical effluent decolouration systems is vague, distinct, and divergent. Biological treatment can be either aerobic, anaerobic or a mixture of both depending on the type of microbes used. Microbial decolourization and oxidation is environmentally friendly and cost-competitive. The processing, quality, adaptability of microorganisms and the reactor type are crucial parameters for removal efficiency. The main advantage of biological treatment in comparison with certain physico-chemical treatments is that over 70% of organic matter may be converted to bio-solids (Palanivelan et al, 2013).

Important biological processes for the treatment of textile wastewater are following.

#### **2.7.2.1 Rotating Biological Contactor (RBC)**

The Rotating Biological Contactor also known as a Bio-Rotor is a method of treatment with attached growth technology. It has circular plastic discs set up on a shaft that immersed partially in a reactor. When the shaft revolves slowly, bio-organisms stick on the disc as biological growth, consuming organic materials from the wastewater as they pass through the

disc surface. Aerobic conditions are kept in the reactor. The disc initiates interaction with bio-film and waste water, combining the mixed liquor and aerating the waste water. However, efficiency is poor when comparing with other biological treatment methods. Mechanical failures are often accompanied with it (Ravichandran & Amarnath, 2012).

#### **2.7.2.2 Biologically Aerated Filter (BAF)**

A biologically aerated filter is a treatment tank eliminating the need of a separate sedimentation tank. It consists of a submerged aerated fixed film biological filtration device that provides a biomass surface and also retains suspended solids that serve as both a biological contactor and a filter. Both the influent and the process air flow move from the bottom upward. In the lower half of the pipe, the maximum biological activity occurs. Limitations include extra charges for repairs, machineries, power etc. (Ravichandran & Amarnath, 2012).

#### **2.7.2.3 Anaerobic filter (AF)**

Anaerobic filter (AF) is another type of anaerobic digester. The digestion tank contains a filter media on which anaerobic bacteria groups attach and organic substances in wastewater are degraded as they travel slowly through it. The filter media may be compressed shale, reticulated polyurethane foam or porous stone. Dead-zone formation, channelling, clogging, etc. are the drawbacks of AF (Ravichandran & Amarnath, 2012).

#### **2.7.2.4 Trickling filter (TF)**

The waste water is sprayed continuously or intermittently on a filter bed. A bio-film which is a rich source of microorganisms will be produced wrapping the filter media by the action of micro-organisms and the organic substances. As the waste water oozes through the filter bed, the organic matter is degraded under aerobic conditions. A high head loss is caused by this filter. It requires a large installing area which increases the expense. These filters cannot treat raw wastewater and primary sedimentation is must. Nuisance due to fly and odour may prevail (Metcalf & Eddy, 2003).

#### **2.7.2.5 Activated Sludge Process (ASP)**

The activated sludge process is one of the most commonly used for secondary wastewater treatment. It is a suspended-growth biological treatment process. It utilizes activated sludge, a

dense microbial culture in suspension to oxidize the organic material under aerobic conditions and create a biological floc for solid separation in the settling units. Mechanical or diffused aeration keeps the aerobic environment in the reactor. Typical retention times are 5 to 14 hours in conventional units rising to 24 to 72 hours in low rate systems (Hait and Mazumder, 2008). The microbial concentration is maintained in the reactor by recycling a certain portion of the sludge and is settled out in a secondary sedimentation tank. The activated sludge process produces new cell mass which will become part of the activated sludge mass. Part of the settled material therefore, must be disposed of, and a portion must be introduced into the incoming raw waste water in order to have an active population of microorganisms that will feed on the organic compounds (Metcalf and Eddy, 2003).

#### **2.7.2.6 Sequencing Batch Reactor (SBR)**

SBR is a modification of the activated sludge process. These differ from activated-sludge plants because these unite all the treatment phases, namely, fill, react, draw and decant phases into a single reactor, while traditional facilities focus on multiple tanks. Suspended growth type or attached growth type SBR may be used (Ravichandran & Amarnath, 2012).

#### **2.7.2.7 Upflow Anaerobic Sludge Blanket (UASB) technology**

UASB is a kind of anaerobic digester used in the treatment of many types of waste water. The technology involves an upward flow of wastewater through an anaerobic sludge bed within a reactor. When the wastewater flows into the sludge, micro-organisms in the sludge decompose organic substances present in the wastewater producing biogas (methane and carbon dioxide). When the gas goes up to exit, hydraulic turbulence occurs in the reactor causing mixing, resulting in further degradation as a result of further microorganism interaction with substrate. Maintaining correct hydraulic conditions is challenging in UASB. Treatment may be unstable with variable hydraulic and organic loads. Long start up time is required (Ravichandran & Amarnath, 2012).

These approaches along with their associated advantages and disadvantages are outlined in Table 2.5.

**Table 2.5 Textile wastewater treatment - current technologies**

Processes	Advantages	Disadvantages
Biodegradation (Punzi et al, 2015)	Rates of elimination of oxidisable substances about 90%	Low biodegradability of dyes
Coagulation-flocculation (Golob et al, 2005)	Elimination of insoluble dyes	Production of sludge blocking filter, increase toxicity
Adsorption on activated carbon (Rahman et al, 2011)	Suspended solids and organic substances well reduced	Cost of activated carbon, desorption difficult
Ozone treatment (Baban et al, 2003)	Good decolorization	No reduction of COD
Electrochemical processes (Thakur et al, 2009)	Capacity of adaption to different volumes and pollution loads	High cost as it requires external energy source
Reverse osmosis (Ozokia and Lib, 2002)	Removal of all mineral salts, hydrolyzes reactive dyes and chemical auxiliaries	Requires high pressure and more energy, membrane fouling, highly dependent on pH, difficult to reject undissociated organic compounds
Nanofiltration(Lau & Ismail, 2009)	Seperation of organic compounds of low molecular weight and divalent ions from monovalent salts	Membrane fouling
Ultrafiltration (Malaeb & Ayoub, 2011)	Low pressure	Insufficient quality of the treated wastewater, high cost

## 2.8 Advanced Oxidation Processes (AOPs)

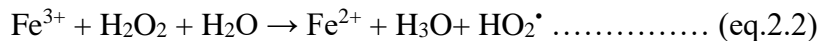
Advanced oxidation processes (AOPs) are the mechanisms of oxidation of organic compounds dissolved or spread in aquatic environments by catalytic, chemical and photochemical approaches. The aim of any AOPs is to generate hydroxyl radicals (OH•) as strong oxidant to destroy compound that cannot be oxidized by conventional oxidant (Gogate & Pandit, 2004). The hydroxyl radical has a strong oxidation capacity (standard potential = 2.73 V versus standard hydrogen electrode) (Torrades et al, 2011). The versatility of AOP is improved by the fact that they offer different possible ways for OH• radicals generation. Various AOPs are H<sub>2</sub>O<sub>2</sub>/Fe<sup>2+</sup> (Fenton), H<sub>2</sub>O<sub>2</sub>/UV/Fe<sup>2+</sup> (photo assisted Fenton), H<sub>2</sub>O<sub>2</sub>/UV, Ozone/H<sub>2</sub>O<sub>2</sub>, Ozone /UV/H<sub>2</sub>O<sub>2</sub>, Ozone/TiO<sub>2</sub>/H<sub>2</sub>O<sub>2</sub>, Ozone/electron-beam irradiation, Ozone/TiO<sub>2</sub>/Electron–beam irradiation, Ozone/ultra-sonics, Ozone/UV, etc. (Vogelpohl & Kim, 2004).

### 2.8.1 Fenton reaction

While the Fenton reaction has been known for more than a hundred years (Fenton, 1894), it has only been in 1968, first suggested as means for wastewater treatment (Bishop et al, 1968). The fundamental mechanism of the Fenton treatment process is chemical oxidation and coagulation of organic compounds by chemical processes. A combination of H<sub>2</sub>O<sub>2</sub> and Fe<sup>2+</sup> ions in acidic medium serves as a very potent oxidizing agent in the Fenton cycle. The classical mechanism is a simple redox reaction that oxidizes Fe<sup>2+</sup> to Fe<sup>3+</sup> and reduces H<sub>2</sub>O<sub>2</sub> to hydroxide ion and hydroxyl radical.



The optimal pH for the Fenton reaction is usually within the range 2 to 4 for the degradation of organic molecules. In the conventional Fenton reaction, carried out in the absence of light, the ferric ion produced in reaction (2.1) can be reduced back to ferrous ion by a second molecule of hydrogen peroxide:



This thermal reduction reaction (2.2) is much slower than the initial reaction (2.1). Although chemically very efficient for the removal of organic pollutants, the Fenton reaction slows down appreciably after the initial conversion of Fe<sup>2+</sup> to Fe<sup>3+</sup> and may require the addition

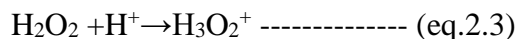
of relatively large amounts of  $\text{Fe}^{2+}$  in order to degrade the pollutant of interest. Another important limitation of the Fenton reaction is the formation of recalcitrant intermediates that inhibit the complete mineralization (Kim et al, 2004).

The high removal efficiencies from Fenton process can be explained by the formation of strong hydroxyl radical ( $\text{OH}^{\bullet}$ ) and  $\text{Fe}^{2+}$  to  $\text{Fe}^{3+}$  oxidation. The Fenton process has dual function of oxidation and coagulation as the  $\text{Fe}^{2+}$  and  $\text{Fe}^{3+}$  ions are coagulants. Iron is a highly abundant non-toxic element and hydrogen peroxide is easy to handle environmentally (Kim et al, 2004).

The parameters that influence Fenton process are pH, dosage of  $\text{Fe}^{2+}$ , dosage of  $\text{H}_2\text{O}_2$ , reaction time and temperature.

#### **a. Effect of pH**

For Fenton method, the optimum pH is in the range 2 to 4. The level of oxidation reduces as pH increases. This is because the iron precipitates as ferric hydroxide at higher (basic) pH levels, and in this form, iron catalytically decomposes  $\text{H}_2\text{O}_2$  into water and oxygen without creating hydroxyl radicals. At pH less than the optimum, the efficiency reduced due to the formation of oxonium ion (eq. 2.3) which stabilizes the performance of  $\text{H}_2\text{O}_2$  lacking the generation of hydroxyl radicals (Hassan and Hameed, 2011).



#### **b. Effect of iron concentration**

There is no evidence of hydroxyl radical formation on the addition of  $\text{H}_2\text{O}_2$  to the wastewater without the addition of iron. The optimum iron catalyst concentration based on the amount of pollutants found in wastewater. Owing to the greater amount of hydroxyl radicals produced, a higher concentration of  $\text{Fe}^{2+}$  ions will increase the rate of decomposition of organic contaminants. In general, as the iron content rises, the rate of contaminant removal accelerates until a stage is reached where additional iron renders it ineffective.

#### **c. Effect of $\text{H}_2\text{O}_2$**

As the dosage of  $\text{H}_2\text{O}_2$  increases, a gradual increase in COD occurs. An excessive concentration of  $\text{H}_2\text{O}_2$  would serve as a radical scavenger decreasing the oxidation rate, while an

unnecessarily low dosage of  $H_2O_2$  will lead to inadequate production of hydroxyl radicals, thereby reducing the oxidation rate (Collivignarelli et al, 2017). The unused portion of  $H_2O_2$  in the Fenton process causes COD contribution (Kang & Hwang, 2000) and hence excess amount more than the optimum dosage is not recommended. Also, the presence of  $H_2O_2$  make harmful effects to many of the microorganisms (Ito et al, 1998) and will affect the overall removal efficiency significantly, where Fenton oxidation is used as a pre-treatment to biological oxidation (Babuponnusami & Muthukumar, 2014).

#### **d. Effect of temperature**

Most studies related to Fenton-based experiments have been conducted at room temperature [Prima et al, 2008; Monteagudo et al, 2011]. The reason is due to the thermal decomposition of  $H_2O_2$  occurs at temperatures above  $50^\circ C$  [Zapata et al, 2010; Ortega-Liebana et al, 2012] and hence, the effectiveness of  $H_2O_2$  usage reduces. Practically, most industrial applications of the Fenton reagent occur at temperatures between  $20-40^\circ C$ . It is necessary to moderate the temperature not only for economic reasons but also for safety reasons. If the reaction temperature is expected to rise beyond  $40^\circ C$  due to exothermic nature, cooling is recommended.

#### **e. Effect of reaction time**

The time needed to complete a Fenton reaction will depend on the many variables discussed above, most notably catalyst dose and wastewater strength. For more complex or more concentrated wastes, the reaction may take several hours. In such cases, performing the reaction in steps may be more effective and safer.

Fenton process was used for the treatment of numerous wastewaters, including the decoloration and oxidation of textile effluents, pharmacy wastewater, landfill leachate disposal, phenol degradation, etc. (Garrido & Theng, 2010). The benefits of the Fenton process include the likelihood of complete mineralization of organic matter, reduction of organic loading in terms of chemical oxygen demand and removal of recalcitrant and hazardous contaminants, thereby allowing for more traditional biological treatment. Fenton process is also a fairly inexpensive system, because compared to many other AOPs, it needs no additional resources. The iron and hydrogen peroxide are both fairly cheap and safe. However, Fenton process

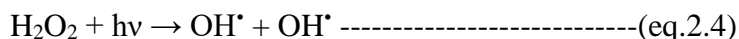
produces large volumes of ferric hydroxide sludge which involves additional separation and disposal processes (Kim et al, 2014). Such disadvantages are resolved by the Photo-Fenton process. The application of UV/solar radiation from an external energy source will reduce the amount of sludge produced (Pawar and Gawande, 2015; Collivignarelli et al, 2017).

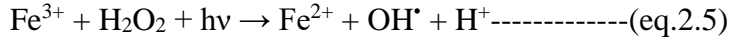
## 2.9 Photo-Fenton process

The photo-Fenton reaction was first investigated by atmospheric researchers to clarify natural mechanisms of hydrogen peroxide production and oxidation of several pollutants in atmospheric water droplets [Faust & Hoigne, 1990]. At the beginning of the 1990s, it was introduced in water treatment technology (Lipczynska-Kochany E, 1992; Sun & Pignatello, 1993; Ruppert et al, 1993). Later on, it was applied to effluent treatment containing many different contaminants, as pesticides (Hincapie et al, 2005; Malato et al, 2003), chlorophenols [Krutzler et al, 1999], natural phenolic pollutants [Gernjak et al, 2003], pharmaceuticals [Perez-Estrada et al, 2005; Arslan & Gurses, 2004], oil mill effluent (Gernjak et al, 2004) etc. Originally toxic waste water has been proven to lose its toxicity upon treatment by photo-Fenton process before total mineralisation has been achieved (Hincapie et al, 2005; Malato et al, 2003). Loss of toxicity is accompanied by an enhancement of biodegradability of the treated waste water (Sarria et al, 2002; Sarria et al, 2003). Consequently, photo-Fenton process and AOPs in general have been proposed as a pre-treatment to biological treatment (Esplugas & Ollis, 1997).

Photo-Fenton process is a Fenton process in presence of UV radiation. If solar light is used in place of UV, it will be solar photo Fenton process. Compared with traditional Fenton approach or photolysis, this process creates more hydroxyl radicals, thereby facilitating the oxidation of organic contaminants. The potential applicability of sunlight as UV light resource is an added advantage of this system as sunlight is naturally abundant and eco-friendly resource (Primo et al, 2008). Solar radiation will provide both UV light between 300–400 nm and visible light between 400–650 nm. ie. it will work for a wide range of wavelengths.

Degradation of contaminants in photo Fenton process may be due to direct photolysis and photo chemical reactions in the presence of light. In addition to Fenton reactions (2.1) and (2.2), additional amounts of hydroxyl radicals are produced from the direct photolysis of H<sub>2</sub>O<sub>2</sub>.





Reaction (2.1) occurs both in the presence and absence of light. The amount of hydroxyl radicals in reaction (2.2) is efficiently produced under acidic condition whereas reaction (2.4) is independent of pH. Reaction (2.5) is the ferric ions catalyzed decomposition of H<sub>2</sub>O<sub>2</sub> which is then followed by light induced formation of ferrous ions and per hydroxyl radicals.

Irradiation with light up to 580 nm leads to photo-reduction of dissolved ferric iron to ferrous iron (Bauer et al, 1999). The primary step is a ligand-to-metal charge-transfer (LMCT) reaction. Subsequently, intermediate complexes dissociate as shown in reaction (2.7) (Zepp et al, 1992).



The ligand can be any Lewis base able to form a complex with ferric ion (OH<sup>-</sup>, H<sub>2</sub>O, HO<sub>2</sub><sup>-</sup>, Cl<sup>-</sup>, R-COO<sup>-</sup>, R-OH, R-NH<sub>2</sub> etc.). Depending on the reacting ligand, the product may be a hydroxyl radical such as in Eq. (2.8) and (2.9) or another radical derivated from the ligand.



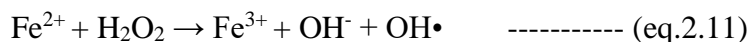
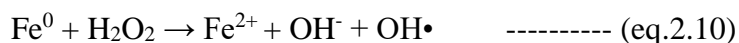
Depending on the ligand the ferric ion complex has different light absorption properties and reaction (2.7) takes place with different quantum yields and also at different wavelengths. Consequently, the pH plays a crucial role in the efficiency of the photo Fenton reaction, because it strongly influences which complexes are formed. Pignatello, 1992, postulated pH 2.8 as an optimum pH for photo-Fenton treatment, because at this pH, precipitation does not take place and the dominant iron species in solution is Fe(OH)<sup>2+</sup>, the most photoactive ferric iron–water complex.

Compared to Fenton process, the key benefit of the photo-Fenton process lies in the substantial reduction in reagent use and sludge output (Collivignarelli et al, 2017). Later studies have reported to solve the Fenton process's pitfalls by adding Nano Zero-Valent Iron (nZVI) along with H<sub>2</sub>O<sub>2</sub>.

## 2.10 Nano Zero-Valent Iron

"Nano" is a term used to describe a billionth of the unit that is mentioned. Nano-technology is related to the synthesis of nano-particles with the goal of achieving human welfares (Sunardi et al, 2017). Nano-technology use is growing due to its overall performance and cost-reduction capability. Nanoscale materials are used in nanotechnology to convert and detoxify contaminants by means of catalytic processes, chemical reduction etc. Nano zero-valent iron (nZVIs) can be highlighted between such nano-particles (Machado et al, 2013). These are nano-sized (< 100 nm) iron particles which, due to their larger specific surface area (about 30 times more than granular iron), can cause higher reaction rates. This property in turn allows a greater exposure of these particles to pollutants. Additionally, as particle size decreases and tends towards 10 nm, thermodynamic properties, such as work-function and free energy can increase reactivity. Also, nZVI has a superior pore penetration ability when compared to larger particulate zero valent iron (Taghizadeh et al, 2013). Nano iron is potentially benign to the environment and, ultimately, is mainly transformed into Fe<sub>3</sub>O<sub>4</sub> and Fe<sub>2</sub>O<sub>3</sub>, which are abundant on earth. Also, iron in oxidation state 0 is very unstable, thus very reactive and represents one of the strongest reducers (Turakhia et al, 2018).

Important reactions in the removal of organic material by H<sub>2</sub>O<sub>2</sub> in the presence of nZVI are:



### 2.10.1 nZVI synthesis

The most widely used techniques for synthesizing nZVIs consist of both chemical and physical methods. The physical methods are split into the bottom-up and top-down strategies. The bottom-up approach is based on creating nano particles by bringing molecules or atoms together through deposition, nucleation, precipitation etc. The top-down method involves

breaking down milli or macro-sized iron materials to produce fragments of a nano scale type. Besides these, sodium borohydride ( $\text{NaBH}_4$ ) reduction produces nZVIs, which is the most commonly used chemical process for its synthesis (Sun et al, 2007; Stefanuik et al., 2015). The most widely used iron precursor for the synthesis of nZVI is ferric chloride. While sodium borohydride has proven to be very effective in producing nZVI, it is dangerous, unsafe and costly. As well, the synthesized nZVI can easily corrode during storage, rendering it less efficient in pollutant degradation (Borja et al, 2015). According to Machado et al. (2013), physical and chemical methods face many problems and limitations, such as high prices and the need for specific and costly equipment for top-down and bottom-up methods, and health concerns linked to  $\text{NaBH}_4$  toxicity, propensity of formation of agglomerates, flammable hydrogen gas production during the process, reduced reactivity and reduced efficiency. These drawbacks provide an inducement to follow the concept of green chemistry, such as synthesizing nano particles from biological materials that can generate biologically sustainable nano particles that are energy intensive, economical and non-toxic. Synthesis of nZVIs from different biogenic substances such as bacteria, algae, fungi, plant extracts, biopolymers such as starch, amino acids, sugar, and glucose etc. is illustrated in some recent studies (Saif et al, 2016).

### **2.10.2 Biological synthesis of nZVI from plant leaf extracts**

Several researchers documented the biological synthesis of iron nano particles using various extracts of plant leaves. Some leaf extracts have high poly phenol content and high antioxidant ability, making them a promising reducing agent for the development of nZVIs. The iron (III) can be reduced by antioxidant compounds producing zero-valent iron (Nadagouda et al, 2010; Schrick et al, 2004; Machado et al, 2013). The plant extracts previously reported are *Mimosa Pudica* (Niraimathee et al, 2016), Green Tea (Shahwan et al, 2011), Henna leaf (Borade et al, 2011), *Parthenium hysterophorus* (Niyas Ahamed et al, 2016), *Murraya Koenigii* (Farrukh & Farrukh, 2015), *A.Bilimbi* (Rosli et al, 2018), *Eriobotrya Japonica* (Onal et al, 2019), *Caricaya Papaya* (Alorkpa et al, 2016), *Neem* (Prashanth & Krishnaiah, 2014), *Tulsi* (Garg & Sardana, 2016), *Guava* (Gayathri & Kiruba, 2014; Jeyasundari et al, 2017), *Amaranthus Dubius* (Harshiny et al, 2015), *Spinacia oleracea* (Turakhia et al, 2018) etc. Various iron compounds are mixed with different plant extracts of certain volumetric ratio to produce green iron nano particles. Iron compounds used in the synthesis of green iron nanoparticles are iron (III) chloride

(Shahwan et al, 2011), iron (II) sulfate (Onal et al, 2019] and iron (III) nitrate (Turakhia et al, 2018). The main advantages of this method are: i) less toxic reducing agent compared with borohydride; ii) prolonged reactivity due to the capping ability that the polyphenol extract matrix induces on the nZVIs (Nadagouda et al, 2010); iii) the utilization of natural products which are considered as wastes; and iv) the fact that the extracts can act as a nutrient source which enhance complementary biodegradation (Hoag et al, 2009; Nadagouda et al, 2010; Machado et al, 2013).

### **2.10.3 Characterization of nano particles**

Particle characterization is the method by which the particle size, form, charging properties, surface properties, microstructure, etc. are defined by specific techniques of characterization. Analysis by UV–Visible spectroscopy is one such method, in which the maximum absorption and wavelength of the synthesized particle can be measured to validate its reduction. Electron microscopy studies such as Scanning Electron Microscopy (SEM), and Transmission Electron Microscopy (TEM) are other important techniques of characterization. SEM will determine the morphology of the synthesized nano particles and the size (average diameter) of the particle will be given by TEM. Fourier- Transform Infrared Spectroscopy (FTIR) is yet another important technique for characterization and identification of a substance which provides information on rotational and vibrational modes of a molecule. The synthesized particles can be analysed under FTIR for the structural conformation (Harshiny et al, 2015).

### **2.11 Biodegradability Index (BI)**

Biodegradability of wastewater indicates the portion of the organic matter in the sample that can be easily removed by microorganisms (Tusseau-Vuillemin et al, 2003). Monitoring the biodegradability of effluent wastewater may provide a key element for pre-evaluation of the efficacy of further treatment processes as well as for assessing the degree of the potential pollution when the effluent is released to nearby watersheds. Biodegradable portion in wastewater is responsible for fast bacterial growth, which may lead to the deterioration of water quality in natural waters (Lai et al, 2011).

Biodegradability Index (BI) is the ratio of BOD<sub>5</sub> to COD of waste water. It can be taken as a measure of biological degradation. BI is the cutoff point between biodegradable and non-biodegradable waste (Abdallaa & Hammam, 2014; Singh et al, 2010). Wastewater with BI

between 0.4 and 0.8 can be considered as readily biodegradable (Metcalf & Eddy, 2003; Al-Momani et al, 2002; Bilinska et al, 2016).

## **2.12 Toxicity assessment**

Effluents from textile processes are highly variable in composition and contain a complex mixture of toxic substances such as dyes and pigments, salts, metals, biocides, surfactants and many other organic and inorganic components (Ellouze et al, 2012; Eremektar et al, 2007; Sharma et al, 2007). The main concern about the release of coloured effluents into the environment is their negative aesthetic impact and eutrophication in the receiving waters; however, many of the coloring and degradation products used in the textile industry have been found to be toxic and geno toxic (Verma, 2008; Tigini et al, 2011; Chhabra et al, 2015; Mountassir et al, 2013; Castro et al, 2019). Textile-generated dye effluents affect visibility and photosynthesis in water bodies and may also be harmful to aquatic life (Kim et al, 2004; Ramesh Babu et al, 2007; Andleeb et al, 2010). The toxicity bioassays therefore continue to be a valuable tool for determining the impact of these complex effluents on living organisms and finding out whether the treated effluents are suitable for disposal into inland waters. Different organisms such as bacteria, algae, fish, etc. may be used in bio-toxicity tests (Davis & Ford, 1992; Metcalf & Eddy, 2003).

## **2.13 Kinetic coefficients**

In the past, designs of biological wastewater treatment processes were based on the factual parameters, namely organic loading, hydraulic loading and detention time which are developed by experience. Presently, the design employs rational as well as empirical parameters based on biological kinetic constants and kinetic equations. The kinetic constants of a biological process are used to predict the effluent substrate and microorganism concentration. There are four kinetic coefficients, namely Biodegradation rate constant ( $k$ ), Half-velocity constant ( $K_s$ ), Yield coefficient ( $Y$ ) and Endogenous decay coefficient ( $k_d$ ).

The elementary equations that express the interconnection between micro-organisms growth and growth limiting substrate utilization in activated sludge processes are rooted on Monod model, which is regarded as the most widely used for finding out the bio-kinetic coefficients. In completely mixed and continuous flow reactor, determination of the bio-kinetic

constants is usually obtained by assembling data from pilot-scale or lab-scale experimental setups conducted at various sludge retention times (SRTs) and/or at various hydraulic retention times (HRTs) (Metcalf and Eddy, 2003).

## **2.14 Sludge volume index (SVI)**

The sludge volume index (SVI) was first introduced in 1934 by Mohlman. It is considered as the standard measure of the physical state of the sludge solids from activated sludge process. SVI is defined as the volume in millilitre occupied by one gram activated sludge after 30 minute settling of aerated mixed liquor. The reciprocal of SVI multiplied by 100 is sludge density index developed by Donaldson, which is also a sludge settleability measure in effluent treatment plant. The general adoption of SVI as a principal measure of the physical properties of sludge solids is specified by its widespread use both in research on waste treatment and in the operation of waste treatment facilities (Dick and Vesilind, 1969).

## **2.15 Moving Bed Biofilm Reactor (MBBR)**

Biological processes provide a cost effective and environmentally safe alternative to wastewater chemical treatment. Bio-film processes proved effective for the removal of organic carbon and nutrients. For these reasons, the process of Moving Bed Biofilm Reactor (MBBR) was developed in Norway at the Norwegian University of Science & Technology in the late 1980s and early 1990s (Ravichandran et al, 2012). The MBBR is a highly efficient biological treatment method built based on conventionally activated sludge process and bio filter process. It is a totally mixed and continuously run bio-film reactor, where biomass is stick on small carrier elements with a lighter density than water and is kept in motion along with a stream of water inside the reactor (Kermani et al, 2009). The basic feature of the MBBR is the specially built bio-film carrier materials, for which the structure, size and construction materials have been carefully considered to optimize performance. One of the key advantages of MBBR carrier materials is that they provide a wide protected area for colonizing bio-films. In the MBBR, surface area may be expanded by building carrier materials with a higher specific surface area, or by adding more carrier materials to the reactor. This provides flexibility for future improvements to the treatment capacity upgrades without requiring the construction of additional reactors. However, the volumetric fill fraction for carrier materials should only be increased to a

certain proportion of the volume of the reactor, otherwise mixing problems tend to arise and there is a limit to the potential for upgrading the surface area for a given volume of the reactor. Microorganisms did not occupy the whole carrier surface, but occur as independent small colonies (Kermani et al, 2009).

### **2.15.1 Advantages of moving bed biofilm process**

The MBBR is a complete mix, continuous flow through process which combines the advantage of fixed film and suspended growth processes. These advantages include:

1. High concentration of micro-organisms enabling rapid degradation rates of pollutants.
2. The reactor volume is totally mixed and consequently there is no stagnant or unused space.
3. As a bio-film system, there is no need for returning the settled sludge to the reactor even at short hydraulic retention times, which simplifies the design and control of effluent clarification
4. Easy to install and maintain, requiring only a tank of adequate size and aerators
5. Treatment performance of MBBRs is proportional to the installed bio-film surface area, so treatment upgrades can be performed by simply adding additional carrier materials to the same tank
6. Compact units with small size.
7. Increased treatment capacity.
8. Enhanced process stability.
9. No need of periodic backwashing.
10. Reduced sludge production and no problems with sludge bulking.

Carrier materials are constantly being moved upwards over the surface of the sieve. This action creates a scrubbing effect that prevents clogging in the reactor (Borkar et al, 2013).

Various factors affecting treatment of textile wastewater in MBBR are contact time, pH and filling ratio of carrier materials in the reactor.

## **2.16 Isolation, identification and inoculation of microorganisms in MBBR**

Microorganisms like bacteria would be isolated from the sludge of textile industry by serial plate dilution method, identified by 16 Svedberg unit ribosomal RNA (16S rRNA) method and inoculated on the bio-film carrier materials of MBBR to increase the efficiency of carrier materials in treating textile wastewater.

### **2.16.1 Serial plate dilution method**

Serial dilutions of suspension of bacteria are plated onto a suitable solid medium. Dilution technique affects overall counting process. The suspension is distributed over the surface of growth medium. The plates are then incubated to form colonies. Multiplication of a bacterium on solid media results in the development of a macroscopic colony visible to naked eye. Every colony is believed to originate from an independent viable cell. The cumulative number of colonies is counted and this number is multiplied by the dilution factor to determine the concentration of cells in the sample of origin. Counting plates would have at least 30-300 colonies.

### **2.16.2 16S rRNA method**

Recognition or identification is achieved by using the 16 S rRNA method. 16S rRNA gene sequencing has been developed as the standard method for bacterial species identification and taxonomic classification. The 16S rRNA sequencing acts as a fast and affordable alternative to phenotypic bacterial identification approaches. Comparison of the bacterial 16S rRNA sequence has been emerged as a valuable genetic technique. The hyper-variable regions of 16S rRNA gene sequences are valuable for bacterial recognition of species-specific signature sequences. It is also capable of reclassifying bacteria into completely new species, or even genera. The sequencing techniques can be used to describe new species that have never been successfully cultured in laboratories (Victoria et al, 2014).

## 2.17 Magnetic field effect in wastewater treatment

Approaches of magnetic fields have been reported for centuries (Colic & Morse, 1999). Michael Faraday presented the idea of induction in 1830, proving that electric current is actuated when a magnetic field flux is traversed by fluid ions or a conductive object. Although applications of magnetic field were swiftly explored to reinforce Faraday's postulation, there was a scarcity of interest from industrialists and researchers worldwide (Shepard et al, 1995). Faunce and Cabell, 1890, later modified the findings for water applications by establishing an electromagnetic device that would be inserted in the cooler system to treat hard water. Implementation of magnetic field in this area has changed markedly as a result of the input on this tool. The first commercial magnetic water treatment system was patented by Theo Vermeiren in Belgium, in 1958. According to Baker and Judd, 1996, the capacity of the magnetic field for water treatment applications remains a contentious topic, and the related phenomenon could not be clarified easily (Fathi et al, 2006). Magnetic applications in water treatment had been attempted by Russian scientists some decades ago (Chhatwani, 2011; Zaidi et al, 2014).

Magnetization has been applied to waste water treatment also. When the wastewater is exposed to magnetic fields, energy will be consumed by the organic molecules present. These energy-enhanced molecules were then entered into an excited state that was unstable in comparison with the ground condition; this improved chemical reaction rate and organic matter degradation has been increased (Mohammed et al, 2014).

Application of magnetic field has the power to enhance the physical characteristics of wastewater in terms of solid-liquid separation mainly through aggregation of colloidal particles. Some studies have reported that magnetized water has a higher conductivity, pH and osmotic pressure than non-magnetized water, and thus has better cell membrane permeability. This will affect the metabolic activities, mainly enzyme activity of bacteria. Again, induction of magnetic field reduced the surface tension in water and adsorbed the paramagnetic oxygen from the atmosphere which increased the oxygen concentration in waste water and thus the organic matter decomposition. These improvements led towards the increase in efficiency of the water treatment performances (Zaidi et al, 2014; Cheng et al, 2014; Yadollahpour et al, 2014).

After induction to a magnetic field, the particles can retain their magnetization properties for a time, which is called the magnetic memory. Higher magnetic memory enhanced the agglomeration of particles. However, strong or weak magnetic memory may hinder or boost the growth pattern of micro-organisms, especially bacteria, thereby affecting the efficiency of wastewater treatment system (Lebkowska et al, 2011). Various bacteria may have various levels of magnetic susceptibility. These bacteria can act differently, either inhibiting or reinforcing. Many can survive under a high magnetic field, while others can bear only low strength field (Zaidi et al, 2014). The correct magnetic field strength spectrum that can positively promote bacterial activity, thus improving the biodegradation cycle is subjective.

Single pass flow is more suitable for improving biological wastewater treatment. As discussed earlier, induced magnetic memory may positively or negatively influence the bacterial activity. Using single pass, the adverse effect can be reduced (Cai et al, 2009; Szczes et al, 2011). However, trial runs should be able to assist in the selection of the flow types.

## **2.18 Optimization of factors influencing the removal process**

The process of regulating the characteristics or inputs of a mathematical process or experiment to find the minimum or maximum result or output is called the optimization. The input consists of variables; the process or function is known as the cost function, objective function, or fitness function; and the output is the cost or fitness. If the process is an experiment, then the variables are physical inputs to the experiment. Conventional methods of studying a process by varying one variable, keeping other factors involved at constant levels does not render the combined effect of all the factors. This method is incapable and time consuming. Recently, many statistical experimental design methods have been engaged in chemical process optimization.

### **2.18.1 Response Surface Methodology (RSM)**

Design of experiments is a very supportive tool as it sets forth statistical models, which aid in realizing the interactions amidst the variables that have been optimized. Response Surface Methodology (RSM) is one of the experimental designing methods which can vanquish the drawbacks of conventional methods. It is useful for the modeling and analysis of programs in which a response of interest is influenced by several variables and the objective is the

optimization of this response. The method was established in 1951 by G.E.P Box and K.B Wilson. It inspects the relationships between various independent variables and one or more response variables. RSM designs allow us to assess interactions and even the quadratic effects and hence it will give an idea of the response surface shape. Response surface designs are types of designs for fitting response surface (Myers et al, 1989). Several phases are comprised in applying RSM as an optimization tool. These are, (i) selection of potent variables with their ranges, (ii) selection of experimental design and conducting of the experiments, (iii) formation of linear regression model equation based on the experimental outputs, (iv) model adequacy verification and (v) model representation through graphs and obtaining optimal conditions.

### **2.18.2 Experimental design**

Before applying the RSM methodology, it is first mandatory to choose an experimental design that will give the experimental runs to be conducted in the laboratory. Different designs which vary in their selection of experimental points and number of runs. Some of the commonly used experimental designs are (i) full three-level factorial design, (ii) central composite design (CCD) and (iii) Box–Behnken design (BBD).

In full three-level factorial design the factors are varied at three levels, -1, 0 and +1 representing minimum, mean and maximum respectively. The number of experiments required is  $3k$  where  $k$  is the number of variables. For more than two independent variables, large number of experiments is required, and hence, other designs are most suited.

Central composite design was introduced in place of full-level factorial design by Box and Wilson in 1951 (Box & Wilson, 1951). It consists of a two-level factorial design, a central point and an additional design in which experimental points are locating at a distance  $\alpha$  from the centre. The number of experimental runs required is  $2k + 2k + c_p$  where  $c_p$  is the number of replicates at the central point. The value of  $\alpha$  is taken as  $\alpha = \sqrt{k}$  (Montgomery, 2010). CCD gives high efficiency up to about five or six factors and then efficiency begins to decrease. CCD can be applied for optimization with a large number of factors if all the experiments can be carried out at the same time rather than one after the other (Massart et al, 1998).

The Box–Behnken design is created by joining two-level factorial design with incomplete block design as proposed by Box and Behnken in 1960 (Box & Behnken, 1960; Khuri & Cornell,

1996). In BBD all experimental points lie on a sphere of radius  $\sqrt{2}$ . Box–Behnken design does not constitute any experimental points at the vertices of the cubic region. It is helpful as testing at these points is expensive or impossible due to practical reasons (Montgomery, 2010). The number of experiments is calculated by the expression  $2k(k-1)+c_p$ , where  $k$  is the number of factors and  $c_p$  is the number of replicates at the central point (Bezerra et al, 2008). BBD requires fewer runs when compared to CCD making its application more economical.

### 2.18.3 Selection of model

In most RSM problems, since the form of the relationship between independent variables and response is unknown, suitable approximation between the factors and response is to be found. The most widely used approximating functions are polynomials. Since the interaction effect between various parameters cannot explain by a simple linear equation, the full quadratic second-order equation with interaction terms is generally used in RSM as given in equation (2.13).

$$Y = \beta_0 + \sum_{i=1}^n \beta_i x_i + \sum_{i=1}^n \beta_{ii} x_i^2 + \sum_{i \neq j=1}^n \beta_{ij} x_i x_j + \varepsilon \text{ ----- (2.13)}$$

where  $Y$  is the response,  $\beta_0$ ,  $\beta_i$ ,  $\beta_{ii}$  and  $\beta_{ij}$  are regression coefficients for intercept, linear, quadratic and interaction coefficients respectively,  $x_i$  and  $x_j$  are coded independent variables and  $\varepsilon$  is the residuals associated to the experiments. This model can anatomize the interactive effects between different independent variables and the critical point (maximum, minimum or saddle points). A second order polynomial equation can be derived as:

$$Y = \beta_0 + \beta_1 x_1 + \beta_2 x_2 + \beta_3 x_3 + \beta_{12} x_1 x_2 + \beta_{13} x_1 x_3 + \beta_{23} x_2 x_3 + \beta_{11} x_1^2 + \beta_{22} x_2^2 + \beta_{33} x_3^2 + \varepsilon \text{ ----- (2.14)}$$

### 2.18.4 Checking the model adequacy

After choosing a suitable mathematical model, the predictive capacity of the model should be validated. This is to assure that the model provides an adequate approximation to the true system. The overall efficiency of a model prediction is generally explained by coefficient of determination ( $R^2$ ).  $R^2$  is the ratio of regression sum of squares to total sum of squares, and it measures the total variation of predicted or model values from the mean. For a model with good prediction efficiency,  $R^2$  value should be close to 1. The model prediction efficiency, however, should not be assessed by  $R^2$  alone (Sarabia & Ortiz, 2009; Montgomery, 2010), since  $R^2$

increases with the increase in the number of variables, disregarding its statistical significance.  $R^2$  value and adjusted  $R^2$  value should be compared (Montgomery, 2010). When there is large difference between  $R^2$  and  $R^2$  adjusted values, it indicates that insignificant terms have been included in the model (Sarabia & Ortiz, 2009; Montgomery, 2010). The difference between the predicted and the actual value is termed as residual and it plays an important role in judging model adequacy. Another statistical term used for measuring the predictive ability of a model is the prediction error sum of squares (PRESS). It is a measure of how well the model for the experiment is likely to predict the response in a new experiment. Small values of PRESS are desirable (Montgomery, 2010). The value of  $R^2$  predicted also describes the prediction capability of the model for new responses which can be calculated from PRESS.  $R^2$  and  $R^2$  predicted should be in close agreement with each other (Myers et al, 2009).

The significance of each factor and interactions between each other is checked with the help of a Fisher test. The larger the magnitude of the F-value and correspondingly the smaller the p-value, the more significant are the corresponding model and the individual coefficients (Montgomery, 2010). If p-value is below 0.05, then the model is significant at 95% confidence interval.

### **2.18.5 Graphical representation of the model**

In RSM, response surface plots and contour plots can be used to visualize regression models. The response surface is a three dimensional graphical representation, whereas a contour plot is two dimensional representation. These graphical plots are useful to recognize the nature of the response at different factor levels. Plot shapes can vary such as circle, ellipse, hyperbolic etc. Circular or elliptical contour plots indicate the maximum and minimum points are located within the experimental region. With a hyperbolic system, the contour plot presents a saddle point – an inflexion point between relative minimums and maximums. It is neither a minimum nor a maximum point. As long as the contour plots are portions of circles or ellipses, it shows that the maximum point is outside the experimental region, while if they are straight lines, the variation of its level will not affect the system. When there are three or more factors, the plot visualization can only be done if the other variables are kept constant (A.T.Nair et al, 2014).

### **2.18.6 Response surface optimization**

Response surfaces can be anatomized to attain the minimum or maximum responses and the corresponding optimum conditions. With multiple responses, the optimum conditions can be met when all the parameters concurrently meet the desirable criteria. The optimum conditions can be obtained graphically by superimposing the contours of the response surfaces of the regression models in an overlay plot. Graphical optimization displays the area of feasible response values in the factor space and the regions that fit the optimization criteria (Ghafari et al, 2009). When there are more than three independent variables it will be difficult to find the conditions that simultaneously satisfy all the responses (Myers et al, 2009; Montgomery, 2010). Here the use of multi-criteria methodology can be followed. Desirability function is the mostly commonly used multi-criteria methodology. In this, each response is converted into an individual desirability function that varies over the range 0 to 1. If the response is at its target, then desirability function is 1, and if a response is outside an acceptable region, then the desirability functions is 0. The simultaneous optimization process is reduced to find the levels of factors that give the maximum overall desirability (Bezerra et al, 2008; Myers et al, 2009; Montgomery, 2010).

## **2.19 Previous studies on textile effluent treatment**

### **2.19.1 Physico-chemical conventional methods**

Patel & Vashi, (2015) discussed about the batch adsorption treatment of textile effluent using naturally produced adsorbents in order to remove BOD, COD, and color. The outcomes of different process parameters like dosage of adsorbent, contact time, temperature, agitator speed and pH are investigated. They remarked that activated neem leaf powder is one of the best adsorbent for textile wastewater treatment.

In another study by the same authors in 2010, the textile mill wastewater was treated with different dosages of coagulants like alum, ferrous sulphate and ferric sulphate at constant contact time and room temperature. Maximum percentage reduction corresponds to 80.2, 74.0 and 84.9% were obtained for COD, BOD and color respectively.

Rahman & Akter, (2016) monitors the possibility of chitin use for the removal of colour from textile effluent. The effects of various parameters such as adsorbent dose, pH and contact time were investigated for this work. 96% color removal has been reported at chitin dosage of 1.5 g in 25 mL solution, pH 5 and contact time 60 minutes.

Senthilkumar et al, (2018), discussed the usage of natural clay as adsorbent for the treatment of textile effluent. Various parameters, namely, adsorbent dose, pH, contact time, temperature and agitation speed has been studied for organic matter degradation. The appositeness of the various adsorption isotherms and kinetic models was investigated. The adsorption kinetics of effluent was found to comply with the pseudo-second-order equation based on the adsorption capacity on the solid phase. The equilibrium data have been explored using Freundlich and Langmuir isotherms. The adsorption data is found to be better fits into the Langmuir isotherm.

Sirianuntapiboon & Saengow, (2004) discussed the adsorption abilities of autoclaved and resting bio-sludge with various types of vat dyes. The adsorption efficiency of the bio-sludge improved with an increment in sludge age. Autoclaved bio-sludge exhibited the highest adsorption efficiency under acidic conditions while the resting bio-sludge exhibited the highest adsorption efficiency under weak alkaline or neutral conditions.

Powdered Activated Carbon (PAC) produced from date seeds was used as an adsorbent for textile effluent color removal. Temperature, pH, agitation speed, adsorbent dosage, particle size, contact time and color concentration were the variables. It was investigated that the mechanism of removal is found to be in good agreement with the Freundlich adsorption isotherm model than that with Langmuir model. The authors revealed that chemi-sorption may be predominant in the adsorption process (Rahman et al, 2017).

Textile effluent treatment through coagulation and adsorption using different dosages of alum, activated carbon, and their mixture was conducted by Aleem et al, (2020). A combination of alum and activated carbon found to be the most efficient treatment.

Another study by Eletta et al, (2018) focussed on sawdust as adsorbent for dye removal from textile effluent. The physico-chemical analysis of the effluent was accomplished before and after the adsorption studies. A maximum adsorption capacity of 98.5% was obtained at the

optimized conditions of 90 min, 275 rpm and 1.5 g for contact time, agitation speed and adsorbent dosage respectively. RSM has been used for optimization.

Dulman & Cucu-Man, (2009) entrenched the experimental surroundings for the removal of various textile dyes using beech wood sawdust as adsorbent. From the six dyes tested, the sorbent shows preference for three dyes: Direct Brown, Direct Brown 2 and Basic Blue 86. The type of dye, concentration, pH, contact time, and adsorbent dosage are affected the adsorption capacity. By comparative kinetic studies, the rate of sorption was found to satisfy with good correlation to pseudo-second-order kinetics. The parameters that characterize the sorption were determined on the basis of Langmuir isotherms. The preference of beech sawdust for dyes increases as follows: Basic Blue 86 < Direct Brown 2 < Direct Brown.

Another study reported the color removal from synthetic wastewater containing Vertigo Blue 49 (CI Blue 49) and Orange DNA13 (CI Orange 13) by adsorption onto CBBA waste material. The effectiveness of CBBA waste material in adsorbing reactive dyes from aqueous solutions was studied as a function of contact time, initial dye concentration and pH by batch experiments. pH 7 was more acceptable for color reduction from both dyes. Dye-stuff adsorption capacities of CBBA for Orange DNA13 and Vertigo Blue 49 were 4.54 and 13.51 mg dye per gram adsorbent, respectively (Dincer et al, 2007).

Smelcerovic et al, (2010) accomplished a study in which a natural waste adsorbent—ash was used for the reduction of a textile vat dye Ostanthren blue GCD. The ash obtained as a waste material during the burning of brown coal. The effect of ash quantity, pH, initial dye concentration and agitation time on adsorption was investigated. It was found that ash is a good adsorbent for textile effluent color removal.

Al-Degs et al, (2000) reported the degradation efficiency of activated carbon towards three highly used reactive dyes in the textile industry. In this work, the adsorption capacities for the anionic reactive dyes, namely; Remazol Reactive Black, Remazol Reactive Yellow and Remazol Reactive Red were studied. The study proved that activated carbon has high removal ability for the three reactive dyes and a signified ability for R. Yellow.

The experiments by Zaharia & Suteu (2013) are concentrated on the study of the effect of pH, adsorbent dosage, time of adsorption and temperature for organic pollutant removals and

color removal by the adsorbent, coal fly ash. The results showed high degree of COD reduction and decoloration at  $\text{pH} \leq 2$ .

.Rao & Rao (2006) in their experiment, adsorption studies were made in treating the solutions of methylene blue (M-B) and Congo red (CR) textile dyes by using flyash. Effects of adsorbent quantity, contact time, pH, initial effluent concentration and temperature have been studied and compared the results with those obtained by using activated carbon. Results proved that flyash is a powerful adsorbent in the treatment of textile effluent.

Mahmood et al, (2005) investigated that water hyacinth has the capability to reduce the pH of textile waste water from alkaline to neutral, COD and BOD reduction in the range of 40 to 70%, total solids with a maximum reduction of 50.64%. The reduction in pH further favoured microbial action to eliminate COD and BOD in effluent.

Shah et al, (2010) also investigated that water hyacinth has the capacity for degrading the dye effluent pollution. The authors reported significant decrease in the TDS, pH, conductivity, DO, hardness, BOD, COD, nitrate nitrogen and ammonium nitrogen in various concentrations of effluent.

Kannadasan et al, (2013) observed the capacity of a natural coagulant derived from a cactus species for turbidity removal from dye industry effluent. Other parameters such as pH as well as colour were also studied. High turbidity removal shows that cactus (*Opuntia*) and water hyacinth (*E.crassipes*) have the capacity to be used for textile effluent treatment applications.

Sabur et al, (2012) reported the textile effluent treatment using coagulants namely, polyaluminium chloride (PAC) and SAFI solutions as coagulants both individually and as their mixture at various ratios. It was seen that the combined effect of both the coagulants is more effective than the individual effect of coagulants for the organic load reduction from the effluent. Solanki et al, (2013) has also reported the use of PAC in textile effluent treatment and compared the results with alum. The study proved that PAC is better coagulant than alum as it is cost effective, forming less sludge and produces larger and more readily settleable flocs. .

Another paper by Bayramoglu et al, (2007) investigated the treatment of textile effluent by Electro-Coagulation (EC) process. Iron and aluminium electrode materials were used as

sacrificial electrode and showed that EC was quick and cost-effective method; devoured less material and generated less sludge, and pH of the medium was more balanced than chemical coagulation process for percentage removal efficiency of COD and turbidity from textile effluent.

Bazrafshan et al, (2014) investigated the efficiency of electro-coagulation process using aluminium electrodes in basic red 18 dye removal from aqueous solutions. Several important parameters, such as initial pH of solution, initial dye concentration, applied voltage, conductivity and reaction time were studied in an attempt to achieve higher removal efficiency. The electrochemical technique showed satisfactory dye removal efficiency and reliable performance in treating of basic red 18.

A study based on the investigation of the performance of a hybrid ultra-filtration/ electro-dialysis process for textile waste water has been reported by Lafi et al, (2018). The ultra-filtration process has been integrated with electro-dialysis and found that the hybrid process was capable of promoting the quality of the treated textile wastewater.

Another study aimed to assess and compare the performance of reverse osmosis (RO) and nanofiltration (NF) membranes in the treatment of biologically treated textile effluent in terms of COD removal, salinity reduction as well as permeate flux. The experimental results showed that the nano-filtration membrane showed better COD removal efficiency compared to the reverse osmosis membrane (Liu et al, 2011).

Uzal et al, (2009) studied the performances of three different nano-filtration (NF) (NF 270, NF 90 and NF 99) and two different reverse osmosis (RO) (HR 98 PP and CA 995 PE) membranes for textile effluent treatment. The permeate quality was acceptable for reuse in terms of color and COD from the tested RO and NF membranes. However, acceptable conductivity was observed for permeate from HR 98 PP RO and NF 90 membranes. On the other hand, in terms of the rate of permeation, NF 270 membrane performed better than the other NF and RO membranes.

Another study reported that ozonation is capable of decomposing the highly structured dye molecules into smaller ones which can be easily biodegraded in an activated sludge process (Lin & Lin, 1993). Meibodi et al, (2013) also reported the influence of ozone as well as electron

beam radiation on decolorization of dye effluents. It was established that ozonation after radiation will result high decolorization.

## **2.19.2 Biological conventional methods**

### **2.19.2.1 Dye degradation by fungus**

Mineralization of dyes has been investigated by white-rot fungi. *Neurospora crassa* and *Phanerochaete chrysosporium* have been used for the removal of color from textile effluent as reported in a study by Singh et al, (2015). *Bjerkandera adusta*, *Trametes versicolor*, *Aspergillus ochraceus*, species of *Pleurotus* and *Phlebia*, etc. have also been successfully attempted (Saratale et al, 2011). The application of this method is limited as it requires long hydraulic retention time for complete degradation (Khan et al, 2013).

### **2.19.2.2 Dye degradation by yeasts**

Azo dye decoloration by yeasts, namely *Candida zeylanoides* and *Candida oleophila* has been reported by Jafaria et al, (2014). Some ascomycete yeast species, such as *Debaryomyces polymorphus*, *Candida tropicalis*, and *Issatchenkia occidentalis*, have been tried to decolorize azo dyes. Some azo and reactive textile dyes can be decolorized by *Galactomyces geotrichum* MTCC 1360 (Saratale et al, 2011). *Trichosporon beigelii* has the ability to degrade Navy blue HER up to 100% as reported by Khan et al, (2013).

### **2.19.2.3 Dye degradation by algae and plants**

Studies reported that photosynthetic organisms namely algae and cyanobacteria are able to decompose azo dyes by an induced form of azoreductase (Sugasini et al, 2014). Biosorption is the mechanism used by algae. Several species of *Chlorella* and *Oscillatoria* have the ability to degrade azo dyes to their aromatic amines and to further convert the aromatic amines into simpler compounds (Saratale et al, 2011). In phyto remediation technique, plants such as *Sorghum vulgare*, *Brassica juncea*, and *Phaseolus mungo* have satisfactorily used for decolorization of textile effluents up to 57, 79% and 53%, respectively. Requirement of nutrient supplies are limited in this method. However, it requires large land area (Saratale et al, 2011).

#### **2.19.2.4 Dye degradation by bacteria**

*Bacillus subtilis*, *Bacillus cereus*, and *Aeromonas hydrophila* were investigated as strong remediating agents as reported by Wuhrmann et al, (1980). Recent research studies on cultures of *Pseudomonas luteola*, *Proteus mirabilis*, and *Pseudomonas* species have shown promising results for decomposition of azo dyes (Chang et al, 2001; Chen et al, 1999; Kalyani et al, 2008). Isolation of pure cultures from textile wastewater will be laborious and time-consuming. In addition, it is not easy to attain complete decolorization by a pure bacterial culture. Mixed bacterial cultures provide better results in decolorization and mineralization. They can efficiently degrade toxic aromatic amines (Saratale et al, 2011).

#### **2.19.3 Fenton treatment on textile effluent**

Papadopoulos et al, (2007) reported the efficiency of Fenton oxidation treatment to decompose the organic compounds present in textile effluent. The experimental results show that the oxidation process causes 45% COD removal and it takes place within four hours. Further reaction time does not increase the overall reduction in the COD removal.

Lin and Peng, (2008) investigated the COD and turbidity reduction of wastewater from a dyeing and finishing mill by using Fenton's treatment. pH, H<sub>2</sub>O<sub>2</sub> dosage, FeSO<sub>4</sub> dosage, reaction time and polyaluminum chloride (PAC) dosage are the independent variables. The Fenton's treatment was found to be effective with COD degradation efficiency of up to 80%.

Patil and Raut, (2014) studied the performance of Fenton's reagent in textile effluent treatment. They reported a color reduction of 98% at pH 3, H<sub>2</sub>O<sub>2</sub> 0.1mol/lit and FeSO<sub>4</sub> 0.2gm/lit, and a COD reduction of 85% at pH 3, H<sub>2</sub>O<sub>2</sub> 0.6mol/lit and FeSO<sub>4</sub> 1.2gm/lit.

Fenton's reagent is found to be a very efficient method for the decomposition of solution of many dyestuffs as reported by Ledakowicz et al, (2012). They proved the inhibition effect due to NaCl present in textile effluent on decolorization. The higher the content of NaCl present in textile effluent, the poorer the degree of decolorization.

Duarte et al, (2013), in their work, the treatment of textile wastewater by the heterogeneous Fenton-like process has been dealt with using a fixed-bed reactor charged with iron-impregnated activated carbon as a catalyst. It was found that the catalyst is stable upto five

successive runs without very much lose in activity. The iron leaching was also found to be very less, which is a crucial factor for the long-term use of catalyst. The operating variables namely contact time, dosage of catalyst and  $H_2O_2$ , temperature and pH, are optimized. The treatment attained 93.2% color reduction and 54.1% TOC reduction.

Meric et al, (2004) reported Fenton's oxidation process for the removal of Reactive Black 5 (RB5) from synthetic wastewater. The parameters, pH, temperature,  $H_2O_2$  dosage and  $FeSO_4$  dosage were optimized and 99% color and 71% COD reduction were reported when RB5 concentration was 100mg/l. The color reduction was above 99% and COD reduction was 84% at RB5 concentration of 200mg/l. Also, toxicity studies on this synthetic sample using daphnids and *Daphnia magna* have also been conducted.

#### **2.19.4 Photo Fenton treatment on textile effluent**

Rahmani et al, (2010) investigated the removal of two azo dyes, namely Acid Orange 7 and Reactive Black (RB5) by Fenton-like process. The use of  $Fe^{2+}$  and Ultra Violet (UV) light produced hydroxyl radicals.  $H_2O_2$  is not supplied externally in this experiment. High reduction of dyes was found in UV system at pH 11, while lower dye removal in the  $Fe^{2+}/UV$  system and  $Fe^{2+}$  system at pH 3. Dye removal was improved by increasing the contact time and the iron content. In the case of Acid Orange 7, color removal in the  $Fe^{2+}$  and  $Fe^{2+}/UV$  systems has improved while in the UV system it has decreased.

Sundararaman et al, (2009) have compared the efficiency of Fenton, photo Fenton, and sono Fenton processes in the removal of colour and COD for Reactive Yellow 16. Fenton, photo Fenton and sono Fenton process caused a COD and color reduction of 80% & 90%, 90% & 98%, and 82% & 95% respectively. The results evinced that the photo Fenton process is found to be more efficient than the other two processes.

The study of elimination of two azo reactive dyes, namely, Reactive Yellow 84 (RY84) and Reactive Red 120 (RR120) by photo-Fenton and Fenton-like oxidation were observed by Mariana N. et al, (2003). The effects of various operating parameters such as contact time, pH, hydrogen peroxide concentration and effect of light on the oxidation of the dye aqueous solutions have been observed. The results show that the solar photo Fenton process performed better than photo Fenton process using UV light in the color reduction of RY84 and RR120.

Dias Fernando et al, (2009) observed the degradation of reactive black 5 in a photo Fenton reactor. The color removal is completed in a short time of about 3 min reaction. TOC removal is strongly dependent on  $\text{Fe}^{2+}$  catalyst and dosage of  $\text{H}_2\text{O}_2$ . The maximum TOC reduction was 90% after a contact time of 90 minutes under the optimum conditions of  $\text{H}_2\text{O}_2$  dosage 280 mg/L and  $\text{Fe}^{2+}$  dosage 78 mg/L.

### **2.19.5 nZVI biological synthesis**

In a research conducted by Borja et al, (2015), nZVI was effectively synthesized from green tea extract. 0.1 M ferric chloride was used as an iron precursor.  $\text{FeCl}_3$ -to-green tea extract ratio, green tea extract flow rate and green tea-to-solvent ratio were optimized. Green tea-to-solvent ratio of 1:20, green tea extract flow rate of 8 mL / min and green tea extract ratio of 1:2 resulted in the maximum yield of nZVI.

*Azadiracta indica* (Neem) extract has been used for nZVI synthesis as reported by Pattanayak and Nayak, (2013). The synthesis was done by mixing 0.001M  $\text{FeCl}_3$  with leaf extract in 1:1 proportion with continuous stirring at 50 to 60°C. Colour change from light green to black and a decrease in pH, indicate the formation of nZVI. Synthesized particle characterization by SEM proved that the particle diameter was in the region of 50 to 100 nm.

Zero valent iron nano particles from *Spinacia oleracea* (spinach) leaf extract were synthesized in another experiment performed by Turakhia et al, (2018), by combining the extract with 0.1 M  $\text{FeCl}_3$  in 2:3 ratio with a continuous magnetic stirring at 10°C for 30 minutes. The presence of black colour has indicated the reduction of ferric ions to  $\text{Fe}^0$  ions. The fluid was then centrifuged at 5000 rpm for 10 minutes at 5°C to isolate the nano particles.

### **2.19.6 Use of nZVI in textile effluent treatment**

The nZVI synthesized from green tea leaf extract was used in a research performed by Ozkan et al, (2018), to eliminate organic matter and colour from textile wastewater. The nZVI was synthesised using green tea extract and 0.01 M  $\text{FeSO}_4 \cdot 7\text{H}_2\text{O}$  as iron precursor in 2:1 ratio at pH 3. When the wastewater sample was subjected to 5 ppm of nZVI, almost 80% color removal along with 18% TOC removal was observed at the end of 90 minutes, indicating its high removal efficiency.

El-Sayed et al, (2017), performed experiment on the use of zero-valent iron nanoparticles in degradation of azo dyes. The extract of guava leaves was used as the reducing agent for the nZVI synthesis. At room temperature with intense stirring, 10 mL extract was applied drop-wise to 50 mL 0.5 M  $\text{FeSO}_4 \cdot 7\text{H}_2\text{O}$ . The change of color from light yellow to black showed the formation of nZVI. Material analysis showed that the particle is in spherical shape and had an average size of 26 nm. This sample was then used to decompose Methyl Orange (MO) dye by batch techniques through adsorption, and to observe the effect of parameters such as pH, nZVI dose and initial dye concentration. Results proved that nZVI of dosage 0.3g/L was used to obtain adsorption capacity of 100% MO within 30 minutes.

In another study reported by Ozkan et al, (2017), pomegranate and green tea leaf extracts were used for nZVI synthesis, and a comparable analysis was done to decolorize textile wastewater. The extracts were prepared during 20 minutes by heating up 20g/ L of dry leaves at 80°C. The synthesis of iron nano particles was achieved by combining the prepared extract and 0.1M  $\text{FeSO}_4 \cdot 7\text{H}_2\text{O}$  in 1:1 volumetric ratio. Nano-particles from pomegranate extract (PG-ZVI) were smaller in size (10.1 nm) compared to the green tea iron nano-particles (GT-ZVI) with an average size of 43.8 nm. Reports showed that nano-particles with PG-ZVI worked better than nano particles with GT-ZVI. The improved efficiency of PG-ZVI nano-particles can be due to increased reactivity, with reduced particle size.

Luo et al, (2014) investigated the biological synthesis of nano zero valent iron using methanolic extract from grape leaf and ferrous chloride ( $\text{FeCl}_2$ ) precursor at room temperature in a ratio of 1:1. Particulate SEM characterisation revealed that the total particle size was 60 nm. The particles were then used for colour removal of Acid Orange II and 80% reduction was reported.

### **2.19.7 MBBR Process**

In a study reported by Yang et al, (2020), three different biological methods—a conventional activated sludge (CAS) system, membrane bioreactor (MBR), and moving bed biofilm reactor (MBBR)—were attempted for textile effluent treatment. The experimental findings proved that MBR was the most effective technology, of which the COD, TSS, and color reduction efficiency were 91%, 99.4%, and 80%, respectively, with a hydraulic retention time

(HRT) of 1.3 days. MBBR had a COD removal performance of 82% under HRT 1 day, while it is 83% under 2 days HRT for CAS. MBBR is an economically fit option for a textile effluent treatment plant as there is 68.4% saving in the capital cost and had the same operational expense as MBR. The environmental impact of MBBR system is also less.

### **2.19.8 Integrated process for textile wastewater treatment**

A hybrid experiment consisting of Moving-Bed Biofilm Reactors (MBBRs) with Polyurethane-Dyeing Sludge Carbonaceous Material (PU-DSCM) foam and chemical coagulation has been studied by Park et al, (2011). The MBBR pilot-scale design was constructed in sequence of two aerobic MBBRs. For biological treatment accompanied by chemical coagulation with  $\text{FeCl}_2$  or aluminium, each reactor was loaded with 20% (v/v) of Polyurethane-Dye Sludge Carbonaceous Material foam (PU-DSCM foam) inoculated with a white-red fungus, *Phanerochaete chrysosporium*. At MLSS concentration of 2900 mg/L attached to the PU-DSCM carrier and 48 hours of short hydraulic retention time (HRT), 79 percent of COD and 54 percent of colour were removed in the MBBR process.

A study on textile effluent was carried out with combined biological-adsorption system by Mirbagheri & Charkhestani, (2015). Extended aeration activated sludge process as biological and slow filtration as adsorption process has been used. In activated sludge system, COD and colour removal at different hydraulic retention times (HRT) were examined. Then the effluent of the biological system comes to the slow filtration pilot to remove the dye completely. In this stage, besides granular activated carbon (GAC) that is very high-cost adsorbent, saw dust and inorganic soils, such as kaolin and talc were tested simultaneously. It has been established that the combined biological-adsorption system could remove about 98.2, 95.6, 92.9, and 91.1% of COD by using GAC, kaolin, saw dust, and talc as an adsorbent, respectively.

Another work by Santos & Boaventura, (2015), evaluate the treatability of a simulated textile wastewater by simultaneously combining biological treatment and adsorption in a SBR (Sequencing Batch Reactor), but using a low-cost adsorbent, waste sludge (WS) from electroplating industry. Direct Blue 85 dye was used in the preparation of the synthetic wastewater. The simulated textile wastewater treatment in SBR exhibited a BOD removal of 53 to 79%, but colour removal was only 10 to 18%. The performance was significantly improved

by the addition of WS, with BOD removals above 91% and average colour removals of 60 to 69%.

Suhas et al, (2019), evaluated the efficacy of combined biological and AOPs treatment (Bio–AOP) using *Aeromonas hydrophila* SK16 and H<sub>2</sub>O<sub>2</sub> (4%) for the remediation of the textile dyes. Bio–AOP treatment showed 100% colour removal of Reactive Red 180 (RR 180), Reactive Black 5 (RB 5) and Remazol Red (RR), while 72% colour removal was observed in individual treatments. Combined treatment significantly reduced BOD and COD of RR180, RB5 and RR to 78 and 68%, 52 and 83% and 42 and 47%, respectively as compared to individual treatment. The Bio–AOP treatment is proved to be more efficient than an individual treatment of textile effluent.

In a study reported by Sosamony & Soloman, (2018), the textile effluent is treated by utilizing Moving Bed Bio-film Reactor (MBBR) with the magnetic field after improving the biodegradability by the solar photo-Fenton process. The carrier materials in MBBR were inoculated with azoarcus bacteria isolated from textile sludge. The fundamental parameters as pH, carrier material filling ratio and contact time were optimized utilizing Box Behnken factorial design. The MBBR process has the most extreme efficiency at pH 7, filling ratio of carrier materials 62% and a contact time 2.4 days. Under these optimum conditions 68.9% BOD and 80% COD are expelled. When the pre-treated wastewater was dealt with MBBR reactor under the influence of magnetic field, the efficiency of the treatment is additionally expanded, so 87.4% COD expulsion and 87% BOD elimination were accomplished at 12 mT attractive field power when exposure time was at 12 hrs.

Xiao-Bao, (2016), established a four-stage lab-scale treatment system [anaerobic MBBR-aerobic MBBR-ozonation-aerobic MBBR in series] to treat textile dyeing wastewater. The MBBRs were operated in a continuous horizontal flow mode. To determine the optimum operating conditions, the effect of hydraulic retention time (HRT) and ozonation time on pollutant removal were analysed by continuous and batch experiments. The optimum operating conditions were found to be 14 hour HRT for both anaerobic and no.1 aerobic MBBRs, 14 iminute ozonation time and 10 hour HRT for no.2 aerobic MBBR. Total removal efficiencies of COD, SS, ammonia and colour reported as 94.3%, 97.8%, 85.3% and 96.3%, respectively. The final effluent could meet the reuse requirements of textile industry.

Shin et al, (2006), scrutinized a combined process involving a Moving Bed Bio-film Reactor (MBBR) and chemical coagulation for textile wastewater treatment. The pilot scale MBBR system consists of three MBBRs (anaerobic, aerobic-1 and aerobic-2 in series), each reactor was filled with 20% (v/v) of polyurethane-activated carbon (PU-AC) carrier for biological treatment followed by chemical coagulation with  $\text{FeCl}_2$ . In the MBBR process, 85% of COD and 70% of colour were eliminated. The dyeing wastewater after biological treatments has been subjected to chemical coagulation. After coagulation with  $\text{FeCl}_2$ , 95% of COD and 97% of colour were removed. The combined process of MBBR and chemical coagulation has a promising potential for dyeing wastewater treatment.

In a study by Dong et al, (2014), an analysis of the performance of integrated moving bed biofilm reactors and a membrane filtration system for the treatment of azo dye reactive brilliant red containing wastewater was conducted. 35% of the bio-film carrier materials are put in the reactor for biological treatment. The average elimination efficiencies of COD, colour and SS were 85, 90 and 94% respectively. The combined MBBRs and membrane system was found to be successful in the treatment of wastewater containing azo dyes.

### **2.19.9 Use of magnetic field in wastewater treatment**

Carlesso et al, (2015), assessed ultra-filtration of a model textile effluent assisted by permanent magnetic field as an alternative to enhance the water permeability recovery. Ultra-filtration was performed in a tangential module and model solutions, composed of carboxy methyl cellulose (CMC) and sodium sulphate. The feed was permeated through poly-sulphone membrane with and without the presence of magnetic field of 0.41T, perpendicular to the membrane surface. Magnetic induction (MI) of feed solution was also observed by recirculation of the feed stream through the magnetic field for 3 hours. Though the feed concentration increase did not influence permeate flux, the presence of salt caused a high flux decline. Effective water permeability recovery was attained when the magnetic field was applied in the ultra-filtration process. The magnetic field application in ultra-filtration of CMC and sodium sulphate solutions has established to be a successful alternative for enhancing the permeability recovery.

In a study by Tetteh and Rathilal, (2020), a composite magnetic coagulant (CMC) containing ferromagnetic nano particle and alum was developed by mixing, drying and calcining for the remediation of textile effluent. Under optimum conditions of 45 mg/L dosage, pH 4 and 50 min. magnetic exposure time, 85% and 82% removal of turbidity and color respectively have been reported. CMC performed better than alum. Therefore, the application of super-paramagnetic nano-composite (CMC) in the water and wastewater settings is considered as an eco-friendly and effective coagulant for the remediation of heavy metals and their derivative pollutants.

Cheng et al, (2014), observed the influence of magnetic porous ceramsite material for coking effluent treatment. The authors proved that ammonia-nitrogen and COD removal in a bio-film reactor using magnetic porous ceramsite material have been improved by 15 to 20% than that without the magnetic material.

Liu et al, (2011), have presented a new method for the treatment of pulp and paper effluent by combining the magnetization with iron-based complex. The iron-based complex was formed by poly-carboxylic acid and ferric sulphate. Results showed that the surface tension and conductivity of the effluent have been greatly influenced after the magnetization process, and the maximum efficiency attained at magnetic intensity of 750 mT and water velocity of 4.4m/s. Besides, the properties of flocs formed by Fe-PA complex were improved by magnetization. The pre-treatment of pulp and paper effluent by magnetization enhanced the removal of COD and reduced about 7.7% of the Fe-PA complex dosage.

Mohammed et al, (2014), studied the impact of constant magnetic field as well as the integration of magnetic field with the adsorption by activated carbon for Palm oil mill wastewater treatment. This new method has been found to be a useful method for removing COD, colour and TSS from palm oil mill wastewater which has been biologically treated.

Geng et al, (2020), investigated the effect of 70 mT magnetic field on wastewater treatment capacity for activated sludge. The effect of the magnetic field on the microbial unigene and metabolic pathways in activated sludge was also investigated. At magnetic field 70 mT, higher pollutant removal in terms of Total Nitrogen was observed.

An improving effect due to the magnetic field on the growth of bacteria and metabolic behaviour in activated sludge was reported by Yavuz and Cebi, (2004), resulting in increased percentage removal of organic contaminants, mainly nitrogen containing pollutants. On exposure to magnetic field of 18 mT intensity, the biodegradation of a synthetic sewage inoculated with activated sludge collected from a municipal wastewater treatment plant increased up to 44 %.

Ji et al, (2010), have also reported the biological decomposition of organic pollutants in real municipal wastewater under magnetic field exposure. The experiment was conducted with varying parameters, biodegradation duration, magnetic field intensity, operating temperature and pH value. The results revealed that activated sludge acclimatization and organic pollutant biodegradation processes were stimulated under magnetic field of 20mT, resulted in a higher efficiency of wastewater treatment.

Liu et al, (2008), observed the anaerobic ammonium oxidizing capacity of anammox consortium boosted under the influence of magnetic field. An anaerobic Total Nitrogen removal in synthetic sewage with lab-cultivated anammox microbial population increased up to 50% at 75mT magnetic field intensity. The results established that an approximate 1/4 saving in cultivation time was achieved by using the magnetic system.

According to Wang et al, (2012), a static magnetic field induce of 48mT enhance the aerobic nitrifying granulation. The element analysis proved that the magnetic field application could promote the accumulation of iron compounds in the sludge. Also, the iron aggregation reduced the full granulation time from 41 to 25days by improving the setting properties of granules and stimulating the secretion of extracellular polymeric substances (EPS).

Niu et al, (2014), investigated the improvement of the cold adaptability by magnetic field at lower temperatures 4 to 15°C. They proved that the biodegradation of synthetic sewage with lab-cultivated sludge was increased at magnetic field intensity in the range 20 to 40 mT.

Tomska and Wolny, (2008), presented the effect of magnetic field of induction 40 mT on organic compounds removal. Moreover, the transformation of nitrogen compounds and the oxygen uptake rate of nitrifying microorganism in activated sludge wastewater treatment process were determined. The results proved that in the case of recirculation of synthetic sewage with

municipal sludge through 40 mT magnetic field, the biodegradation increased up to 16%. The nitrification rate has also been improved.

According to Zaidi et al (2014), presently, there is no confirmation findings on the suitable range of magnetic field intensity that can positively enhance the bacterial activity, thus enhancing the biodegradation process. Due to different response of different microbial species, preliminary laboratory experiments are crucial for each individual case, to find the efficient magnetic field strength and proper exposure time regarding the real biodegradation process factors.

#### **2.19.10 Response surface methodology in research**

Recently, wide attention has been received in research works for RSM. Examples include, pulp and paper mill effluent treatment by coagulation (Mosaddeghi et al, 2020), saline wastewater treatment (Darvishmotevalli et al, 2019), organic removal from milk processing wastewater (Abdulgader et al, 2020), hospital wastewater treatment by electro-coagulation (Murdani et al, 2018), dye removal using coagulation/flocculation (Moghaddam et al, 2010), ammonia nitrogen removal from fresh leachate using combination of ultrasound and ultraviolet (Zarghi et al, 2020), dye mineralisation by UV/H<sub>2</sub>O<sub>2</sub> process (Olya et al, 2008), Fenton's peroxidation on the removal of organic pollutants from olive oil mill wastewater (Ahmadi et al 2005) etc.

# CHAPTER 3

## METHODOLOGY

### 3.1 Sampling of original textile wastewater

The samples of original untreated textile wastewater were collected from a Textile industry situated in Thrissur, Kerala. The samples were collected for 6 months (November, 2016 to April, 2017) with 5 days interval. For each day's sampling, 5 samples of volume 1L each were collected at 1-hour interval to make a representative composite sample. The collected wastewater samples were stored at 4°C and analyzed to determine the characteristics.

### 3.2 Analytical methods

The parameters pH, BOD, COD, conductivity, color, etc. were analyzed as per procedures in standard methods (APHA, 1971). The methods/instruments used for analysis are listed below in Table 3.1.

**Table 3.1 Methods/instruments used for analysis**

Parameter	Instrument	Method
pH	Water Quality Analyser	Electrometric method
BOD	BOD incubator	Dissolved oxygen determination by Winkler method
COD	Reflux Apparatus	Potassium dichromate reflux method
Color	UV- Visible Spectrophotometer	Spectrophotometry
Chloride	Titration	Mohr method
Turbidity	Nephelometric Turbidimeter	Nephelometric method
Sulphide	Titration	Iodometric method
Alkalinity	Titration	Double end point titration method

### 3.3 Treatment of effluent using MBBR with textile sludge

#### 3.3.1 Experimental setup of MBBR

The schematic diagram of experimental setup for the study is shown in Fig.3.1.

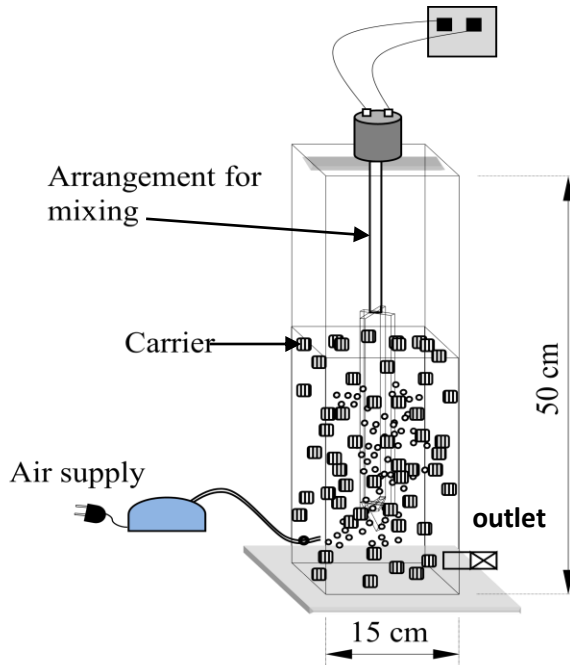


**Fig. 3.1 Schematic diagram of experimental set-up of MBBR**

A reactor made of acrylic glass reactor with a total capacity of 11.25 litres was used in the study. The size of the reactor was 15 X 15 cm with height 50 cm. 70% of volume, ie. 35cm has been taken as the effective depth of wastewater inside the reactor. Carrier materials of various percentages by volume have been filled inside the reactor. At the time of each testing the volume of wastewater inside the reactor was kept as 7.875 litres. Aerators were provided for aeration from the bottom side of the reactor. Aeration rating of 3 l/min maintained inside the reactor to make the carrier elements with wastewater in circulation and to attain the necessary DO concentration. Acrylic sheet paddles was connected with a motor and kept at the middle to stir the carrier elements with the wastewater. These paddles were rotated at speed 30 rpm.

### 3.3.2 Carrier materials

Moving bed biofilm carrier materials (MBBC) were prepared using corrugated cylinders made of PVC with 1.5 cm as the internal diameter, 2 cm as the external diameter and 1.4 cm as the height as shown in Fig. 3.2. These carrier elements have been used for attaching microorganisms which have  $0.94\text{g/cm}^3$  density and  $350\text{m}^2/\text{m}^3$  specific surface area.



**Fig 3.2 carrier elements**

### 3.3.3 Seeding and attachment of microorganisms

Biological sludge from aeration tank of textile industry was collected and diluted with tap water to increase the sludge volume. Nutrients namely glucose ( $\text{O}(\text{CHOH})_4\text{CH}_2\text{OH} = 3\text{g/L}$ ) and urea ( $\text{NH}_2\text{CONH}_2 = 4\text{g/L}$ ) were added into the sludge to enhance the growth of microorganism and its pH was adjusted to 7. Microorganisms were allowed to grow for a week at room temperature. Then carrier materials were introduced and air flow was set at 3 litres/min.

Required volume percentage of carrier materials and wastewater were introduced in the reactor. Sufficient fluidization was attained for the bio film carrier materials by means of aeration provided from the bottom side of the reactor. The MBBR process was conducted with varying pH, contact time and filling ratio of carrier materials. The responses, namely percentage COD and BOD removals have been measured. The experiments were done by changing the parameters one at a time, keeping the others constant.

## **3.4 Treatment of textile effluent using MBBR with bacteria inoculated carriers**

### **3.4.1 Isolation, identification and inoculation of bacteria**

Biological sludge was collected from the aeration tank of Textile industry. This sludge was used for isolating the microorganisms. Isolation, Identification and Inoculation were done in Department of Microbiology, Kerala Agriculture University, Vellanikkara.

#### **3.4.1.1 Isolation**

Serial dilution plate count method was used for the isolation of bacteria. Nutrient Agar media was prepared first. 10 ml of each sample was mixed with 90 ml sterile water blank in a conical flask ( $10^{-1}$  dilution). 1 ml from this dilution has been pipetted from the conical flask to 9 ml sterile water blank in the test tube ( $10^{-2}$  dilution). This process was repeated till  $10^{-6}$  dilutions obtained. 1 ml of suspension was pipetted from  $10^{-6}$  dilutions, to sterile, petri-dishes separately. The melted and cooled media were poured in respective plates. The suspension was mixed with media by rotating the petri-dishes in clockwise and anti-clockwise direction. The plates were allowed to solidify, inverted, incubated at  $28\pm 2^{\circ}\text{C}$  for 24 to 48 hours and observed for single isolated colonies of respective microorganism (Cappuccino et al.,1992).

#### **3.4.1.2 Identification**

Identification was done by 16 S rRNA method (16 Svedberg unit Ribosomal RNA).

##### **1<sup>st</sup> step - Polymerase Chain Reaction Amplification (PCR Amplification)**

23 $\mu\text{l}$  master mix containing 12.5 $\mu\text{l}$  Emerald mix, 1 $\mu\text{l}$  Primer and 9.5 $\mu\text{l}$  distilled water was prepared and it was mixed in a short spin at 10000 rpm for 2 to 3 seconds. Culture was prepared by adding one touch from streaked culture to 10 $\mu\text{l}$  sterilized distilled water. Denaturation of the culture was done at  $98^{\circ}\text{C}$  in 2 minutes in a Master cycler Gradient which was then centrifuged at 10000 rpm for 2 minutes. Supernatant of the culture was taken out from the centrifuge and 2 $\mu\text{l}$  of supernatant was mixed with 23 $\mu\text{l}$  of master mix. The mixture prepared above was again mixed in a short spin at 10000 rpm for about 2 to 3 seconds. 25 $\mu\text{l}$  of master

mix was kept as blank. 34 cycles were repeated (Claudia et al., 2001). After PCR Amplification, sample was taken out and Agarose Gel Electrophoresis was done.

### **2<sup>nd</sup> step - Agarose Gel Electrophoresis**

1% Agarose was prepared by adding 1 g Agarose to 98ml distilled water and 2ml loading buffer (TAE). The prepared Agarose was taken in a conical flask and heated for proper mixing and then cooled. 1 $\mu$ l Erythro Bromide (ETBr) was added to the conical flask and was thoroughly mixed. The mixture prepared above was poured in a stacking tray with comb. After solidifying, the gel was formed and the comb was removed from the stacking tray. Stacking tray with gel was placed in a buffer tank which contain loading buffer (TAE). 5 $\mu$ l 1kb DNA ladder (marker), 2 $\mu$ l blank and 2 $\mu$ l sample were kept in corresponding well in stacking tray. 100V current was applied. DNA of the sample would migrate to positively charged region. After that gel was transferred from stacking tray to UV transilluminator. DNA appeared as orange fluorescent band in the transilluminator (Claudia et al, 2001).

#### **3.4.1.3 Inoculation**

The colonies of identified bacteria was transferred to peptone nutrient medium and allowed to grow and multiply for 24 hrs at room temperature. Then the carrier materials were kept in the bacterial culture for 12 hrs, dried in the air and filled inside the MBBR reactor.

This MBBR with bacteria inoculated on carrier materials as discussed previously was termed as Modified MBBR. The remaining procedure was as explained in section 3.3.

### **3.5 Pretreatment of textile effluent before biological treatment**

As the biodegradability of textile effluent is low, steps are taken to improve the biodegradability by pre-treating with advanced oxidation processes before biological treatment. The AOPs considered are

- i) Homogeneous Photo Fenton process (HPF)
- ii) Homogeneous Solar Photo Fenton process (HSPF)
- iii) Advanced Photo Fenton process (APF)
- iv) Advanced Solar Photo Fenton process (ASPF)

After selecting suitable pretreatments, biological treatment, Moving bed Biofilm Reactor (MBBR) has been tried for making the effluent safe for disposal.

### 3.6 Homogeneous photo-Fenton process (HPF)

#### 3.6.1 Chemicals

The chemicals used in the experiment include 1N  $\text{H}_2\text{SO}_4$  or NaOH to adjust the pH,  $\text{FeSO}_4$  and 30%  $\text{H}_2\text{O}_2$  to generate hydroxide radicals.

#### 3.6.2 Experimental procedure

The schematic diagram of the experimental set-up of UV photo-Fenton reactor is shown in Fig.3.3. 11watts UV lamp was used as source of radiation in the experiment. The set up was covered with aluminium foil in order to avoid the escape of UV light and also to prevent the radiation from UV light.

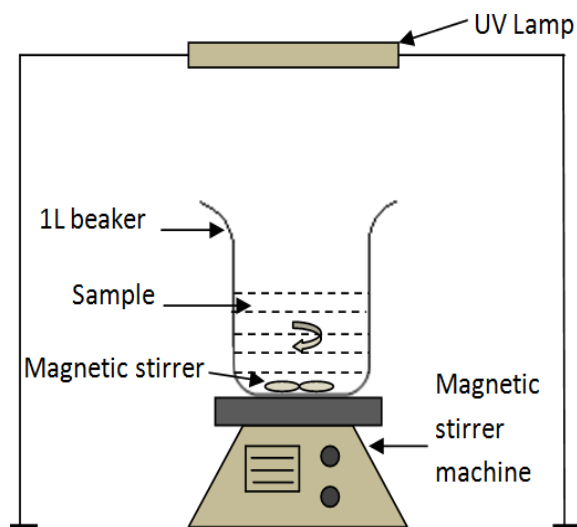


**Fig.3.3 Schematic diagram of UV photo-Fenton reactor**

Before starting the Fenton experiment, the pH of the wastewater sample was adjusted to desired range using 1N  $\text{H}_2\text{SO}_4$  or NaOH. After adding pre-determined amount of  $\text{H}_2\text{O}_2$  and  $\text{FeSO}_4$  into the wastewater sample of 1 litre volume, the solution was stirred using magnetic stirrer to ensure homogenous mixing for 30 minutes. To stop the reaction of  $\text{H}_2\text{O}_2$ , the pH was raised to 12 using NaOH. Large amounts of small flocs have been produced by the oxidation

process that contained iron hydroxide as a precipitated by-product, which is required to be discarded. Calcium hydroxide was used in flocculation step as coagulant (Pawar and Gawande, 2015). After coagulation, flocculation and sedimentation, the COD of the supernatant was measured. The parameters which are varied during the experimentation are pH,  $\text{Fe}^{2+}$  dosage and  $\text{H}_2\text{O}_2$  dosage.

### **3.6.3 Design of experiments**

The software Minitab version 16 was used to design the number of experiments to be performed, analyze the experimental data and assess the experimental results. In order to investigate the effects of influencing factors and to obtain the optimum condition, Response Surface Methodology (RSM) was used. The Box-Behnken design (BBD), an experimental design for RSM is a useful statistical tool for the optimization of different processes. In this method, the leading objective is to optimize the response surface that is influenced by different parameters. RSM also points out the interrelation between the response variable and the input parameters (Zaidi et al, 2016).

All the experimental analysis and optimization are done using Box-Behnken Design in this thesis work.

## **3.7 Homogeneous solar photo Fenton process (HSPF)**

### **3.7.1 Chemicals**

Same as in section 3.6.

### **3.7.2 Experimental procedure**

The solar photo-Fenton experiment was carried out in a glass beaker of capacity 1 litre. 1N  $\text{H}_2\text{SO}_4$  or NaOH was used for adjusting the pH value of the sample. The experimental setup was placed under the sunlight and given volume of  $\text{FeSO}_4 \cdot 7\text{H}_2\text{O}$  and  $\text{H}_2\text{O}_2$  was added. The reaction time started with the addition of  $\text{H}_2\text{O}_2$  and the reagents has to be thoroughly mixed. The solar light intensity was measured using light meter.

The factors influencing the photo-Fenton reaction are pH,  $\text{Fe}^{2+}$  concentration and  $\text{H}_2\text{O}_2$  concentration and optimization of parameters for maximum COD removal has been studied using BBD in RSM.

## 3.8 Synthesis of nano zero valent iron (nZVI)

### 3.8.1 Preparation of leaf extract

For the biological synthesis of nano zero-valent iron, aqueous extract of *Amaranthus dubius* leaves were used. The collected leaves were first washed thoroughly in deionized water to remove the dust and dirt present on its surface. The leaves were then chopped into small pieces. For the preparation of extract, 20g leaves were weighed and placed in 250 mL beakers. 100 mL distilled water was added to the beaker and it was boiled for 45 minutes at 50°C. The beakers were then allowed to cool. After cooling, it was filtered using the Whatmann filter paper to separate the leaf extract and set aside at 4°C for further use (Harshiny et al, 2015).

### 3.8.2 Synthesis of nano zero valent iron

For the synthesis of nano zero-valent iron particles, the prepared leaf extract was added drop wise to 0.1 molar ferric chloride solution in the ratio 1:1. The pH of the leaf extract should be adjusted to 6 using 0.1 N HCl and 0.1 N NaOH. The extract is added to ferric chloride solution with constant stirring. On addition of the extract to ferric chloride solution, the yellowish green solution turns blackish green, indicating the formation of Fe<sup>0</sup> particles as black precipitate. The resulting mixture was then centrifuged at 5000 rpm for obtaining the nano particles. It was then washed with ethanol and dried in hot air oven at 60°C for 120 min.



Fig.3.4 nZVI powder.

Fig.3.4 showed the nZVI stored in sealed bottles under dry conditions.

### **3.8.3 Characterization techniques**

The absorbance spectrum of the samples was measured using a UV- Spectrophotometer. The functional groups of the nano particles were recorded by Fourier Transform Infrared (FTIR) spectrophotometer. The size of the nano particles were analyzed using Transmission Electron Microscope (TEM) and the surface area was analyzed using Brunauer-Emmett-Teller (BET) analysis.

## **3.9 Advanced photo Fenton process (APF)**

### **3.9.1 Chemicals**

The chemicals used in the experiment include 1N H<sub>2</sub>SO<sub>4</sub> or NaOH to adjust the pH, nZVI and 30% H<sub>2</sub>O<sub>2</sub> to generate hydroxide radicals.

### **3.9.2 Experimental procedure**

Same as described in section 3.6.2 except that Fe<sup>2+</sup> ions are replaced by nZVI.

## **3.10 Advanced solar photo Fenton process (ASPF)**

### **3.10.1 Chemicals**

Same as described in section 3.9.1

### **3.10.2 Experimental procedure**

Same as described in section 3.6.2 except that Fe<sup>2+</sup> ions are replaced by nZVI.

## **3.11 Reusability of nZVI and iron leachability**

Reusability of nVI was studied for effluent after APF and ASPF processes under optimum conditions. After the first cycle of treatment, the suspension solution was centrifuged to obtain a precipitate to separate the catalyst from the reaction solution, which was washed with DI water and vacuum-dried at 40 ± 5 °C overnight (Bao et al, 2019). The regenerated nZVI has been introduced to the effluent sample with the same COD value for second cycle of treatment.

The same procedure is repeated for successive cycles of experiment and effluent samples are measured for COD reduction. The amount of leached iron ions has also been noted after each cycle.

### 3.12 Determination of kinetic coefficients k and K<sub>s</sub>

The raw effluent with COD concentration S<sub>0</sub> as well as the effluent after all the four pre-treatment processes, HPF, HSPF, APF and ASPF have been run for various hydraulic detention time (θ) and observed the effluent COD concentration (S) and MLSS (X).

Let S<sub>0</sub> be the raw influent concentration, S the effluent concentration, θ the hydraulic detention time and X concentration of microorganism.

A mass balance for the mass of substrate in the complete mix reactor at steady state conditions results in the following expression.

$$(S_0 - S) - \frac{\theta(kXS)}{(K_s+S)} = 0 \text{ ----- (eq.3.1)}$$

Rearranging,

$$\frac{(X\theta)}{(S_0-S)} = \frac{1}{S} \frac{K_s}{k} + \frac{1}{k} \text{ ----- (eq.3.2) which is a straight line equation.}$$

A graph with (Xθ)/(S<sub>0</sub>-S) in y-axis and (1/S) in x-axis will be a straight line with (K<sub>s</sub>/k) as slope and (1/k) as y-intercept (Metcalf & Eddy, 2003).

A graph is drawn with 1/S in x-axis and (Xθ)/(S<sub>0</sub>-S) in y-axis which will be a straight line with K<sub>s</sub>/k as slope and 1/k as y-intercept. K<sub>s</sub> and k can thus be determined.

### 3.13 Calculation of sludge volume index (SVI)

The most common method to evaluate how well a sludge settles and compacts is to measure the SVI. This is the volume in millilitre occupied by one gram of sludge after settling the aerated sludge for 30 minutes (Willen, 1995). SVI is used to describe the settling characteristics of sludge in the aeration tank in Activated Sludge Process. It is a process control parameter to determine the recycle rate of sludge. It was instigated by Mohlman in 1934, and has become the basic measure of the physical characteristics of activated sludge processes.

$$\text{SVI (mL/g)} = \frac{\{\text{settled sludge volume (mL/L)} \times 1000\}}{\{\text{Mixed Liquor Suspended Solids (MLSS)}\}(\text{mg/L})} \text{----- (eq.3.3)}$$

### 3.14 Bioassay experiment for toxicity assessment

Toxicity tests were done for raw and treated effluents. The static nonrenewal bioassay method was employed for this test [APHA, 2005]. Static bioassay conducted as a short term toxicity test. To evaluate the toxicity, death of the organisms was the criterion. The static bioassay tests were conducted at room temperature using *Poecilia libestes reticulate* (Guppy fish) as the test organism. The fish were bought up from a local fish supplier of Trichur City (Kerala State) for experimental purpose. The length of fish ranged from 1.0 to 1.3 cm and weight 0.18 to 0.26 gm. Only healthy fish were selected for toxicity testing experiments. The bioassay studies were carried out in containers of 10 litre capacity with ten fish in each container. Similar control was run parallel with dilution water (well water) only. Previously cleaned containers were washed with 20ppm of potassium permanganate. Various dilutions of effluents were prepared by mixing with well water. Toxicity has to be assessed for five effluents, one raw effluent and the other 4 are effluent after treatment by HPF, HSPF, APF and ASPF processes. Pilot experiments were conducted to choose the mortality range between 10% and 90%. Based on the pilot experiments, the dilutions were fixed as 2 to 10% for raw effluent and 30 to 100% for treated effluent to determine the toxicity for 24 hrs and 96 hrs. 2% dilution means 2% effluent gets mixed with 98% well water. Aeration is done by an aerator pump. The control group was kept in well water without addition of effluent. The experiments were conducted under the natural solar light with no food being given to the fish before 24 hours of the experiment and during the experiment. The results of fish survival were recorded after 24 hrs and 96 hrs. The results of experiments were acceptable only in cases where fish in the control were observed to have a mortality rate of less than 10%. The graphs with %survival versus %dilution for untreated textile effluent and textile effluent after HPF, HSPF, APF, and ASPF processes are plotted to find the value of LC<sub>50</sub> which is the concentration at which 50% survival of fish possible.

### 3.15 Pretreatments selected

The pretreatments were selected based on Biodegradability Index (BI). BI is the ratio of BOD to COD of the effluent.  $BI \geq 0.40$  means the effluent can be readily decomposed by

biological treatment. In addition, the value of kinetic coefficients,  $k$  and  $K_s$ , and SVI has been taken as the norms for checking the biodegradability enhancement.

### **3.16 Variation of BI with time**

The selected pretreatments have been varied with respect to time in order to find whether the BI value has reached 0.40 earlier. After pretreating with suitable pretreatment, the effluent was subjected to treatment through MBBR with bacteria inoculated carriers.

### **3.17 Experimental design of MBBR**

Experimental set up and inoculation of carrier materials are same as given in section 3.4. Various factors affecting treatment of textile wastewater in MBBR were contact time, pH and filling ratio of carriers in empty reactor. The effluent COD and BOD were measured. Optimization of varying parameters was done by Box Behnken method using Minitab software. Based on preliminary studies, the range of parameters has been fixed as pH from 6 to 9, contact time from 1 to 3 days and filling ratio of carrier materials from 40% to 80%. The oxygen transfer efficiency is adversely affected at filling ratio of carrier materials less than 40%. If filling ratio is greater than 80%, then sufficient mixing will not be obtained.

### **3.18 MBBR under magnetic field**

Magnetic field was applied to the wastewater in the MBBR reactor to determine its influence on the process. Magnetic field was created by winding copper wires around the reactor and passing DC current through it. The intensity of magnetic field was calculated using Biot-savart law which is given by

$$B = \mu N I / L \quad \text{----- (eq.3.4) (Philips \& Sanny, 2008)}$$

Where  $B$  is the field intensity in Tesla (T),  $\mu$  is the magnetic permeability of air,  $N$  is the no. of turns of coil,  $I$  is the current passing through the coil in Ampere (A) and  $L$  is the length of coil.

The schematic diagram of the experimental setup for MBBR with magnetic field was as in fig.3.5.

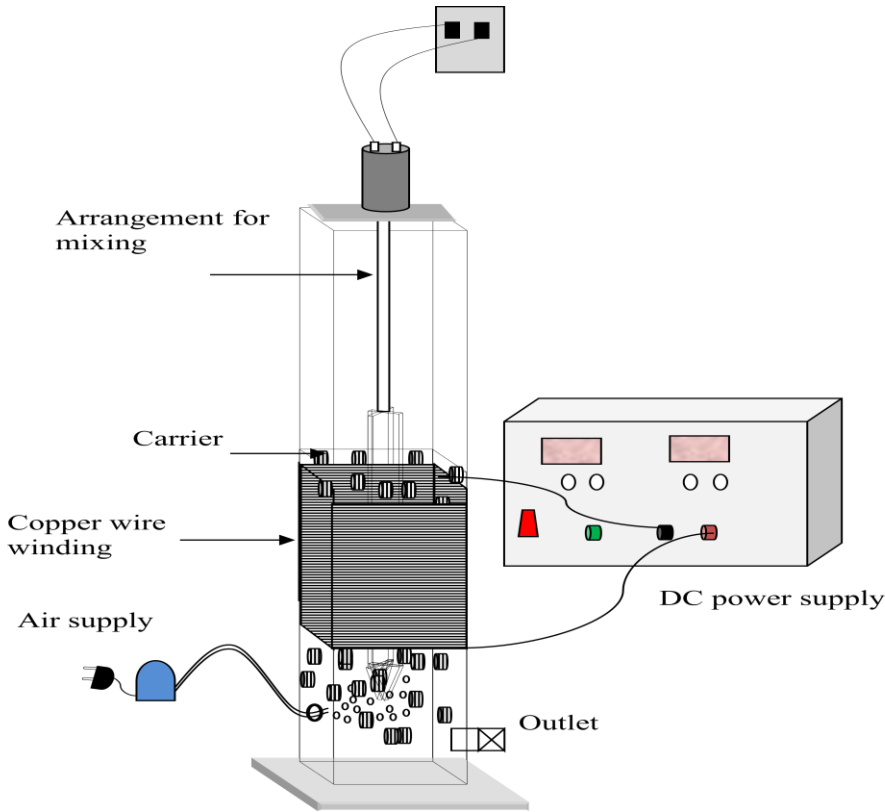


**Fig.3.6 Schematic Diagram of Experimental Set Up of MBBR with Magnetic Field**

The effect of field on MBBR process was studied by varying the field exposure time and field intensity. The reactor was operated at optimum pH, filling ratio of carriers and contact time as obtained under previous section when working without magnetic field. The MBBR was operated at various magnetic field intensity and exposure time. The experiment was conducted with one parameter varying at a time keeping the other constant. The range of magnetic intensity was 0 to 14 mT and that of exposure time was 0 to 14 hours. For each run of the experiment, percentage removal of BOD and COD were calculated in order to find the optimum conditions.

### **3.19 Cost estimation and economic evaluation**

Cost estimation and economic evaluation is important in designing, constructing and predicting the future economical requirements of a treatment plant. Here, capital cost, operating

cost including chemical expenses, energy requirements, sludge handling etc. and total cost have been calculated for Integrated HSPF-MBBR system and Integrated ASPF-MBBR system for comparison. Capital costs are converted to annual costs using capital recovery factor (CRF). Taking 8 hours per day as the working time, interest rate (i) as 10%, design period (n) as 15 years for photo Fenton reactor and capacity of the plant as 100m<sup>3</sup>/day,

$$\text{Annualized capital cost} = \text{cost} * \text{CRF} \text{ ----- (eq.3.5)}$$

$$\text{Annualized capital cost} = \text{cost} * \frac{\{i(1+i)^n\}}{\{(1+i)^n - 1\}} \text{ ----- (eq.3.6) (Papavinasam, 2015)}$$

$$\text{Operating cost} = \text{chemical cost} + \text{energy cost} + \text{sludge handling cost}$$

$$\text{Electrical energy, kWh} = \text{VI}t \text{ ----- (eq.3.7) where V=electrical voltage in kV, I=current in Amp, t=time in hours.}$$

The rate of electric energy prevailing in the area is Rs 5.50/kWh.

$$\text{Sludge handling cost} = \text{Rs } 10/\text{kg.}$$

$$\text{Total cost} = \text{Annualized capital cost} + \text{operating cost.}$$

# CHAPTER 4

## RESULTS AND DISCUSSIONS

### 4.1 Sample characterization

The characteristics of textile effluent samples collected at different period have been given in Appendix 1 and the average characteristics are tabulated in Table 4.1.

**Table 4.1 Characteristics of Textile Effluent**

Parameters	Value
BOD (mg/l)	210 ± 18.4
COD (mg/l)	980 ± 75.2
pH	12 ± 0.9
Alkalinity (mg/l)	1200 ± 110
Turbidity (NTU)	64 ± 6.7
Sulphide (mg/l)	44 ± 5.9
Chloride (mg/l)	180 ± 15.6
Conductivity (mS/cm)	0.85 ± 0.05
Hardness (mg/l as CaCO <sub>3</sub> )	140 ± 9.8

### 4.2 Treatment of textile effluent using MBBR with carrier materials inoculated with textile sludge

The MBBR process with carrier materials inoculated with sludge collected from aeration tank of textile industry has been conducted with contact time, pH and filling ratio of carrier materials as variables. The experiment was done by varying one variable at a time, keeping the others constant.

#### 4.2.1 Effect of contact time on COD removal

After fixing filling ratio of carriers as 50% of reactor volume and pH as 6, the contact time of the effluent in reactor has been varied. Aeration was provided at a rate of 3 l/min. The effluent COD was measured at various contact time and the corresponding percentage removal of COD has been computed. Fig.4.1 explains the variation of %COD removal with contact time.

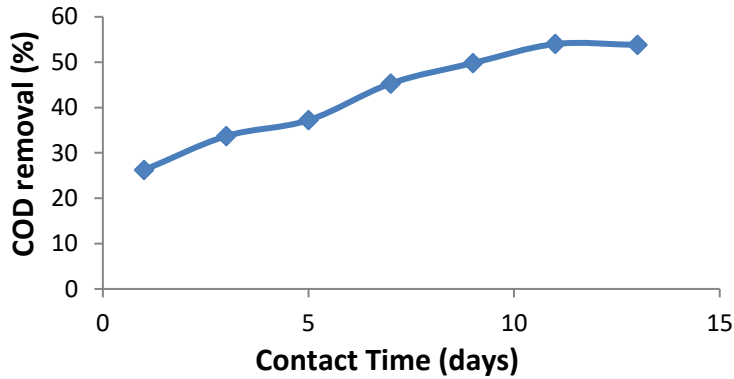


**Fig.4.1 Variation of COD removal with contact time**

The COD of wastewater was decreased day by day and became nearly constant. The maximum COD removal has been attained at 11<sup>th</sup> day.

#### 4.2.2 Effect of pH on COD removal

The pH range for biological sludge is normally lies in the range of 6-8. Keeping the carrier material filling ratio as 50% and contact time as 11 days, pH has been varied. Variation in percentage COD removal with pH has been plotted in Fig.4.2.

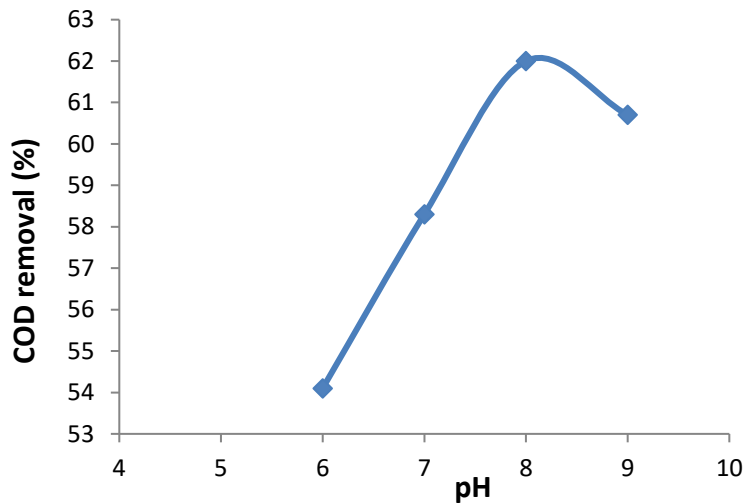


**Fig.4.2 Variation of COD removal with pH**

Maximum %COD removal has been recorded at pH 8 which means that the growth rate of bacteria responsible for the degradation is optimum at this pH.

#### **4.2.3 Effect of filling ratio of carrier materials on COD removal**

As percentage of carrier materials increases, the surface area for the microbial growth also increases. Hence filling ratio of carrier materials has been taken as one of the varying parameter. Keeping the pH as 8 and contact time as 11 days, filling ratio has been varied and percentage COD removal versus filling ratio has been plotted in Fig.4.3.

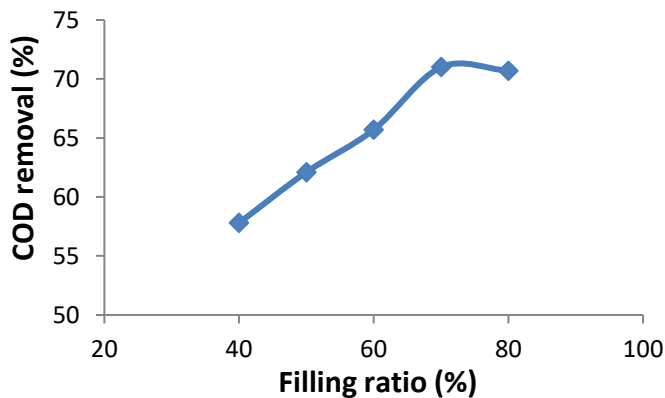


**Fig.4.3 Variation of COD removal with filling ratio**

COD removal has been increased with the increasing filling ratio of carrier materials from 40% to 70% and then decreased. Increase in removal is due to the increase in the bacterial mass taking part in the degradation. The decrease in COD removal may be due to the prevention of free movement of carrier materials inside the reactor. Also, the excessive carrier filling ratio increased the collision between the carriers, resulting in the bio-film desorption on the surface of carriers. Therefore, the amount of bacteria in the reactor would not increase greatly with the increase in carrier ratio, resulting in decrease in organic degradation. Maximum COD removal of 71 % was obtained at 70% filling ratio of carrier materials. Under these optimum conditions of pH 8, contact time 11days and carrier material filling ratio 70%, percentage of BOD removal has also been measured as 78%.

As the BOD of the effluent after treatment is 46mg/l which is less than 100mg/l and COD of the effluent is 284mg/l, it meets the effluent standards for irrigation purpose as per Environmental Protection Rules, 1984, Schedule IV, Part A. However, as the BOD is greater than 30mg/l and COD greater than 250mg/l, it does not meet the effluent standards for disposing into inland waters as per E(P) Rules.

### **4.3 Treatment of textile effluent using MBBR with bacteria inoculated carriers**

The isolation, identification and inoculation of predominant bacteria present in the textile sludge have been done as per section 3.4.1. The predominant bacteria have been found out as azoarcus. The Quadrant streaked culture of azoarcus bacteria is shown in Fig.4.4.



**Fig 4.4 Quadrant streaked culture of azoarcus bacteria**

The azoarcus bacterial colonies are inoculated on PVC carrier media. MBBR with bacteria inoculated carrier media has been run at varying parameters contact time, pH and filling ratio of carrier materials.

#### **4.3.1 Effect of contact time on COD removal**

The contact time of the effluent in MBBR reactor has been varied, keeping the pH and filling ratio of carrier materials as 6 and 50% respectively. The percentage removal of COD has been computed at various contact times and plotted as shown in Fig.4.5.

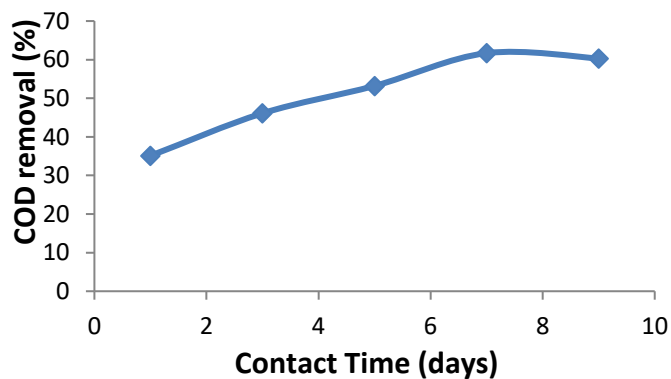


**Fig.4.5 Variation of COD removal with contact time**

The percentage COD removal of wastewater was increased with increasing contact time up to an optimum value. The maximum COD removal was attained at 7<sup>th</sup> day. When the contact time increases, the microorganisms attain maximum contact with the organic content in wastewater resulting in more COD degradation. The decrease in the COD removal after 7<sup>th</sup> day may be due to the lack of substrate concentration.

#### 4.3.2 Effect of pH on COD removal

Fixing the carrier filling ratio as 50% and contact time as 7 days, pH has been varied and variation in percentage COD removal plotted in Fig.4.6.

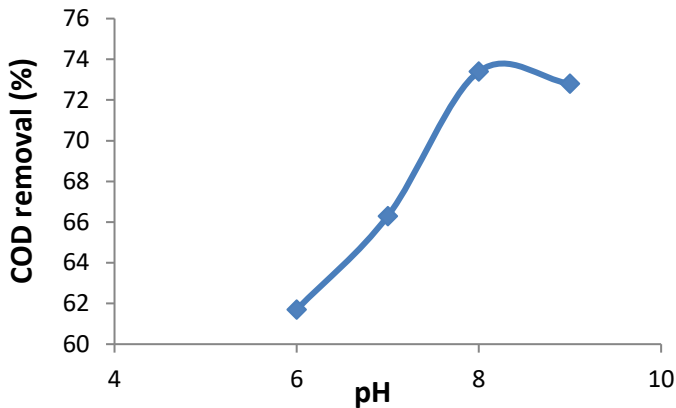


**Fig.4.6 Variation of COD removal with pH**

Maximum removal was recorded at pH 8. The pH tolerance of bacteria is important because dyes bind to cotton fibre materials by substitution or addition mechanisms under alkaline conditions (Rajeshwari et al, 2011). The efficiency of bacteria responsible for organic content degradation is optimum at pH 8.

#### 4.3.3 Effect of filling ratio of carrier materials on COD removal

Keeping the pH as 8 and contact time as 7 days, filling ratio of carrier materials has been varied and the percentage COD removal has been plotted in Fig.4.7.

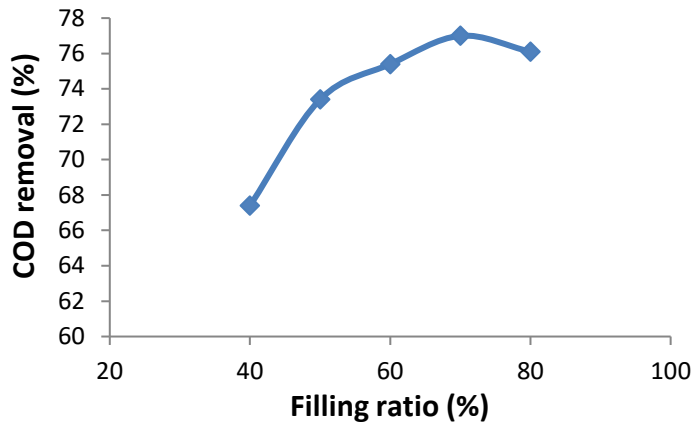


**Fig.4.7 Variation of COD removal with filling ratio**

COD removal was increased with the increasing filling ratio of carriers from 40% to 70% and then decreased. Maximum COD removal of 77% was obtained at 70% filling. The mass of bacterial population taking part in the organic content degradation increases with the increase in percentage of carrier materials. When the filling ratio is increased beyond 70%, the movement of carrier materials gets interrupted resulting in reduction in the efficiency of degradation. BOD removal measured under these conditions was 82%. As the BOD of the effluent after treatment is 38mg/l and COD of the effluent is 225mg/l, it meets the effluent standards for irrigation purpose. However, it cannot be disposed into inland waters, as it does not conforming to that standards.

#### **4.4 Homogeneous photo Fenton process (HPF)**

Since the biodegradability index (BI) of the raw textile effluent is 0.21, it takes long time for treatment through MBBR and it is not possible to dispose the effluent into inland waters after MBBR treatment only. Hence, advanced oxidation processes have been attempted as

pretreatment to increase the BI. One of the AOPs suggested is HPF process. The UV bulb of 11W is used as source of UV radiation.

#### 4.4.1 Optimization using BBD for COD reduction in HPF process

Box-Behnken Design (BBD) has been used for optimizing the variables and evaluating the results. Table 4.2 shows the levels of varying factors and Table 4.3 gives the design of experimental runs given by BBD with %COD removal as response.

**Table 4.2 Levels of varying factors for BBD in HPF/HSPF Process**

variables	Variable levels	
	Low	High
pH	2	4
H <sub>2</sub> O <sub>2</sub> (mM)	40	80
Fe <sup>2+</sup> (mg/l)	10	50

**Table 4.3 Design of experimental runs for BBD in HPF process**

Run	pH	H <sub>2</sub> O <sub>2</sub> (mM)	nZVI(mg/l)	COD Re%
1	3	80	10	58.51
2	4	40	30	67.70
3	3	80	50	68.06
4	4	60	10	59.60
5	4	60	50	64.70
6	3	60	30	77.01
7	3	40	10	61.03
8	2	60	50	74.71
9	4	80	30	62.86

10	3	60	30	76.49
11	3	40	50	68.87
12	2	40	30	63.87
13	2	80	30	71.96
14	2	60	10	58.06
15	3	60	30	76.60

#### 4.4.2 Regression model for COD reduction in HPF process

ANOVA Table with estimated regression coefficients and p-values for varying parameters and their interactions are given in Table 4.4.

**Table 4.4 Estimated Regression Coefficients for COD removal in HPF**

Term	Coefficient	SE Coeff	T	p
constant	-73.3178	11.8992	-6.162	0.002
pH	42.1688	4.8365	8.719	0.000
H <sub>2</sub> O <sub>2</sub> (mM)	1.9902	0.2418	8.230	0.000
Fe <sup>2+</sup> (mg/l)	1.7321	0.1804	9.600	0.000
pH*pH	-4.9762	0.7066	-7.042	0.001
H <sub>2</sub> O <sub>2</sub> *H <sub>2</sub> O <sub>2</sub>	-0.0128	0.0018	-7.254	0.001
Fe <sup>2+</sup> *Fe <sup>2+</sup>	-0.0186	0.0018	-10.552	0.000
pH*H <sub>2</sub> O <sub>2</sub>	-0.1616	0.0339	-4.761	0.005
pH*Fe <sup>2+</sup>	-0.1444	0.0339	-4.253	0.008
H <sub>2</sub> O <sub>2</sub> *Fe <sup>2+</sup>	0.0011	0.0017	0.630	0.557
R <sup>2</sup> = 98.57%    R <sup>2</sup> (pred)= 77.44%    R <sup>2</sup> (adj) = 96.00%				

Here, low p value (<0.05) and high T value for a term indicates that the term has high significance on percentage COD reduction. It was found that all terms are significant in percentage COD reduction except the interaction term between H<sub>2</sub>O<sub>2</sub> and Fe<sup>2+</sup>. When simple or multiple linear regression is considered, the size of the coefficient for each independent variable gives the size of the effect that the variable have on the dependent variable, and the sign of the coefficient (positive or negative) indicates the direction of the effect. In regression with multiple independent variables, the coefficient tells how much the dependent variable is expected to increase when that independent variable increases by one, holding all the other independent variables constant. pH is the most significant parameter with high regression coefficient in percentage COD reduction followed by H<sub>2</sub>O<sub>2</sub> dosage and Fe<sup>2+</sup> dosage in HPF process. The predominance of pH may be due to the sensitivity of the parameter owing to the narrow band (2 to 4) at which the process becomes optimum (Kris & Suresh, 2020).

R<sup>2</sup>, which is the coefficient of determination, is the proportion of the variance in the dependent variable that is predictable from the independent variable. R<sup>2</sup> value tells how well the model fits the observed data. Here, R<sup>2</sup> value 98.57% indicates that 98.57% of the variations in percent removal of COD are clarified by the independent variables. R<sup>2</sup>(adj) 96.00% suggests a satisfactory fitting of the model. It specifies that all the variables are apt to the model and the model has been improved by all of them. R<sup>2</sup>(pred) 77.44% stipulates that the model appreciably predicts responses for new observations.

A second-order polynomial model was fitted to predict the COD removal as follows.

$$\text{COD removal \%} = -73.3178 + 42.1688X_1 + 1.9902X_2 + 1.7321 X_3 + -4.9762 X_1^2 + -0.0128X_2^2 + -0.0186 X_3^2 + -0.1616 X_1X_2 + -0.1444 X_1X_3 + 0.0011 X_2X_3 \text{ ----- (Eq.4.1)}$$

Where  $X_1 = \text{pH}$ ,  $X_2 = \text{H}_2\text{O}_2$  dosage,  $X_3 = \text{Fe}^{2+}$  dosage

#### 4.4.3 Optimization results of COD reduction in HPF process

Optimization plot for %COD removal by HPF process is given in Fig.4.8. From the figure, it is clear that the optimum conditions are pH 2.69,  $\text{H}_2\text{O}_2$  dosage 62.22mM and  $\text{Fe}^{2+}$  dosage 37.88mg/l which ensures 77.94% COD removal.

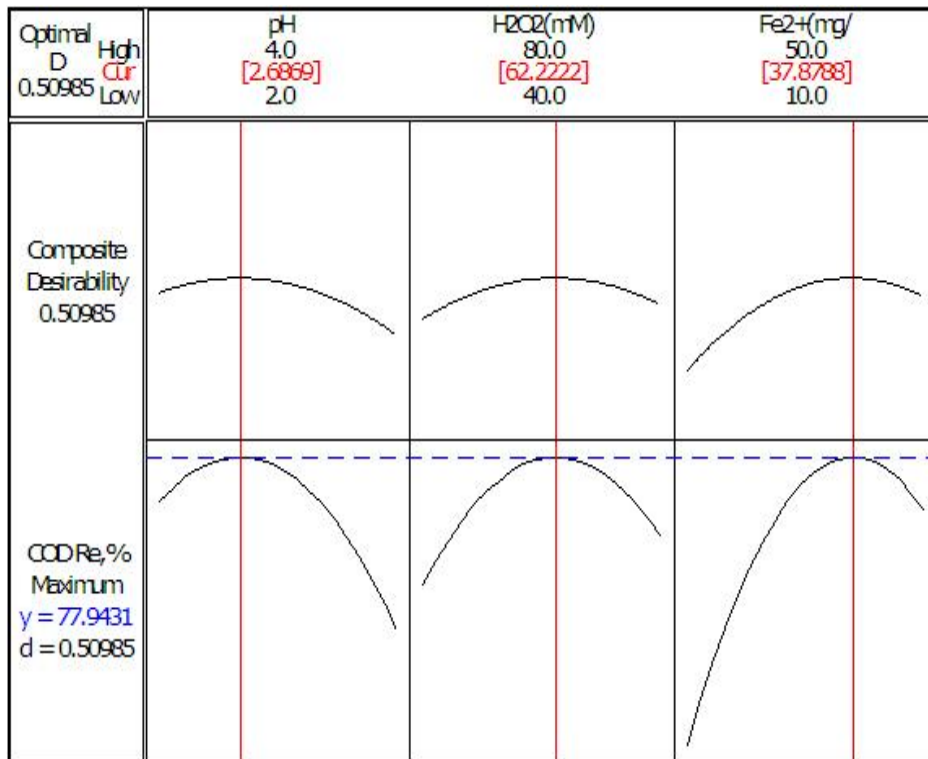


**Fig.4.8 Optimization Plot for %COD removal in HPF Process**

#### 4.4.4 Contour plots for COD reduction in HPF process

Two dimensional contour plots generated by the model represent the relationship between independent and dependent variables graphically. Graphical representations of 2D contour plots for regression analysis of percentage COD reduction is shown in Fig.4.9. The contour plots give the interaction between two independent variables on the response, keeping

the others fixed as optimum. The response variable is shown by the contour lines whereas the independent variables are shown on the two axis of the contour plot. The contours were curved because the model includes statistically significant quadratic terms. It is obvious from contour plots that COD removal efficiency increases as H<sub>2</sub>O<sub>2</sub> dosage increases up to 62.2mM and pH 2.7, keeping Fe<sup>2+</sup> dosage as 37.9mg/l. Similarly, on increasing the Fe<sup>2+</sup> dosage above 37.9mg/l, efficiency decreases. It can be seen from all the three interaction plots that increase in pH, Fe<sup>2+</sup> dosage and H<sub>2</sub>O<sub>2</sub> dosage above the optimum, results a decrease in the efficiency of COD removal.

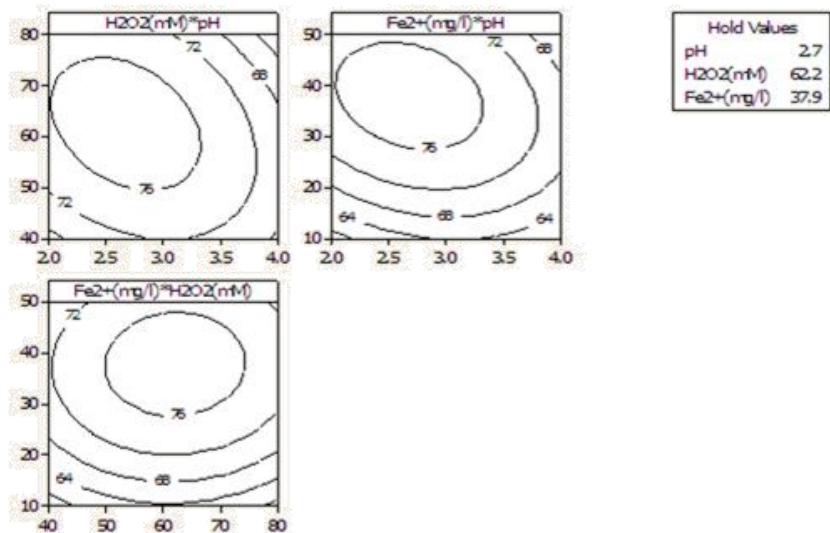
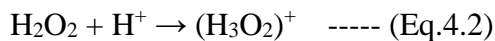


**Fig.4.9 Contour plots for %COD removal in HPF process**

#### **4.4.5 Effect of parameters on COD reduction in HPF process**

At pH less than 2.7, the reaction of hydrogen peroxide with Fe<sup>2+</sup> (ferrous ion) could be slowed down because H<sub>2</sub>O<sub>2</sub> can stay stable probably by solvating a proton to form an oxonium ion (e.g., H<sub>3</sub>O<sub>2</sub><sup>+</sup>) as presented by Eq.4.2. An oxonium ion makes H<sub>2</sub>O<sub>2</sub> electrophilic which enhance its stability and reduce the reactivity with ferrous ion.



At the same time the formed complex species  $[\text{Fe}(\text{H}_2\text{O})_6]^{2+}$  and  $[\text{Fe}(\text{H}_2\text{O})_6]^{3+}$  also react more slowly with  $\text{H}_2\text{O}_2$ . In addition, the scavenging effect of the  $\text{OH}^\bullet$  radical by  $\text{H}^+$  is severe (Eq.4.3).



On the other hand, at pH higher than 2.7, the oxidation efficiency decreased rapidly due to the stability of  $\text{H}_2\text{O}_2$  which starts to rapidly decompose into molecular oxygen without formation of appreciable amounts of hydroxyl radicals. It is expected that the formed  $\text{O}_2$  is not capable to efficiently oxidize the organics in the mild operating conditions used (Hassan and Hameed, 2011). In the presence of excess  $\text{H}_2\text{O}_2$  dosage, its scavenging effect towards hydroxyl radicals is significant resulting in the formation of less reactive species  $\text{HO}_2^\bullet$  which reduces its efficiency (Duc,2013). Efficiency increases with increase in  $\text{Fe}^{2+}$  dosage. At high dosage of ferrous ions, efficiency reduced which is due to the self-inhibition effect of hydroxyl radical by converting it to hydroxyl ions during oxidation of  $\text{Fe}^{2+}$  (Hassan and Hameed,2011).

## **4.5 Homogeneous solar photo Fenton process (HSPF)**

### **4.5.1 Optimization using BBD for COD reduction in HSPF process**

Solar irradiation is used as the source of light in HSPF process. The levels of varying factors are same as in Table 4.2 and Table 4.5 gives the design of experimental runs for BBD with %COD removal as response. Solar light intensity has been measured as  $30 \pm 2 \text{ W/m}^2$ .

**Table 4.5 Design of experimental runs for BBD in HSPF process**

Run	pH	H <sub>2</sub> O <sub>2</sub> (mM)	nZVI(mg/l)	COD Re%
1	3	40	50	63.84
2	3	60	30	70.10
3	3	60	30	70.10
4	4	40	30	62.28
5	4	80	30	58.56
6	2	60	10	52.80
7	2	40	30	56.84
8	3	40	10	53.81
9	3	80	10	55.42
10	3	60	30	70.10
11	3	80	50	62.48
12	4	60	10	52.80
13	2	80	30	65.64
14	2	60	50	70.78
15	4	60	50	59.86

**4.5.2 Regression model for COD reduction in HSPF process**

ANOVA Table with estimated regression coefficients and p-values for varying parameters and their interaction terms are given in Table 4.6.

**Table 4.6 Estimated Regression Coefficients for COD removal in HSPF**

Term	Coefficient	SE Coef	T	p
constant	-76.9197	18.2026	-4.225	0.008
pH	39.2075	7.4002	5.298	0.003
H <sub>2</sub> O <sub>2</sub> (mM)	1.9749	0.3700	5.337	0.003

Fe <sup>2+</sup> (mg/l)	1.7579	0.2761	6.368	0.001
pH*pH	-4.5487	1.0812	-4.207	0.008
H <sub>2</sub> O <sub>2</sub> *H <sub>2</sub> O <sub>2</sub>	-0.0118	0.0027	-4.367	0.007
Fe <sup>2+</sup> *Fe <sup>2+</sup>	-0.0162	0.0027	-6.004	0.002
pH*H <sub>2</sub> O <sub>2</sub>	-0.1565	0.0519	-3.013	0.030
pH*Fe <sup>2+</sup>	-0.1365	0.0519	-2.628	0.047
H <sub>2</sub> O <sub>2</sub> *Fe <sup>2+</sup>	-0.0019	0.0026	-0.715	0.507
R <sup>2</sup> = 96.47%   R <sup>2</sup> (pred)= 83.59%   R <sup>2</sup> (adj) = 90.13%				

Here also, all the terms except the interaction term between H<sub>2</sub>O<sub>2</sub> and Fe<sup>2+</sup> are significant in COD reduction. pH has the predominant effect in COD reduction as discussed in HPF process. A high R<sup>2</sup> and R<sup>2</sup>(adj) indicates that the model is perfectly fit with the experimental data and all the variables have improved the model.

A second-order polynomial model was fitted to predict the COD removal as follows.

$$\text{COD removal \%} = -76.9197 + 39.2075X_1 + 1.9749X_2 + 1.7579 X_3 + -4.5487 X_1^2 + -0.0118X_2^2 + -0.0162 X_3^2 + -0.1565 X_1X_2 + -0.1365 X_1X_3 + -0.0019 X_2X_3 \quad \text{----- (Eq.4.4)}$$

Where X<sub>1</sub> = pH, X<sub>2</sub> = H<sub>2</sub>O<sub>2</sub> dosage, X<sub>3</sub> = Fe<sup>2+</sup> dosage

#### 4.5.3 Optimization results of COD reduction in HSPF process

Fig.4.10 shows the optimization plot for percentage COD removal. From the optimization plot it is obvious that 71.7% COD removal obtained at optimum pH 2.63, H<sub>2</sub>O<sub>2</sub> dosage 63.03mM and Fe<sup>2+</sup> dosage 39.5mg/l.

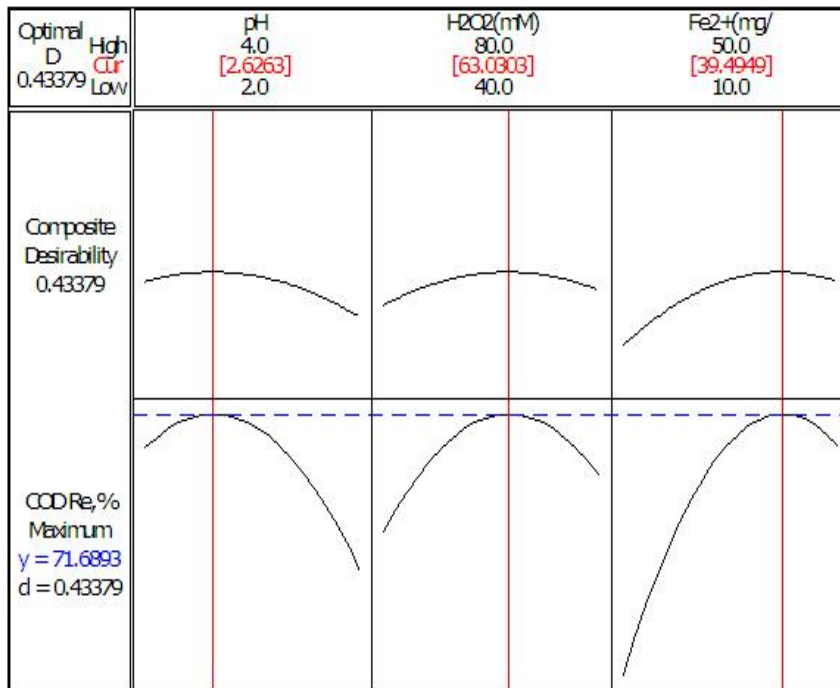


**Fig. 4.10 Optimization Plot for %COD removal in HSPF Process**

#### 4.5.4 Contour Plots for COD reduction in HSPF process

Fig.4.11 presents the contour plots which explore the relationship between two independent variables with COD reduction, with the constant variable optimum. A reduction in the efficiency of COD removal can be seen with the increase in pH, Fe<sup>2+</sup> dosage and H<sub>2</sub>O<sub>2</sub> dosage above the optimum. The reasons have been as explained in section 4.4.5.

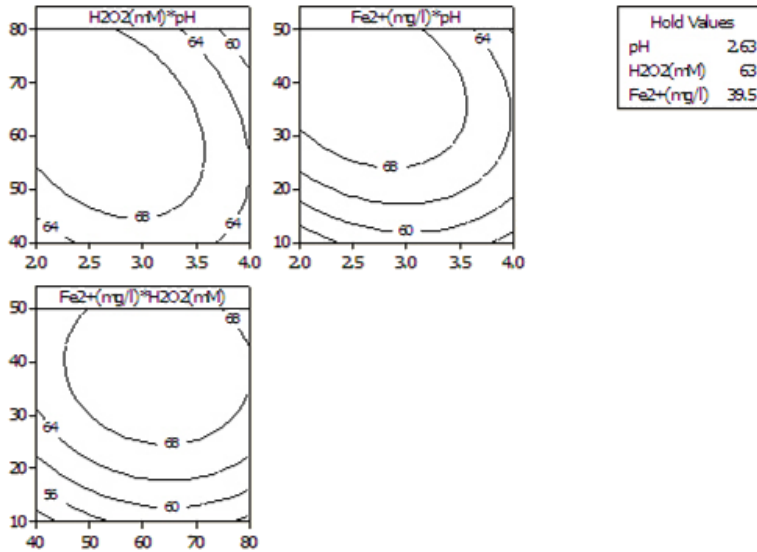


**Fig.4.11 Contour Plot for %COD removal in HSPF Process**

## **4.6 Biosynthesis and characterization of nano zero valent iron (nZVI)**

### **4.6.1 UV Spectroscopy analysis**

nZVI has been synthesized from *Amaranthus Dubius* leaf extract and characterization has been done. The UV spectra of nZVI is shown in Fig.4.12. Absorption peaks from 204nm to 290nm indicates the formation of nanoparticles. Absorption peaks are due to the excitation of surface plasmon vibrations in the iron nano particles, which are identical to the characteristics UV visible spectrum of metallic iron (Pattanayak and Nayak, 2013).

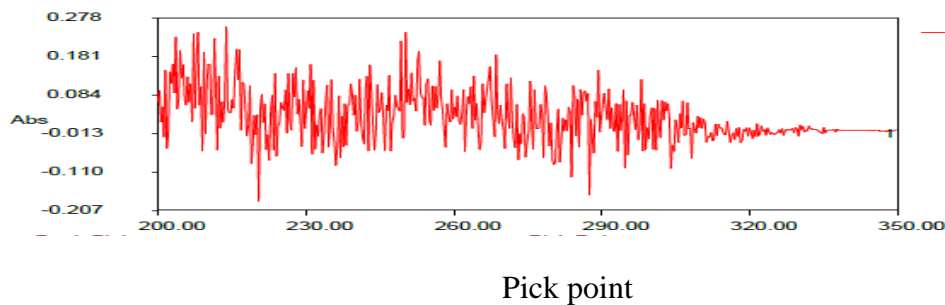


**Fig.4.12 UV Spectra of nZVI**

## 4.6.2 FT-IR analysis

FTIR spectrum of nZVI has been given in Fig.4.13. Amaranthus Dubius leaf consists of pectin and flavonoid, which contains functional groups such as aldehydes, ketones, carbohydrates and hydroxyl groups. The functional groups in the synthesis of nZVI can be identified from FTIR analysis. Stretch band at  $3396\text{ cm}^{-1}$  is due to the presence of photochemicals such as amaranthine, isomaranthine, etc. and phenolic groups like  $-\text{OH}$  and  $-\text{NH}$ . The peak  $1625\text{ cm}^{-1}$  reveals the presence of strong  $\text{C}=\text{O}$  bonding in aldehydes and ketones. The peak  $1401\text{ cm}^{-1}$  related to  $\text{CH}_2$  symmetric bending mode of the methyl groups of carboxylate (Harshiny et al, 2015; Farshchi et al, 2018). The polyphenol and functional groups mentioned above are responsible for the reduction of  $\text{Fe}^{3+}$  to  $\text{Fe}^0$ .

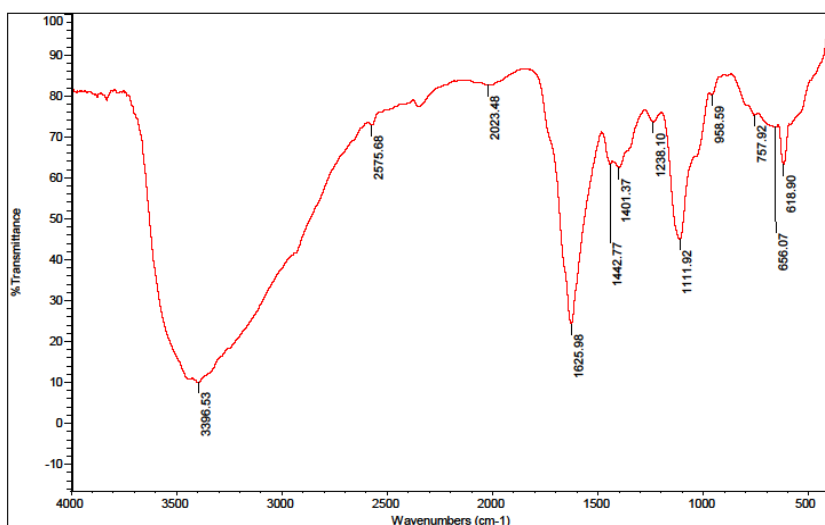


**Fig.4.13 FTIR Spectrum of nZVI**

### 4.6.3 TEM analysis

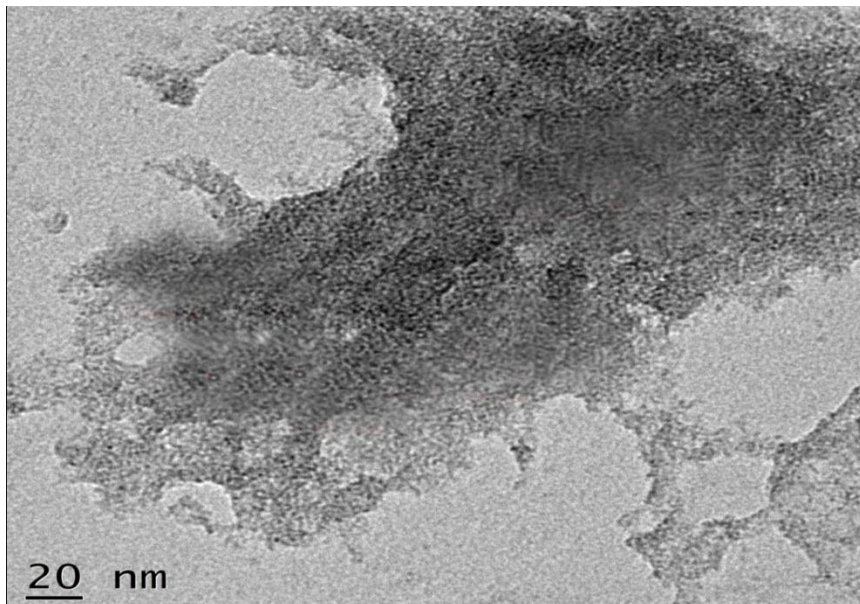


**Fig.4.14 TEM Image of nZVI**

The TEM results in Fig.4.14 confirm the presence of nanoparticles in the size range 2.5nm to 10nm. FeNps form irregular clusters, but demonstrate some dispersion. The metallic iron and iron oxide phases can be distinguished from the corresponding color contrast. The lighter regions are mainly on the surface of the particle and the dark regions are concentrated in the centre of the particle. The core was formed by metallic iron and the surface formed by iron oxides.

### 4.6.4 BET surface area analysis

The BET surface area analysis results show that surface area is 3.74 m<sup>2</sup> per gram of nZVI with mean pore diameter 4.3 nm and total pore volume 0.00401 cm<sup>3</sup>/gram. The BET surface area is high compared to commercially available Fe powder (<10μm) which has a surface area around 0.9 m<sup>2</sup>/gram.

Hence, it can be concluded that nZVI can be successfully synthesized from *Amaranthus Dubius* leaf extract and it can be competitively used for the wastewater treatment as commercially available iron powder.

## 4.7 Advanced photo Fenton process (APF)

### 4.7.1 Optimization using BBD for COD reduction in APF process

The biosynthesized nZVI can be used in photo Fenton process replacing ferrous ions and this process is termed as Advanced Photo Fenton (APF) process. 11W Philips UV bulb is used as source of UV radiation.

Table 4.7 shows the levels of varying factors and Table 4.8 gives the design of experimental runs for BBD with %COD removal as response.

**Table 4.7 Levels of varying factors for APF Process**

variables	Variable levels	
	Low	High
pH	2	4
H <sub>2</sub> O <sub>2</sub> (mM)	40	80
nZVI (mg/l)	10	50

**Table 4.8 Design of experimental runs for BBD in APF process**

Run	pH	H <sub>2</sub> O <sub>2</sub> (mM)	nZVI(mg/l)	COD Re%
1	2	80	30	81.20
2	3	40	50	78.17
3	2	60	50	83.90
4	4	40	30	77.18
5	2	40	30	73.28
6	4	60	50	74.12
7	3	40	10	69.02
8	3	80	50	76.12
9	4	80	30	72.68
10	3	60	30	86.58
11	4	60	10	69.40
12	3	60	30	84.49
13	2	60	10	68.56
14	3	80	10	67.52
15	3	60	30	85.59

**4.7.2 Regression model for COD reduction in APF process**

ANOVA Table with estimated regression coefficients and p-values for varying parameters and their interaction terms are given in Table 4.9.

**Table 4.9 Estimated Regression Coefficients for COD removal in APF process**

Term	Coef	SE Coef	T	p
constant	-59.8439	13.1979	-4.534	0.006
pH	36.4450	5.3644	6.794	0.001
H <sub>2</sub> O <sub>2</sub> (mM)	2.1036	0.2682	7.843	0.001
nZVI(mg/l)	1.7829	0.2001	8.909	0.000
pH*pH	-4.1404	0.7838	-5.283	0.003

H <sub>2</sub> O <sub>2</sub> *H <sub>2</sub> O <sub>2</sub>	-0.0136	0.0020	-6.926	0.001
nZVI*nZVI	-0.0188	0.0020	-9.592	0.000
pH*H <sub>2</sub> O <sub>2</sub>	-0.1553	0.0377	-4.123	0.009
pH*nZVI	-0.1328	0.0377	-3.526	0.017
H <sub>2</sub> O <sub>2</sub> *nZVI	-0.0003	0.0019	-0.183	0.862
R <sup>2</sup> = 98.15%    R <sup>2</sup> (pred)= 75.55%    R <sup>2</sup> (adj) = 94.83%				

It was found that except the interaction term between H<sub>2</sub>O<sub>2</sub> and nZVI, all other terms are significant and they have high significance on percentage COD reduction. High correlation coefficient for pH implies its dominant significance in COD removal as discussed in HPF and HSPF process. R<sup>2</sup> values confirm satisfactory fitting of the model.

A second-order polynomial model was fitted to predict the COD removal as follows.

$$\text{COD removal \%} = -59.8439 + 36.4450X_1 + 2.1036X_2 + 1.7829X_3 + -4.1404X_1^2 + -0.0136X_2^2 + -0.0188X_3^2 + -0.1553 X_1X_2 + -0.1328 X_1X_3 + -0.0003 X_2X_3 \text{ -----(Eq.4.5)}$$

Where X<sub>1</sub> = pH, X<sub>2</sub> = H<sub>2</sub>O<sub>2</sub> dosage, X<sub>3</sub> = nZVI dosage.

#### 4.7.3 Optimization Results of COD reduction in APF process

Fig.4.15 shows the optimization plot for %COD removal in APF process. COD reduction of 86.85% is obtained at pH 2.65, H<sub>2</sub>O<sub>2</sub> dosage 61.8mM and nZVI dosage 37.5mg/l.

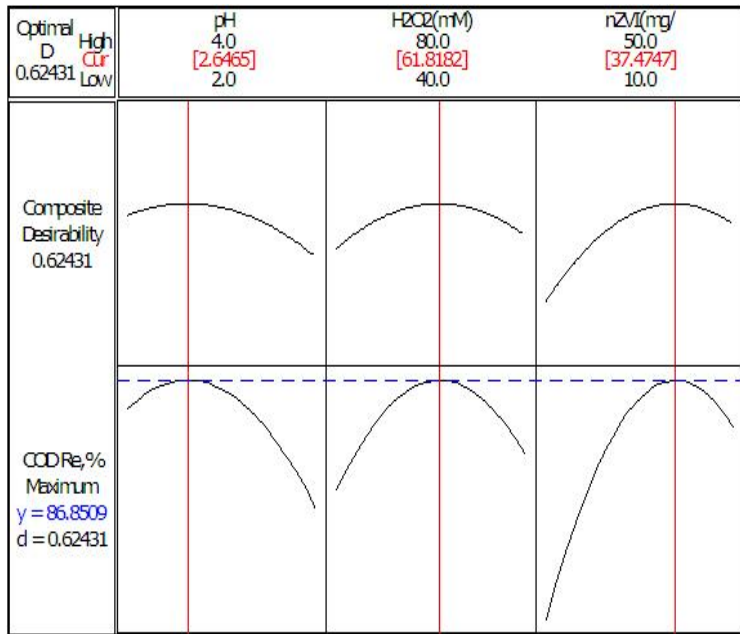


**Fig.4.15 Optimization Plot for %COD removal in APF Process**

#### 4.7.4 Contour plots and effects of parameters on COD reduction in APF process

Contour plots corresponding to the percentage COD removal in APF process is given in

Fig.4.16.

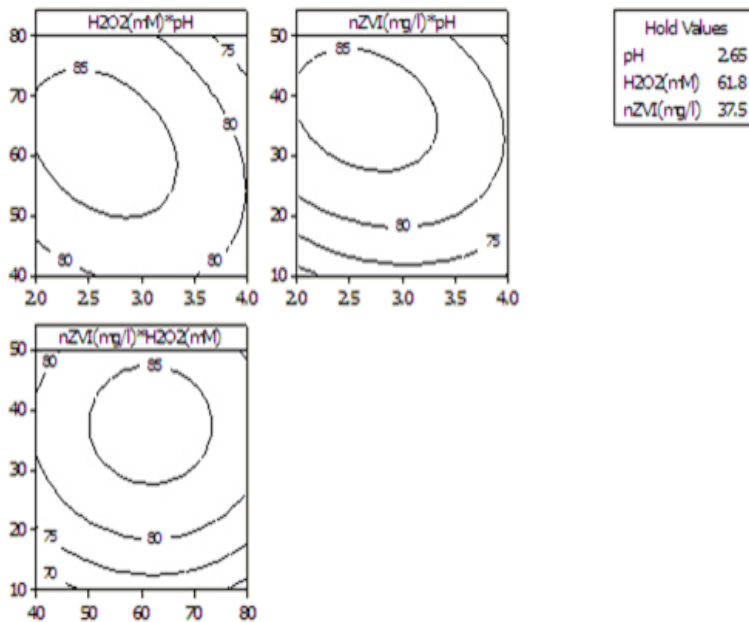


**Fig.4.16 Contour Plots for %COD removal in APF Process**

For pH values above the optimum, the degradation efficiency reduces since iron precipitates as hydroxide derivate, reducing the availability of ferrous ions and the radiation transmission. Another reason for the inefficient removal at high pH is due to the dissociation and auto-decomposition of  $H_2O_2$  (Ebrahiem et al, 2017). As  $H_2O_2$  dosage increases the reduction rates increases. This is because excess  $H_2O_2$  produce more hydroxyl free radical resulting in increased removal %. But Further increase leads to a decrease of COD removal due to the recombination of hydroxyl radical and also the reaction between  $OH\cdot$  and  $H_2O_2$  which results in the scavenging of  $OH\cdot$  radical generating less reactive hyperoxy radicals. As catalyst (nZVI) dosage increases, COD removal during the initial stage increases due to the increase in surface area of the catalyst for accelerating the decomposition of  $H_2O_2$  which in turn increase the number of hydroxyl radicals significantly. A decrease at a later stage may be due to the reduction in active sites of catalysts and also, due to the reaction leading to the ferrous ion and hydroxyl radical recombination. Therefore, the oxidation of organic pollutants was hindered at high nZVI dosage (Ertugay and Acar, 2013). It is obvious that by replacing ferrous ions with nZVI, the COD reduction increases, which proves the improved performance of the reactor.

## **4.8 Advanced solar photo Fenton process (ASPF)**

### **4.8.1 Optimization using BBD for COD reduction in ASPF process**

Solar Photo Fenton process can also be repeated replacing ferrous ions with nZVI and the process is called Advanced Solar Photo Fenton (ASPF) process. Solar light intensity is the same as in HSPF process. The varying parameters and levels of varying parameters are same as in the APF process.

**Table 4.10 Design of Experimental Runs for COD removal in ASPF process**

Run	pH	H <sub>2</sub> O <sub>2</sub> (mM)	nZVI(mg/l)	COD Re%
1	4	60	10	67.72
2	3	80	10	60.52
3	3	60	30	79.58
4	3	80	50	70.22
5	4	80	30	65.68
6	3	40	10	61.82
7	2	60	50	77.50
8	3	40	50	71.87
9	2	80	30	74.44
10	4	60	50	67.88
11	2	60	10	60.86
12	2	40	30	66.84
13	4	40	30	71.28
14	3	60	30	79.78
15	3	60	30	78.59

**4.8.2 Regression model for COD reduction in ASPF process**

ANOVA Table with estimated regression coefficients and p-values for varying parameters and their interaction terms are given in Table 4.11.

**Table 4.11 Results of Regression Analysis of BBD in ASPF**

Term	Coeff.	SE Coeff.	T	p
constant	-62.7518	15.7934	-3.973	0.011
pH	35.5675	6.4193	5.541	0.003
H <sub>2</sub> O <sub>2</sub> (mM)	1.9790	0.3210	6.166	0.002

nZVI(mg/l)	1.7930	0.2395	7.487	0.001
pH*pH	-3.8121	0.9379	-4.065	0.010
H <sub>2</sub> O <sub>2</sub> *H <sub>2</sub> O <sub>2</sub>	-0.0124	0.0023	-5.272	0.003
nZVI*nZVI	-0.0182	0.0023	-7.746	0.001
pH*H <sub>2</sub> O <sub>2</sub>	-0.1650	0.0451	-3.662	0.015
pH*nZVI	-0.1435	0.0451	-3.185	0.024
H <sub>2</sub> O <sub>2</sub> *nZVI	-0.0002	0.0023	-0.097	0.926
R <sup>2</sup> =97.40%    R <sup>2</sup> (adj)=92.73%    R <sup>2</sup> (pred)=83.02%				

The parameters with low p value (<0.05) and high T value (absolute value) confirms their high significance in COD reduction. Hence, all parameters except the interaction term between H<sub>2</sub>O<sub>2</sub> and nZVI dosage are significant in COD reduction. High value of correlation coefficient for pH proves its dominant significance followed by H<sub>2</sub>O<sub>2</sub> and nZVI dosage in the efficiency. The coefficient of determination, R<sup>2</sup>, is the proportion of the variance in the dependent variable that is anticipated from the independent variable. Here, R<sup>2</sup> value 97.04% indicates that 97.04% of the variations in percent removal of COD are clarified by the independent variables. R<sup>2</sup>(adj) value is also satisfactory. The model appreciably predicts responses for new observations, as confirmed by high R<sup>2</sup>(pred).

A second-order polynomial model was fitted to predict the COD removal as follows.

$$\text{COD removal \%} = -62.7518 + 35.5675 X_1 + 1.9790 X_2 + 1.7930 X_3 - 3.8121 X_1^2 + 0.0124 X_2^2 + 0.0182 X_3^2 - 0.1650 X_1 X_2 - 0.1435 X_1 X_3 - 0.0002 X_2 X_3 \quad \text{----- (Eq.4.6)}$$

Where X<sub>1</sub> = pH, X<sub>2</sub> = H<sub>2</sub>O<sub>2</sub> dosage, X<sub>3</sub> = nZVI dosage.

### 4.8.3 Optimization results of COD reduction in ASPF process

From the optimization plot (Fig.4.17), it is clear that the solar photo Fenton process with nZVI results a COD removal of 79.76% at pH 2.6, H<sub>2</sub>O<sub>2</sub> dosage 62.6mM and nZVI 38.7mg/l. The contact time has been fixed as 30minutes. The biodegradability index after 30minutes under these optimized conditions was 0.42. It is clear that %COD removal increases in ASPF process than that in HSPF process which may be due to the large surface area owned by nZVI.

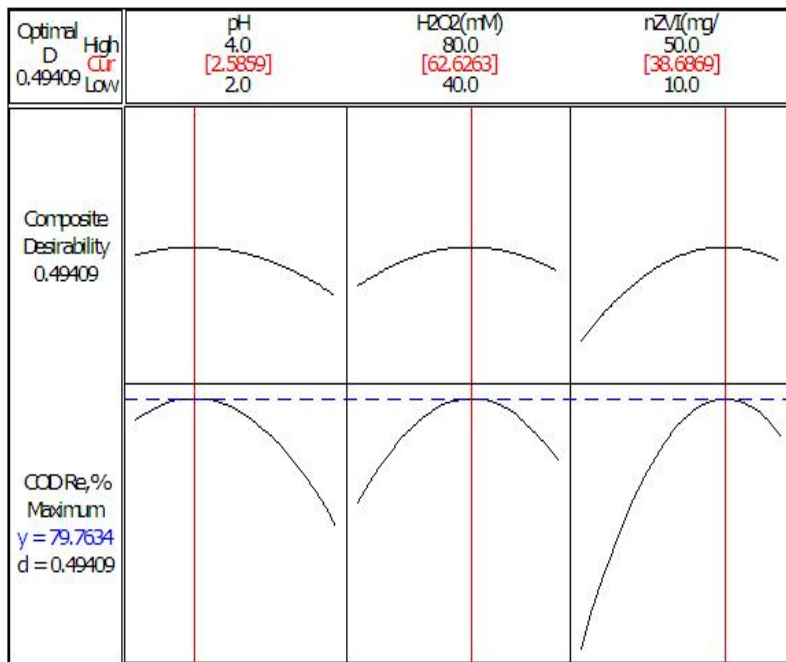


**Fig.4.17 Optimization Plot for %COD removal in ASPF process**

### 4.8.4 Contour plots and effects of parameters on COD reduction in ASPF process

Fig.4.18 shows the contour plots for COD removal at optimum values of variables. As the model includes statistically significant quadratic terms, the contour lines are curved. COD removal efficiency increases as H<sub>2</sub>O<sub>2</sub> dosage increases upto 62.6mM and pH 2.6, keeping nZVI dosage as 38.7mg/l, as seen in the contour plots. The efficiency decreases on increasing the nZVI dosage above 38.7mg/l. It can be seen that increase in pH, nZVI dosage and

H<sub>2</sub>O<sub>2</sub> dosage above the optimum, results a decrease in the efficiency of COD removal. The reasons have been as explained in section 4.6.4.

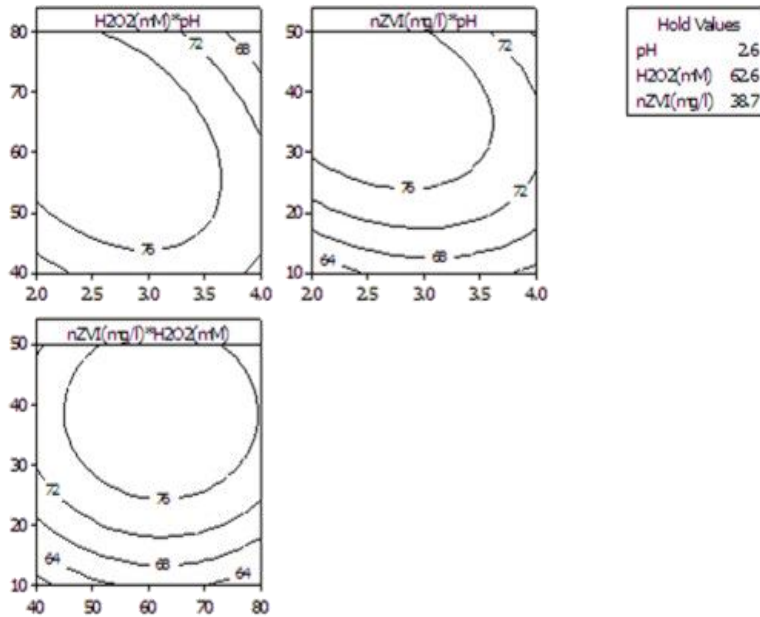


**Fig.4.18 Contour Plots for %COD removal in ASPF process**

### 4.9 Comparison of pretreatments

Table 4.12 and Fig.4.19 shows the comparison of performances of the four processes, namely HPF, HSPF, APF and ASPF. The %BOD removal and BI have also been found out under optimized conditions and the results are tabulated.

**Table 4.12 Comparison of Results of AOPs**

Process	pH	H <sub>2</sub> O <sub>2</sub> (mM)	Fe <sup>2+</sup> /nZVI (mg/l)	UV/Solar light	C.T, mts	%COD removal	%BOD removal	BI
HPF	2.69	62.20	37.88	11 W	30	77.97	64.00	0.35
HSPF	2.62	63.00	39.49	30±2W/m <sup>2</sup>	30	71.69	44.50	0.42
APF	2.64	61.80	37.47	11 W	30	86.85	79.10	0.34
ASPF	2.58	62.63	38.70	30±2W/m <sup>2</sup>	30	79.76	61.43	0.41

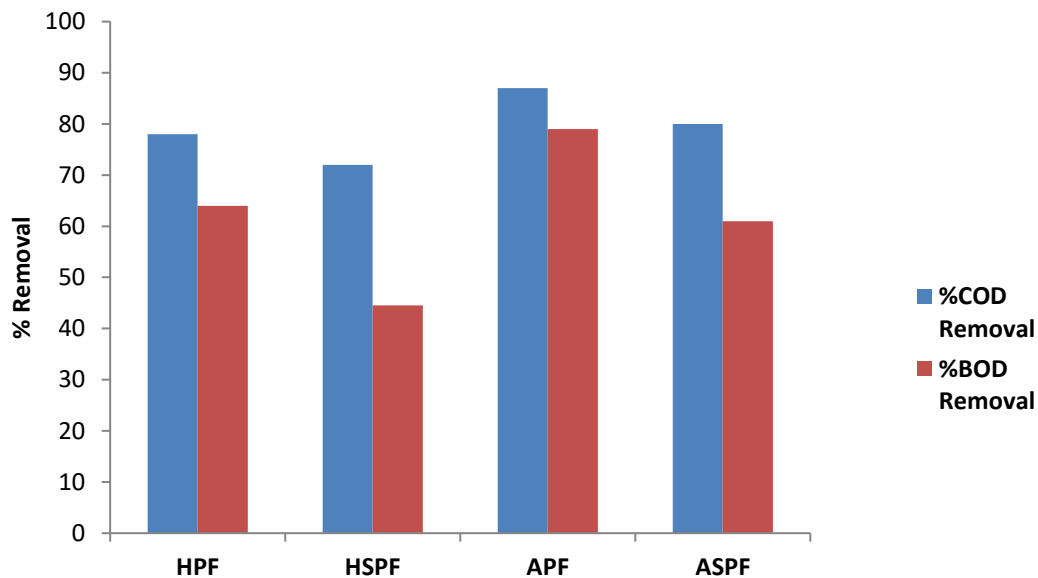


**Fig.4.19 Percentage removal versus Process Graph**

#### 4.10 Validation of the models

To ensure that the model provides an adequate approximation to the real system, it is necessary to check the fitness of the model. Validation of the model is done by conducting the experiments at randomly selected values. The observed COD reduction efficiency is obtained from the experiment and the predicted values are computed using the regression equations. Table 4.13 shows observed and predicted values of COD reduction for randomly selected points.

**Table 4.13 Validation of the Models**

Process	pH	H <sub>2</sub> O <sub>2</sub> (mM)	Fe <sup>2+</sup> /nZVI(mg/l)	%COD reduction	
				observed	Predicted
HPF	2.6	45	25	67.9	68.5
	3.5	70	42	63.9	65.8
HSPF	2.8	50	25	65.1	66.4
	3.5	70	45	63.8	65.5
APF	2.5	70	25	81.1	82.8
	3.5	45	45	85.6	86.8
ASPF	2.5	56	35	77.2	78.7
	3.0	65	40	76.9	78.6

Since the difference between observed and predicted value is small, the model is acceptable.

#### 4.11 Reusability of nZVI and iron leachability

The reusability and regeneration tendency of the catalyst nZVI after APF and ASPF processes were assessed. The amount of leached iron ions has also been measured. The results of four successive runs in COD removal is shown in Table 4.14 and Fig.4.20 and it has been found that nZVI can be used effectively up to third cycle without very much loss in efficiency and after that the degradation efficiency is reduced too much in both processes. The reduction in the removal efficiency after third cycle of experiment could be attributed to the reduction of active sites of nZVI upon adsorption of degradation by-products and small amounts of iron leaching during Fenton reaction.

**Table 4.14 Reusability of nZVI**

Process	%COD removal			
	I <sup>st</sup> cycle	II <sup>nd</sup> cycle	III <sup>rd</sup> cycle	IV <sup>th</sup> cycle
APF	86.85	83.12	81.65	58.95
ASPF	79.76	74.10	71.40	53.10

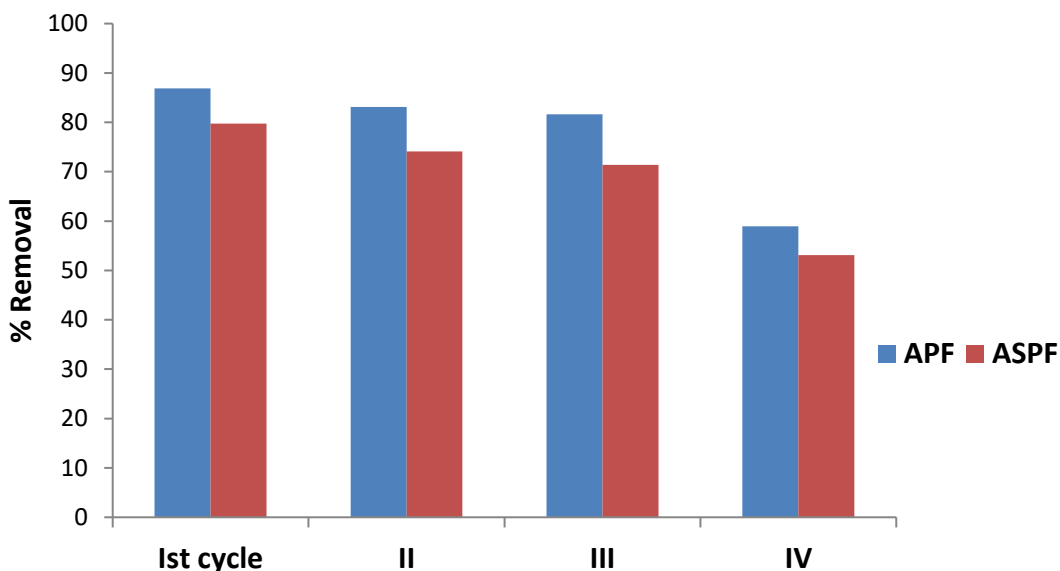


**Fig.4.20 Reusability of nZVI**

**Table 4.15 Percentage of Iron leaching**

Process	% Iron leaching			
	I <sup>st</sup> cycle	II <sup>nd</sup> cycle	III <sup>rd</sup> cycle	IV <sup>th</sup> cycle
APF	16.82	11.73	9.34	6.95
ASPF	13.75	10.34	8.90	5.72

The amount of leached iron ions are reported in Table 4.15. It has been found that the percentage of leached iron ions were 16.82 and 13.75 in APF and ASPF respectively after the first cycle of experiment, which have been reduced to 9.34 and 8.90 after third cycle. After fourth cycle, these values have been very much decreased. This is very promising result against the value of 77% reported by Mahdiah et al, 2021 for commercially available nZVI. nZVI absorb leached  $Fe^{2+}$  and  $Fe^{3+}$  ions and continuously feed reaction during Fenton process, generating higher amount of hydroxyl radicals.  $Fe^{2+}$  and  $Fe^{3+}$  ions have the possibility of being absorbed by biosynthesized nZVI to avoid leaching and make the continuous supply to reaction possible. nZVI exhibits excellent reusability. The high removal efficiency and low levels of

iron leaching suggests that nZVI synthesized from Amaranthus Dubius leaf is a highly efficient and cost effective catalyst for photo Fenton oxidation of textile effluent.

#### 4.12 Toxicity assessment after AOPs

The graphs with %survival versus %dilution for untreated textile effluent and textile effluent after HPF, HSPF, APF, and ASPF processes are given in figures 4.21 to 4.25. Toxicity Graphs after 24 hours and 96 hours survival are presented. Corresponding LC<sub>50</sub> values are tabulated in Table 4.16.

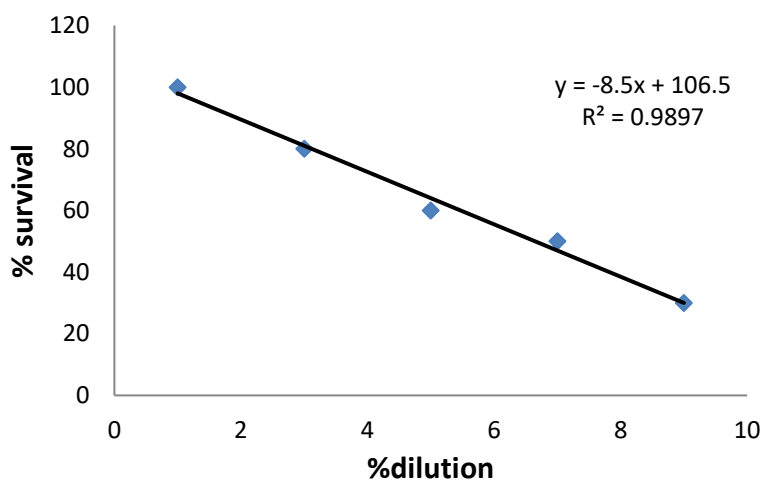


**Fig.4.21 Toxicity graph (96hrs) for raw effluent**

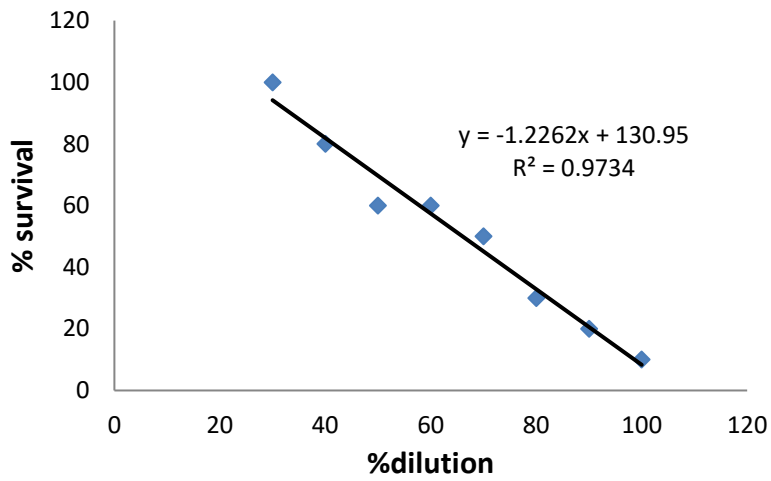


**Fig.4.22 Toxicity graph (96hrs) for effluent after HPF process**

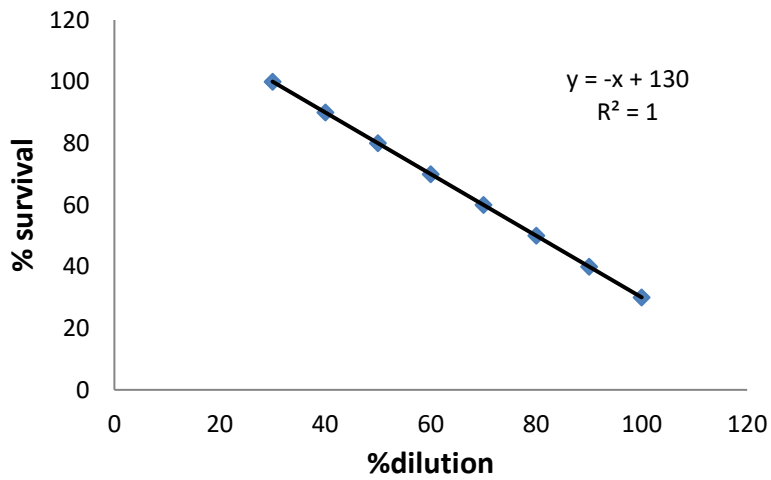


**Fig.4.23 Toxicity graph (96hrs) for effluent after HSPF process**

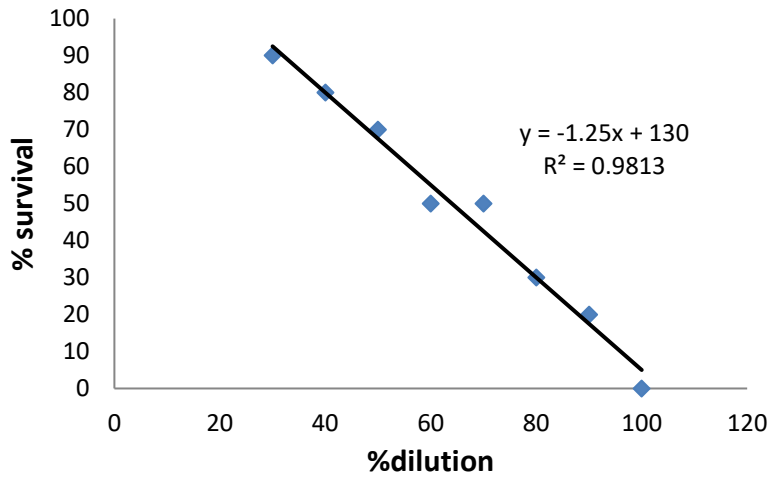


**Fig.4.24 Toxicity graph (96hrs) for effluent after APF process**

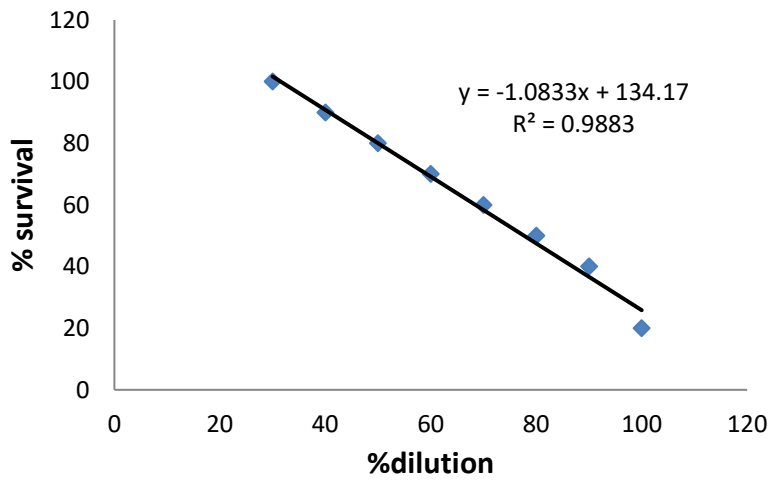


**Fig.4.25 Toxicity graph (96hrs) for effluent after ASPF process**

**Table 4.16 LC<sub>50</sub> Values of Textile effluent**

	LC <sub>50</sub> after 24hrs	LC <sub>50</sub> after 96hrs
Raw effluent	9.7%	6.7%
Effluent after HPF	80.0%	66.0%
Effluent after APF	71.5%	64.0%
Effluent after HSPF	90.9%	80.0%
Effluent after ASPF	85.0%	77.7%

It is established that the toxicity effects reduces due to the AOPs with more positive effect towards solar light based processes, while it is slightly less effective for nZVI based photo Fenton processes. Toxicity tests appealed that though the applied treatment for the decolorization and degradation is effective, the partial mineralization may form intermediate degradation products which are responsible for inducing toxicity to the effluent [Luna et al, 2014]. Solar irradiation has more ability to reduce these intermediate compounds than UV irradiation. It improves toxicity reduction by photolysis of hydroxide complexes and high photo activity under UV-visible light by increasing the quantum yield for Fe<sup>2+</sup> production [Manenti et al, 2015; Gutierrez-Mata et al, 2017] and it is found that these effects are more under solar light than UV light. LC<sub>50</sub> after the ASPF process is smaller than that of HSPF at initial stages. This may be due to the rapid oxidation of nZVI which releases excess Fe<sup>2+</sup>, causing the formation of reactive oxygen species and excessive utilization of O<sub>2</sub>, and creating a highly toxic effect on organisms [El-Temsah et al, 2016; Chen et al, 2011; Sevcu et al, 2011]. Though these effects higher in initial stages, complete oxidation of nZVI neutralizes these effects to become negligible at later stages [Lee et al. 2008; Fajardo et al. 2013]. This may be the cause of not much drastic change in LC<sub>50</sub>(96hrs) values of the effluents after HSPF and ASPF processes. Also, an increase in the nZVI aggregation rate due to the small size of particles causes the formation of bulky aggregates

that settle more rapidly [Tratnyek & Johmson, 2006; Phenrat et al, 2007; Lowry & Gasmon, 2009], resulting in reducing toxicity.

### 4.13 Determination of k, Ks and SVI

The reactor with wastewater is run at various detention times and the observations are given in Table 4.17 and figures 4.26 to 4.30. Values of  $X\Theta/(S_0-S)$  and  $1/S$  have also been calculated. Values of k and Ks can be found out from slope (Ks/k) and y-intercept ( $1/k$ ).

**Table 4.17 Observations at various detention times for k and Ks**

Influent	So,(mg/l)	$\Theta$ , (d)	S,(mg/l)	X,mg/l	$X\Theta/(S_0-S)$	1/S	k & Ks from Slope & y-intercept of graph	
Raw influent	980	2	780	880	8.8000	0.001282	slope	3596
	980	3	718	928	10.6260	0.001393	intercept	5.39
	980	4	662	966	12.1509	0.001511		
	980	5	576	972	12.0297	0.001736	k, d <sup>-1</sup>	0.185
	980	6	510	916	11.6936	0.001961	Ks, mg/l	667
Effluent after HPF	216	2	156	120	4.0000	0.006410	slope	412.9
	216	3	137	127	4.8228	0.007299	intercept	1.51
	216	4	111	134	5.1048	0.009009		
	216	5	96	137	5.7083	0.010417	k, d <sup>-1</sup>	0.662
	216	6	85	141	6.4580	0.011765	Ks, mg/l	273.4
Effluent after HSPF	277	2	210	152	4.5373	0.004762	slope	470.9
	277	3	188	146	4.9213	0.005319	intercept	2.241
	277	4	155	150	4.9180	0.006452		
	277	5	136	160	5.6738	0.007353	k, d <sup>-1</sup>	0.446
	277	6	121	164	6.3077	0.008264	Ks, mg/l	210
Effluent after APF	129	2	78	98	3.8431	0.012821	slope	229.6
	129	3	68	102	5.0164	0.014706	intercept	1.246
	129	4	53	108	5.6842	0.018868		

	129	5	43	110	6.3953	0.023256	k, d <sup>-1</sup>	0.803
	129	6	37	115	7.5000	0.027027	Ks, mg/l	184.3
Effluent after ASPF	198	2	152	132	5.7391	0.006579	slope	623
	198	3	135	150	7.1429	0.007407	intercept	1.94
	198	4	111	158	7.2644	0.009009		
	198	5	97	165	8.1683	0.010309	k, d <sup>-1</sup>	0.515
	198	6	88	169	8.2182	0.011364	Ks, mg/l	321

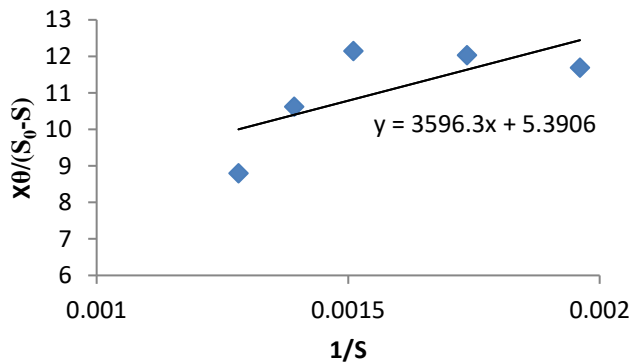


**Fig.4.26  $X_0/(S_0-S)$  Vs  $1/S$  graph for k and Ks of raw effluent**

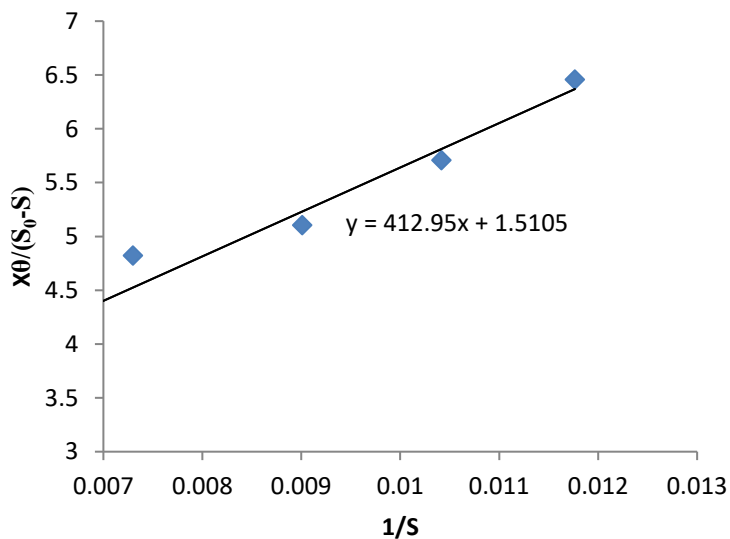


**Fig.4.27  $X_0/(S_0-S)$  Vs  $1/S$  graph for effluent after HPF process**

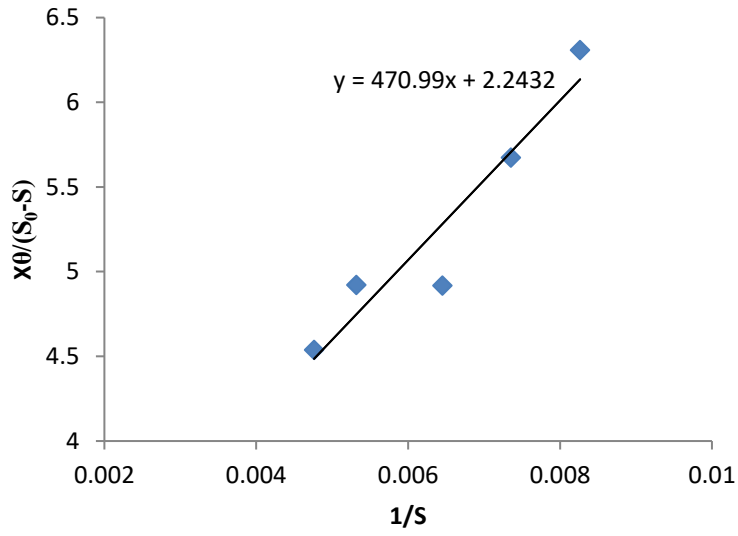


**Fig.4.28  $X\theta/(S_0-S)$  Vs  $1/S$  graph for effluent after HSPF process**

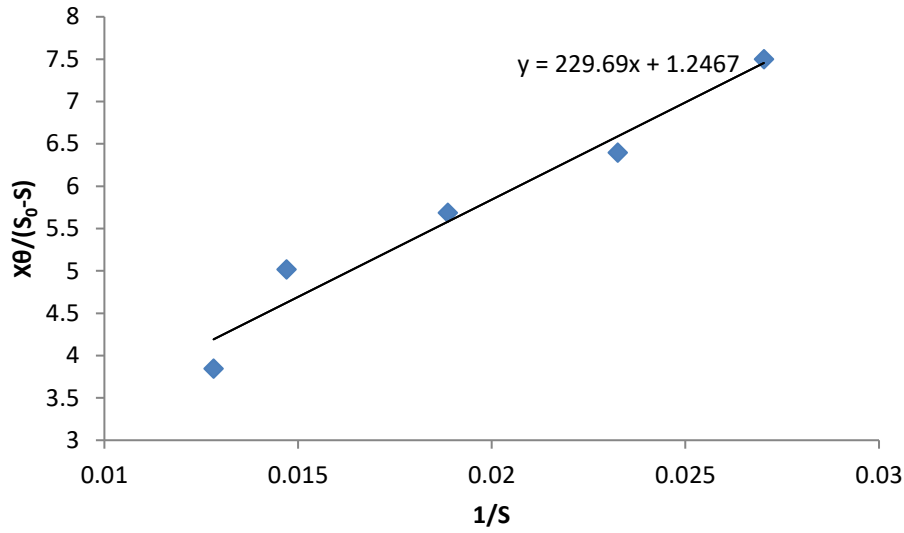


**Fig.4.29  $X\theta/(S_0-S)$  Vs  $1/S$  graph for effluent after APF process**

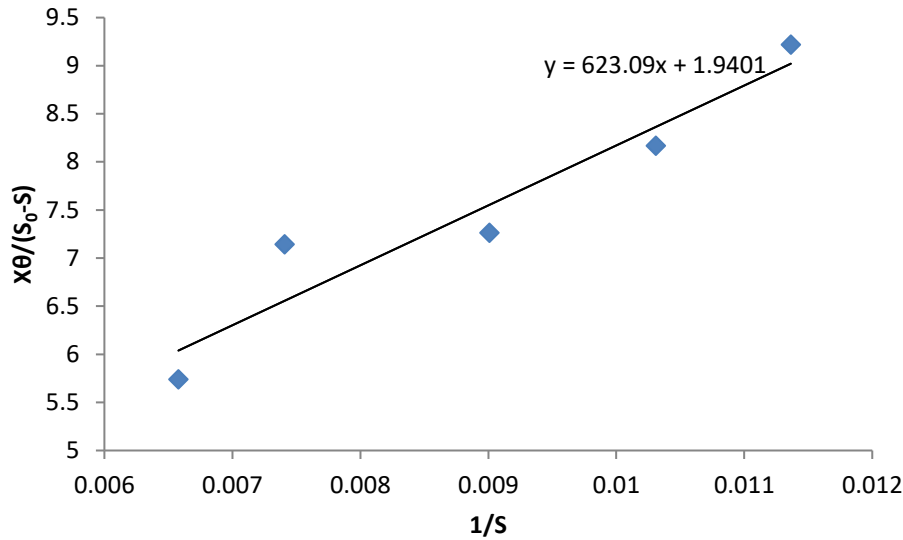


**Fig.4.30 X0/(S0-S) Vs 1/S graph for effluent after ASPF process**

SVI is calculated by measuring the settled sludge volume and mixed liquor suspended solid concentration. Total sludge produced from all the four processes has also been measured and presented in terms of kg of COD removed. The values of k, Ks, SVI and sludge formed are given in Table 4.18.

**Table 4.18 Values of k, Ks and SVI**

Process	k, d <sup>-1</sup>	Ks, mg/l	SVI, ml/g	Sludge, (kg/kg COD removed)
Raw waste	0.185	667	243	
Effluent after HPF process	0.662	273.4	185	0.0018
Effluent after HSPF process	0.446	210.0	98	0.0010
Effluent after APF process	0.803	184.3	162	0.0013
Effluent after ASPF process	0.515	321.0	85	0.0011

Improved value of k due to the treatment appeals increase in the utilization capacity of organic matter by the microorganisms and the subsequent decrease in Ks shows the increase in

specific growth rate of microorganisms [Metcalf & Eddy, 2003]. These two factors clearly define the enhanced biodegradability after HPF, HSPF, APF and ASPF processes. The  $k$  value is more for the effluent after HPF and APF processes, due to the increased biochemical degradation rate. This may be the cause of low BI for the effluent after these processes. The value of SVI in the range 50-150 mL/g shows the satisfactory sludge settling characteristics [Bartosz et al, 2017]. High SVI value in raw effluent sludge is due to the presence of filamentous bacteria which creates treatment problems [Chan & Koe, 1991]. Reduction in SVI reflects the absence of these bacteria after all the four treatments. The effluent after HSPF and ASPF processes have SVI in the range 50-150 mL/g as solar irradiation is found to have better ability to destroy the filamentous bacteria. High value of SVI shows that the sludge characteristics for the effluent after APF and HPF processes are not much satisfactory. All the four processes create small quantities of sludge.

#### **4.14 Gas chromatographic analysis after ASPF process**

GC-MS Analysis for the raw effluent and effluent after ASPF process has been done to determine the characteristics. Fig.4.31 & 4.32 presents the gas chromatograms for the effluent before and after treatment. The peaks in the effluent before treatment are due to dyes and their derivatives. Most of the peaks are eliminated or reduced after treatment through ASPF process which can be seen in figures. Table 4.19 shows the compounds which are eliminated or reduced by treatment.

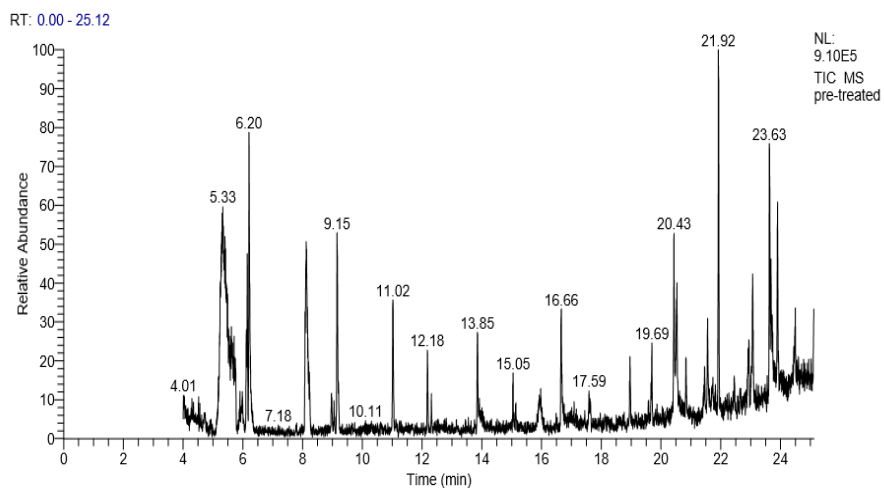


**Fig.4.31 Gas Chromatogram for untreated textile effluent**

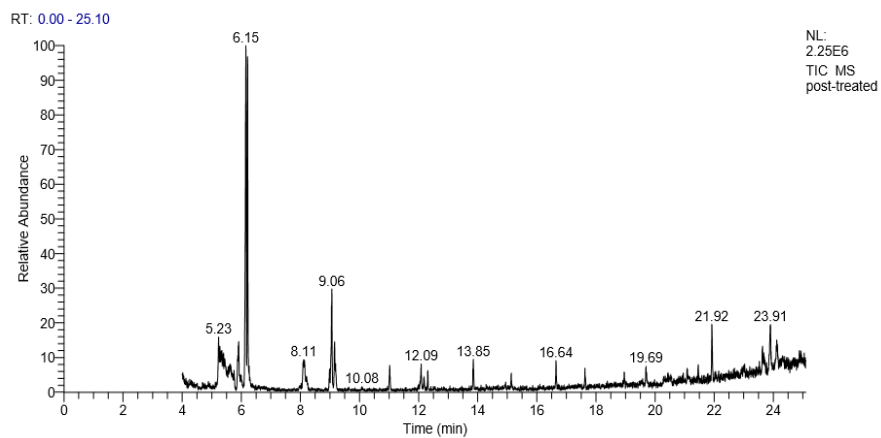


**Fig.4.32 Gas chromatogram for effluent after ASPF treatment**

**Table 4.19 GC results before and after treatment**

Name of Compound	RT	Area,%		% reduction
		Before	After	
Cyclotrisiloxane, hexamethyl	5.33	14.35	3.04	78.8
Benzyl alcohol, benzyldimethyl silyl ether	6.15	4.64	31.28	-
Cyclotetrasiloxane, octamethyl	8.12	11.48	0.04	99.7
Diisopropoxy hexamethyl trisiloxane	9.15	5.03	3.29	34.6
Cyclopentasiloxane, decamethyl	11.02	3.03	1.41	53.5
Isopropoxy hexamethyl tris tetrasiloxane	16.66	2.60	1.30	50.0
Cyclooctasiloxane, hexadecamethyl	18.96	1.21	0.14	88.4
Octasiloxane hexadecamethyl	20.53	2.81	0	100.0
Hexadecanoic acid, methyl ester	21.92	8.26	3.53	57.3
Cyclodecasiloxane, eicosamethyl	22.94	1.19	0	100.0
Octadecanoic acid, methyl ester	23.63	10.03	1.11	88.9
Heptacosanoic acid, methyl ester	23.90	3.62	0	100.0

The compounds, Octasiloxane hexadeca methyl, Cyclodecasiloxane eicosamethyl and Heptacosanoic acid methyl ester have been fully eliminated by the treatment. The compounds Cyclotrisiloxane hexamethyl, Cyclotetrasiloxane octamethyl, Diisopropoxy hexamethyl trisiloxane, Cyclopentasiloxane decamethyl, Isopropoxy hexamethyl tris tetrasiloxane, Cyclooctasiloxane hexadecamethyl, Hexadecanoic acid methyl ester and Octadecanoic acid methylester have been reduced. Only one compound namely benzyl alcohol, benzyl dimethyl silyl ester increased after treatment. Benzyl alcohol is the solvent used in textile industry and this compound and its derivatives are found at short retention time with low molecular weight which are not toxic and will be easily mineralized. Gas chromatogram results prove that the

presence of solar light and nZVI in Fenton process successfully reduced the carcinogenic and harmful compounds present in the textile effluent and enhanced the biodegradability.

#### 4.15 Selection of pretreatment

The biodegradability index is greater than 0.40 and SVI is in the range 50-150 mL/g for the effluent after HSPF and ASPF processes. The increase in k value and decrease in Ks value indicates that the treatments enhanced the biodegradability and it is ready for subsequent biological treatment. The toxicity has been very much reduced after these treatments. Solar based pretreatments are cost-effective and eco friendly also. The effluent after HSPF as well as ASPF pretreatment becomes biologically compatible and its complete mineralization can be achieved by biological means. Hence, HSPF and ASPF treatments are taken as pre-treatments for the textile effluent to improve the biodegradability before MBBR treatment.

#### 4.16 Variation of BI with time

The pretreatments HSPF and ASPF are optimized at constant time, 30 minutes. These processes have been run at optimized conditions by varying contact time to assess whether the BI value attained 0.4 before 30minutes. Table 4.20 and Fig.4.33 shows variation of BI with time.

**Table 4.20 BI Vs Time in HSPF and ASPF process**

Time in mts.	BI	
	HSPF	ASPF
5	0.18	0.30
10	0.30	0.32

15	0.34	0.40
20	0.35	0.39
25	0.40	0.41
30	0.41	0.42

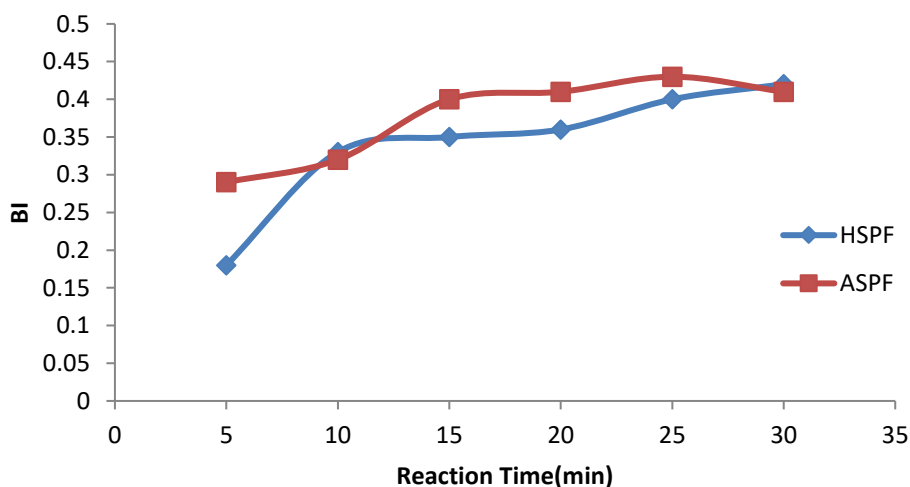


**Fig.4.33 Variation of BI with time**

From the graph, it is clear that the HSPF process and ASPF process attains BI 0.4 at 25minutes and 15minutes respectively. The COD degradation rate is more than that of BOD degradation rate in these processes which cause the increase of BI with time. Also, this degradation is taking place rapidly in ASPF process due to the presence of nZVI. Hence, the optimum conditions for HSPF pre-treatments are pH 2.6,  $\text{Fe}^{2+}$  dosage 39.5mg/l,  $\text{H}_2\text{O}_2$  dosage 63mM, contact time 25minutes and  $30 \pm 2 \text{ W/m}^2$  solar light intensity. The other pre-treatment is ASPF process at pH 2.6,  $\text{H}_2\text{O}_2$  dosage 62.6mM, nZVI dosage 38.7mg/l, contact time 15minutes and  $30 \pm 2 \text{ W/m}^2$  solar light intensity.

## 4.17 MBBR process after HSPF pretreatment

### 4.17.1 Design of experiment with analysis

Experimental runs to be performed to optimize the MBBR treatment are obtained using Box Behnken statistical design considering the factors pH, filling ratio of carrier materials and contact time. COD removal, BOD removal and color removal for each run have been determined. Table 4.21 gives the levels of factors in the BBD and Table 4.22 gives the experimental runs. Ranges of parameters are fixed after doing preliminary studies.

**Table.4.21 Levels of factors for BBD in MBBR Process**

Variables	Variable Levels	
	Low	High
pH	6	9
Filling Ratio (F.R) % of carrier materials	40	80
Contact Time(C.T) days	1	3

**Table 4.22 Experimental runs in BBD for MBBR after HSPF Pretreatment**

Run No.	pH	F.R. (%)	C.T., (d)	%COD removal	%BOD removal	%Color removal
1	9	60	1	62.25	45.99	80.13
2	9	60	3	68.20	54.88	89.20
3	6	40	2	66.78	51.89	86.82
4	9	80	2	64.64	52.83	87.30
5	6	60	1	61.58	41.98	78.98
6	7.5	80	3	68.98	55.76	90.30
7	7.5	80	1	60.43	39.46	74.32
8	7.5	40	1	62.83	42.94	77.48
9	7.5	60	2	78.62	66.98	91.12
10	9	40	2	70.37	57.45	82.22

11	6	60	3	76.97	64.05	88.60
12	7.5	60	2	78.42	66.98	89.02
13	7.5	60	2	79.08	67.84	89.86
14	6	80	2	74.87	61.34	82.14
15	7.5	40	3	70.99	57.78	78.44

**Table 4.23 Results of Regression Analysis for COD removal in MBBR after HSPF**

Term	Coeff.	SE Coeff.	T	p
constant	-175.961	22.8524	-7.700	0.001
pH	35.826	4.9099	7.297	0.001
F.R.%	2.489	0.2761	9.013	0.000
C.T.,days	45.892	4.8038	9.553	0.000
pH*pH	-1.800	0.3087	-5.831	0.002
F.R.*F.R.	-0.014	0.0017	-7.908	0.001
C.T.*C.T.	-7.407	0.6945	-10.666	0.000
pH*F.R.	-0.115	0.0222	-5.178	0.004
pH*C.T.	-1.573	0.4448	-3.537	0.017
F.R.*C.T.	0.005	0.0334	0.146	0.890
R <sup>2</sup> =98.56%    R <sup>2</sup> (adj)=95.96%    R <sup>2</sup> (pred)=77.41%				

**Table 4.24 Results of Regression Analysis for BOD removal in MBBR after HSPF**

Term	Coeff.	SE Coeff.	T	p
constant	-243.025	29.1079	-8.349	0.000
pH	39.583	6.2539	6.329	0.001
F.R.%	2.958	0.3517	8.411	0.000
C.T.,days	68.011	6.1188	11.115	0.000
pH*pH	-1.922	0.3932	-4.889	0.005
F.R.*F.R.	-0.018	0.0022	-7.986	0.000
C.T.*C.T.	-11.217	0.8846	-12.681	0.000
pH*F.R.	-0.117	0.0283	-4.139	0.009
pH*C.T.	-2.197	0.5666	-3.877	0.012
F.R.*C.T.	0.018	0.0425	0.429	0.685
R-sq=98.83%    R-sq(adj)=96.74%    R-sq(pred)=81.90%				

**Table 4.25 Results of Regression Analysis for color removal in MBBR after HSPF**

Term	Coeff.	SE Coeff.	T	p
constant	54.7563	25.8637	2.117	0.008
pH	0.2125	5.5569	0.038	0.007
F.R.%	0.4923	0.3125	1.575	0.005
C.T.,days	14.3913	5.4368	2.647	0.006
pH*pH	-0.2861	0.3493	-0.819	0.450
F.R.*F.R.	-0.0118	0.0020	-6.026	0.002

C.T.*C.T.	-5.1288	0.7860	-6.525	0.001
pH*F.R.	0.0813	0.0252	3.231	0.023
pH*C.T.	-0.0917	0.5034	-0.182	0.863
F.R.*C.T.	0.1877	0.0378	4.972	0.004
R <sup>2</sup> =97.34%      R <sup>2</sup> (adj)=92.55%      R <sup>2</sup> (pred)=64.59%				

Tables 4.23, 4.24 and 4.25 gives the regression coefficients for %COD removal, % BOD removal and %color removal respectively. The low p value and high T value indicate that, all terms except the interaction term between filling ratio of carrier materials and contact time are significant in %COD and %BOD reduction. High value of regression coefficient for contact time unveiled its predominant significance in COD and BOD elimination. This may be because of the release of extracellular enzymes excreted by the bacteria responsible for the organic content degradation which depends mainly on contact time (Metcalf & Eddy, 2003). The square factor of pH and interaction between pH and contact time are not significant in color removal. High R<sup>2</sup> value indicates that the model fits with the data. R<sup>2</sup>(adj) value reveals that the model satisfied with the independent variables. High R<sup>2</sup>(pred) value confirms that the model is ready for predicting the response with new sets of observations.

#### 4.17.2 Optimization of results

Optimization plot (Fig.4.34) given by BBD for percentage removals indicates that under optimum conditions of pH 7.06, percentage filling ratio of carriers 62.2% and contact time 2.41 days, MBBR with bacteria inoculated carrier materials after pre-treating by HSPF process assured COD reduction 79.9%, BOD reduction 68.9% and color reduction 91%.

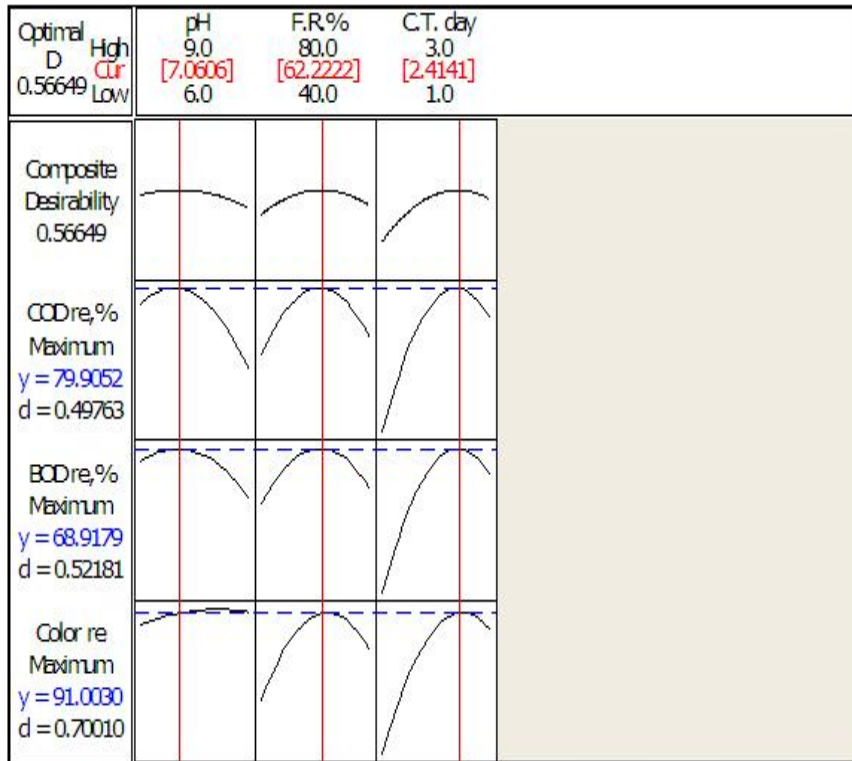


Fig. 4.34 Optimization Plot for % removals in MBBR after HSPF pretreatment

#### 4.17.3 Contour plots and Main effects plots for %removals

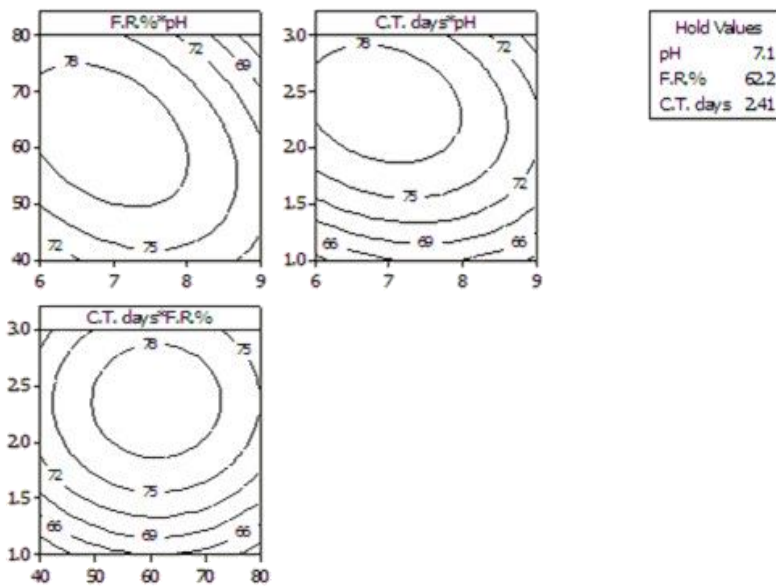
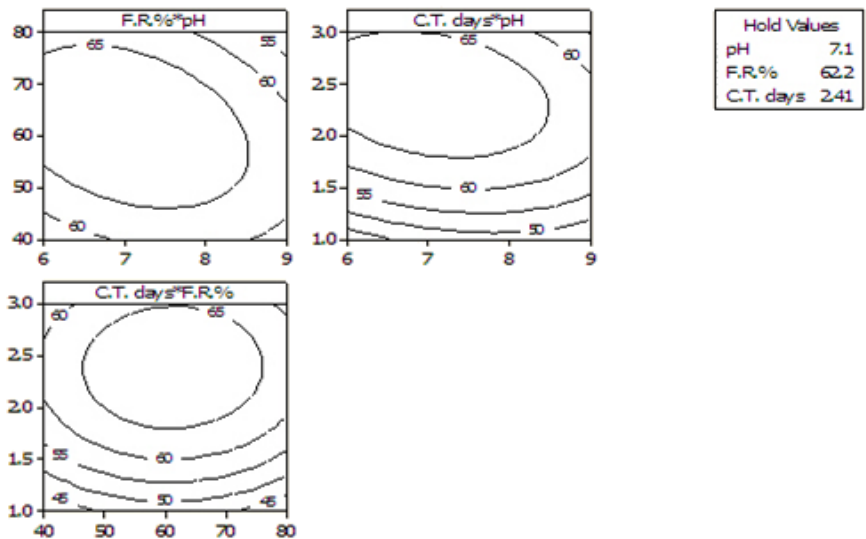
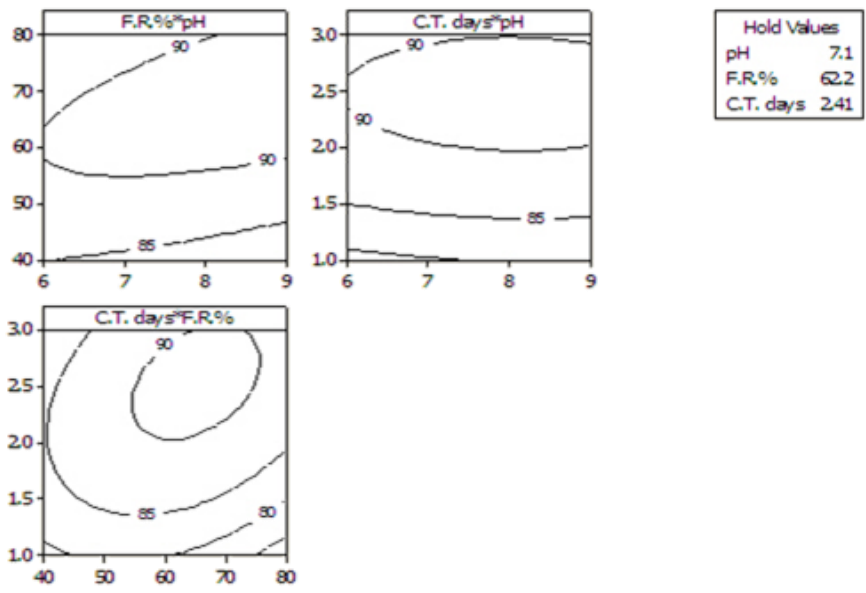


Fig.4.35 Contour Plots for COD removal in MBBR after HSPF pretreatment



**Fig.4.36 Contour Plots for BOD removal in MBBR after HSPF pretreatment**



**Fig.4.37 Contour Plots for color removal in MBBR after HSPF pretreatment**

Contour plots in figures 4.35 to 4.37 explore the relationship of any two variables, pH, filling ratio or contact time with responses, %COD reduction, %BOD reduction or %Color reduction. These are drawn under optimum conditions of variables. It can be shown by the

contour plots that the percentage removals have been increased with variables pH, F.R and C.T. up to the optimum value. On increasing above the optimum, the removals have been decreased. When filling ratio of carrier materials is very low, oxygen transfer efficiency will be poor which will adversely affect the organic removal. On increasing the filling ratio, the bacterial load will be increased which will increase the organic removal also. When it is more than 62.2%, proper mixing will not occur inside the reactor which will reduce the reduction efficiency. Maximum efficiency is observed in pH 7.1 as the azoarcus bacteria inoculated in the carrier materials shows optimum growth in that pH. As contact time increases removal efficiency increases up to 2.41 days and after that slight decrease in efficiency because of bacterial death due to lack of feed which increases the biological load.

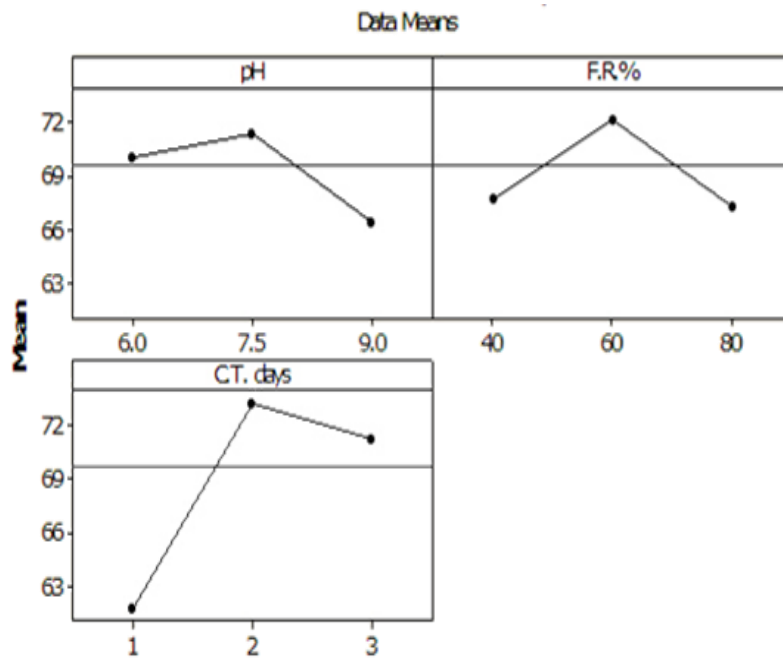


**Fig.4.38 Main effects plot for COD removal in MBBR after HSPF process**

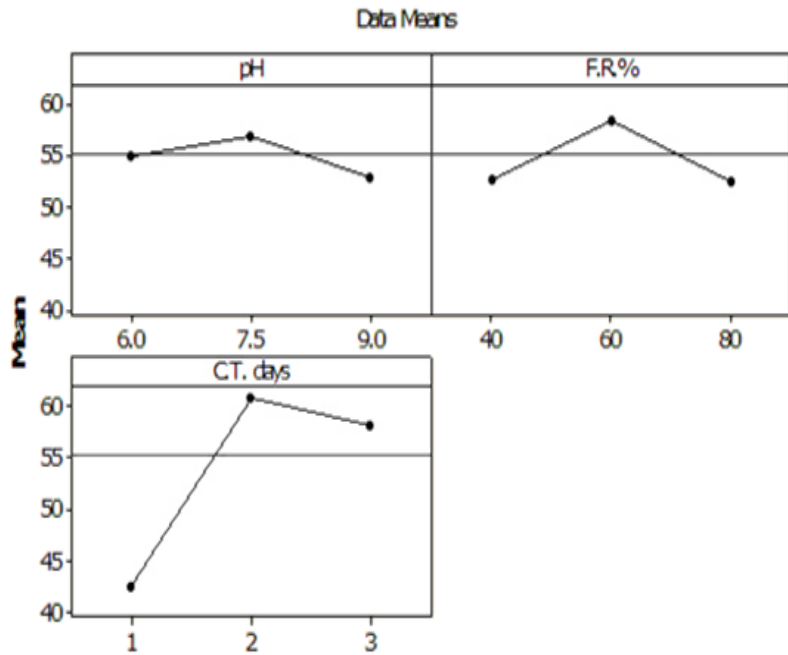


**Fig.4.39 Main effects plot for BOD removal in MBBR after HSPF process**

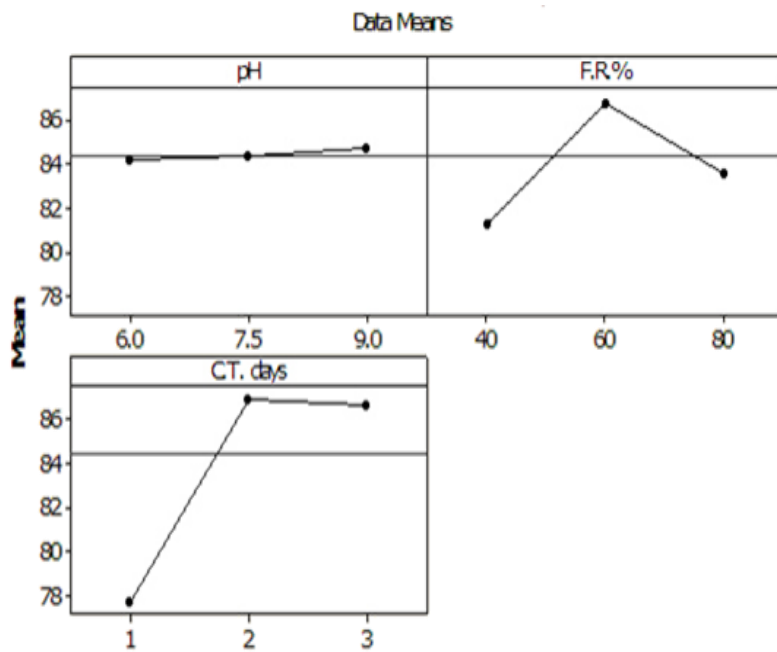


**Fig.4.40 Main effects plot for color removal in MBBR after HSPF process**

Main effects plot (Fig.4.38, 4.39 & 4.40) for %COD removal, %BOD removals and %color removal show the same trend as in the case of contour plots. Contact time shows more

significance than other two variables in percentage removals as discussed earlier in the regression analysis.

After treatment through MBBR pretreated by HSPF process, the effluent COD is 197mg/l and BOD is 65mg/l. As the effluent BOD less than 100mg/l is the effluent standard for irrigation purpose as per E(P) rules, the effluent can be disposed as irrigation water. However, it is greater than 30mg/l which is the effluent standard for disposing into inland waters, the effluent cannot be disposed into inland waters. Hence a modification is needed for meeting the effluent standards disposing into inland waters.

#### **4.18 MBBR induced with magnetic field**

The effect of magnetic field is studied by varying the exposure time and magnetic field intensity and observing the %COD and BOD reduction. MBBR has been run under the optimum conditions of pH 7.06, filling ratio of carrier materials 62.2% and contact time 2.41days. Experiment was conducted by varying one variable, keeping the other constant. Table 4.26 and Fig.4.41 shows the variation of %COD removal for various exposure time by keeping the magnetic field intensity as 5mT. The maximum COD removal is obtained at 12 hours.

**Table 4.26 Variation of COD removal with exposure time for MBBR with magnetic field after HSPF**

Exposure time (hrs)	0	4	8	12	16
%COD removal	79.9	81.2	82.5	83.2	83.1

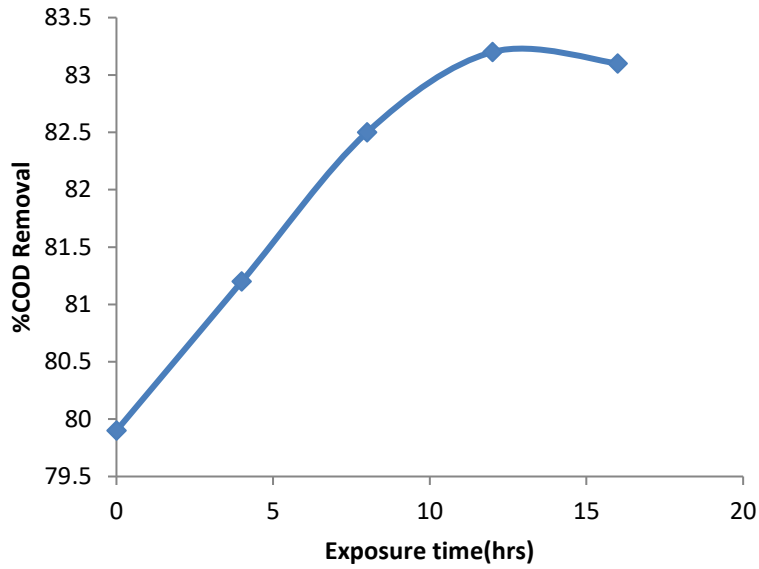


**Fig.4.41 COD removal versus exposure time in magnetic field induced MBBR after HSPF**

By keeping the exposure time as 12 hours, the magnetic field intensity has been varied and %BOD and %COD removal have been computed. The maximum BOD and COD removals are obtained as at 12mT as in Table 4.27 and Fig.4.42.

**Table 4.27 Variation of COD and BOD removal with field intensity for MBBR with magnetic field after HSPF**

Field intensity, mT	4	6	8	10	12	14
%COD removal	80.2	82.3	84.8	85.9	86.9	85.3
%BOD removal	69.1	72.3	76.2	80.8	85.8	85.0

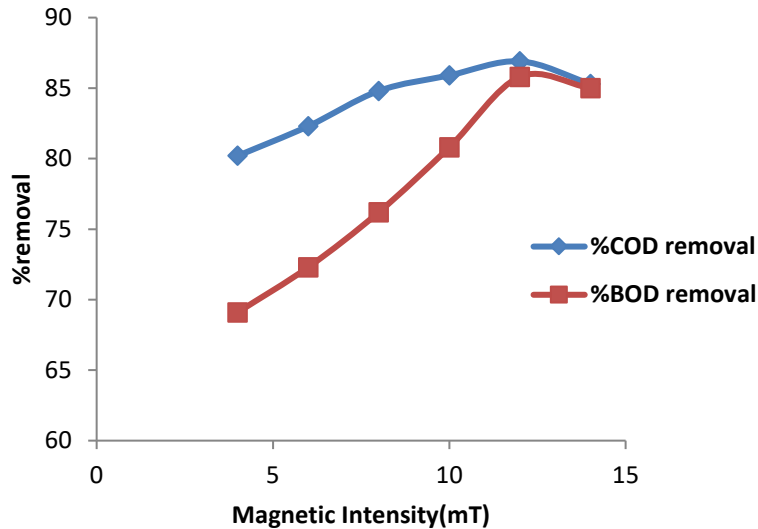


**Fig.4.42 % removals versus field intensity in magnetic field induced MBBR after HSPF**

The percentage removals increased with respect to magnetic field intensity upto 12 mT. The maximum tolerance limit of field intensity of azoarcus bacteria is 12 mT at an exposure time of 12 hours. The induction of magnetic field enhances the enzyme activity of bacteria. This is due to the improvement in physical properties like conductivity, surface tension etc, which cause the adsorption of paramagnetic oxygen from atmosphere, resulting in higher oxidation efficiency (Zaidi et al, 2014). By exposing the MBBR to magnetic field intensity 12mT at an exposure time of 12hours, BOD reduced to 29.8mg/l and COD reduced to 128.4mg/l. Hence the effluent can be disposed into inland waters.

## **4.19 MBBR process after ASPF pretreatment**

### **4.19.1 Design of experiment with analysis**

Experimental runs to be performed to optimize the MBBR treatment are obtained using Box Behnken statistical design considering the factors pH, filling ratio and contact time. COD removal, BOD removal and color removal for each run have been determined. Table 4.28 gives

the experimental runs. Ranges of parameters are same as explained in Table 4.21.

**Table 4.28 Experimental runs in BBD for MBBR process after ASPF pretreatment**

Run No.	pH	F.R. (%)	C.T. (d)	%COD removal	%BOD removal	%Color removal
1	6	60	3	53.88	43.50	80.62
2	9	40	2	84.30	63.04	84.03
3	6	80	2	80.92	60.90	88.18
4	7.5	60	2	83.20	69.95	94.15
5	9	60	3	56.82	46.46	89.98
6	7.5	60	2	81.42	69.92	94.40
7	7.5	40	3	54.84	44.08	82.40
8	7.5	80	3	60.44	50.48	86.42
9	7.5	40	1	70.90	52.87	76.73
10	6	60	1	69.86	53.58	79.32
11	9	80	2	72.90	54.02	81.45
12	9	60	1	65.84	43.90	71.82
13	7.5	60	2	82.12	71.90	94.32
14	7.5	80	1	64.02	45.02	66.44
15	6	40	2	74.57	54.38	77.40

**Table 4.29 Results of Regression Analysis for COD removal in MBBR after ASPF**

Term	Coeff.	SE Coeff.	T	p
constant	-84.455	21.592	-3.911	0.011
pH	23.3547	4.6391	5.034	0.004
F.R.%	1.2264	0.2609	4.701	0.005
C.T.,days	48.8983	4.5389	10.773	0.000

pH*pH	-1.1165	0.2916	-3.828	0.012
F.R.*F.R.	-0.0039	0.0016	-2.381	0.063
C.T.*C.T.	-18.1346	0.6562	-27.636	0.000
pH*F.R.	-0.1479	0.0210	-7.039	0.001
pH*C.T.	1.1600	0.4203	2.760	0.040
F.R.*C.T.	0.1560	0.0315	4.949	0.004
R <sup>2</sup> =99.51%    R <sup>2</sup> (adj)=98.62%    R <sup>2</sup> (pred)=93.48%				

**Table 4.30 Results of Regression Analysis for BOD removal in MBBR after ASPF**

Term	Coeff.	SE Coeff.	T	p
constant	-217.439	28.5915	-7.605	0.001
pH	49.003	6.1430	7.977	0.000
F.R.%	2.278	0.3455	6.595	0.001
C.T.,days	39.561	6.0102	6.582	0.001
pH*pH	-3.057	0.3862	-7.917	0.001
F.R.*F.R.	-0.014	0.0022	-6.475	0.001
C.T.*C.T.	-16.851	0.8689	-19.394	0.000
pH*F.R.	-0.129	0.0278	-4.654	0.006
pH*C.T.	2.107	0.5565	3.785	0.013
F.R.*C.T.	0.178	0.0417	4.267	0.008
R <sup>2</sup> =99.01%    R <sup>2</sup> (adj)=97.23%    R <sup>2</sup> (pred)=86.66%				

**Table 4.31 Results of Regression Analysis for color removal in MBBR after ASPF**

Term	Coeff.	SE Coeff.	T	p
constant	-118.966	42.9652	-2.760	0.039
pH	31.498	9.2312	3.412	0.019
F.R.%	2.584	0.5191	4.977	0.004
C.T.,days	11.076	9.0318	1.226	0.005
pH*pH	-2.019	0.5803	-3.480	0.018
F.R.*F.R.	-0.017	0.0033	-5.347	0.003
C.T.*C.T.	-9.311	1.3057	-7.131	0.001
pH*F.R.	-0.111	0.0418	-2.662	0.045
pH*C.T.	2.810	0.8363	3.360	0.020
F.R.*C.T.	0.179	0.0627	2.852	0.036
R <sup>2</sup> =96.73%    R <sup>2</sup> (adj)=67.70%    R <sup>2</sup> (pred)=90.84%				

Table 4.29, 4.30 and 4.31 show the regression coefficients for COD, BOD and color removals. All the terms are significant in BOD and color reduction. All the terms except square of filling ratio of carrier materials are significant in COD reduction. Regression coefficient says that contact time is the most significant term in COD removal, while in the case of BOD and color reduction, it is the pH. This may be due to the mineralization required in COD removal for which contact time is the most important, while in the case of BOD and color removal, growth rate of bacteria is the most important for which role of pH is very significant. Filling ratio of carrier materials has the least significance in COD, BOD and color removal. High R<sup>2</sup> values

indicate that the model fits with the data and it can be used effectively for predicting the responses with new observations.

#### 4.19.2 Optimization of results

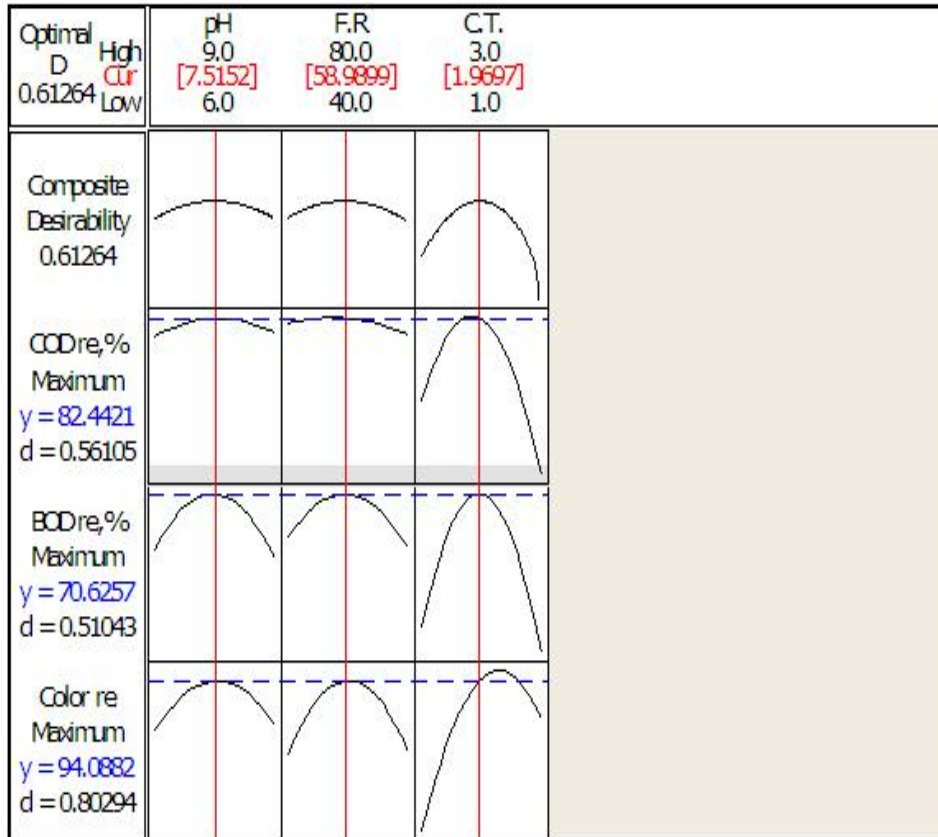


**Fig.4.43 Optimization plot for % removals in MBBR after ASPF pretreatment**

A COD removal of 82.4%, BOD removal of 70.6% and color removal of 94.1% can be seen from the optimization plot (Fig.4.43) under optimum conditions pH 7.5, filling ratio of carrier materials 59% and contact time 1.97 days.

### 4.19.3 Contour plots and Main effects plots for %removals

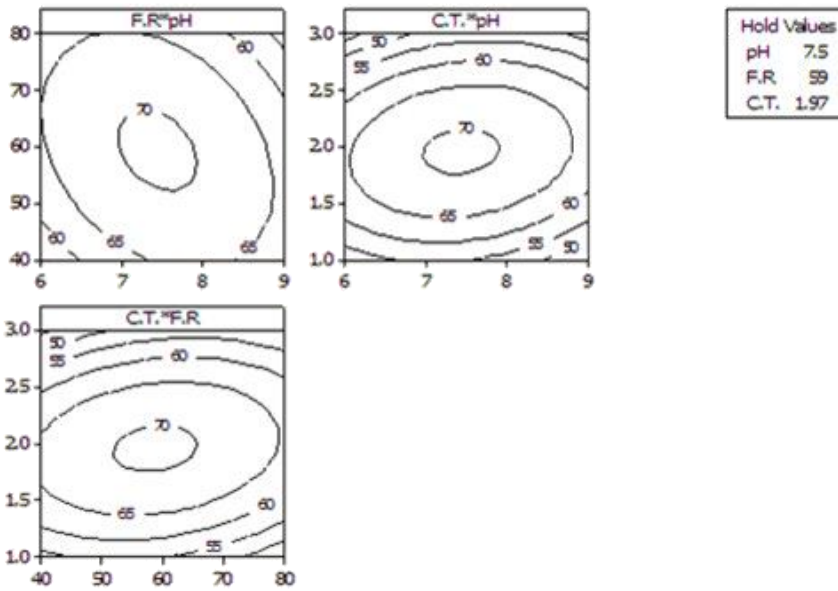


Fig. 4.44 Contour Plots for %BOD removal in MBBR after ASPF pretreatment

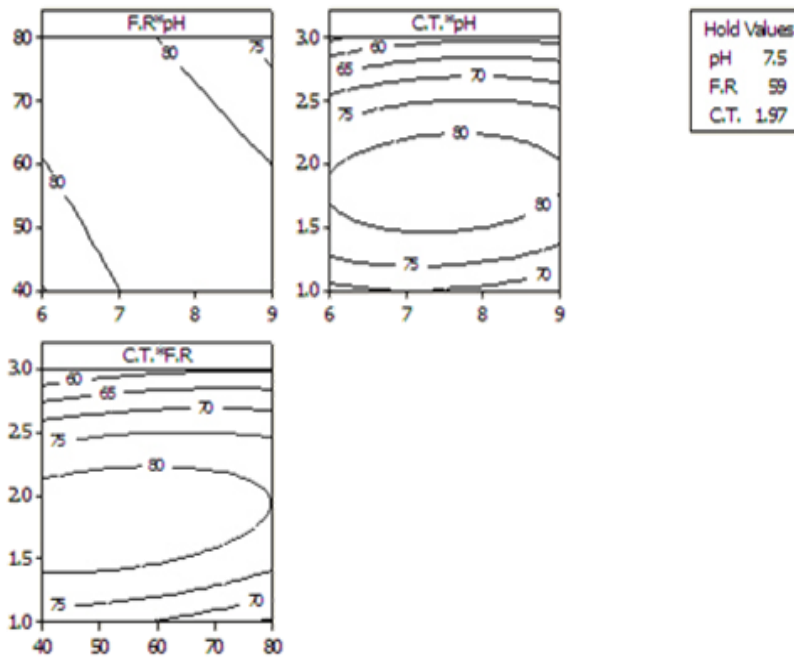
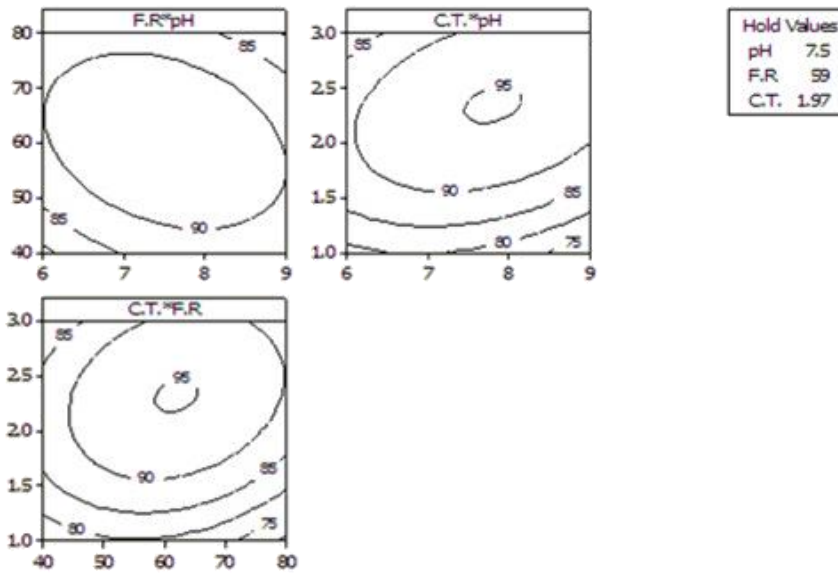
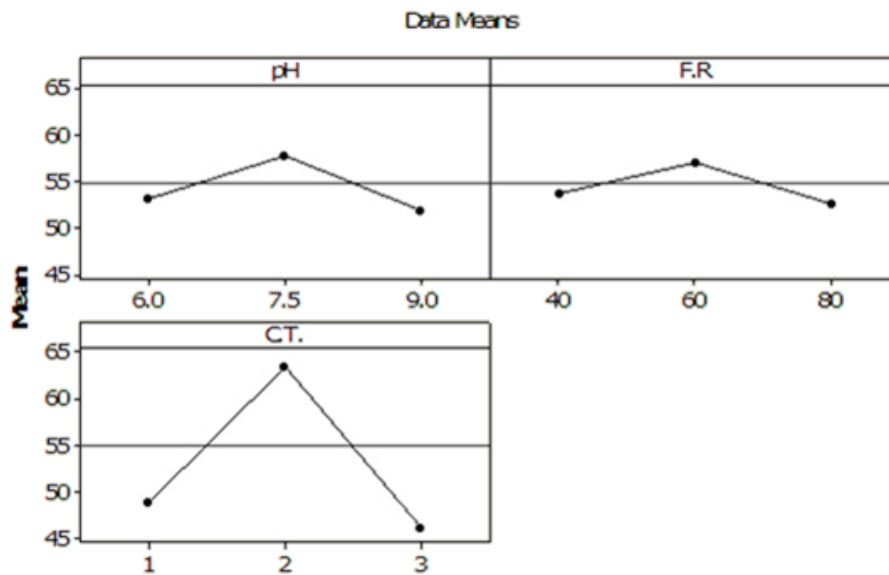


Fig.4.45 Contour Plots for %COD removal in MBBR after ASPF pretreatment



**Fig.4.46 Contour Plots for %color removal in MBBR after ASPF pretreatment**

Contour plots are drawn for percentage of BOD, COD and color removals in figures 4.44, 4.45 and 4.46. The behavior is the same as in the case of contour plots of MBBR after HSPF process. Increase in pH, carrier materials filling ratio and contact time above the optimum value cause a decrease in efficiency of degradation.



**Fig.4.47 Main effects plot for BOD removal in MBBR after ASPF process**

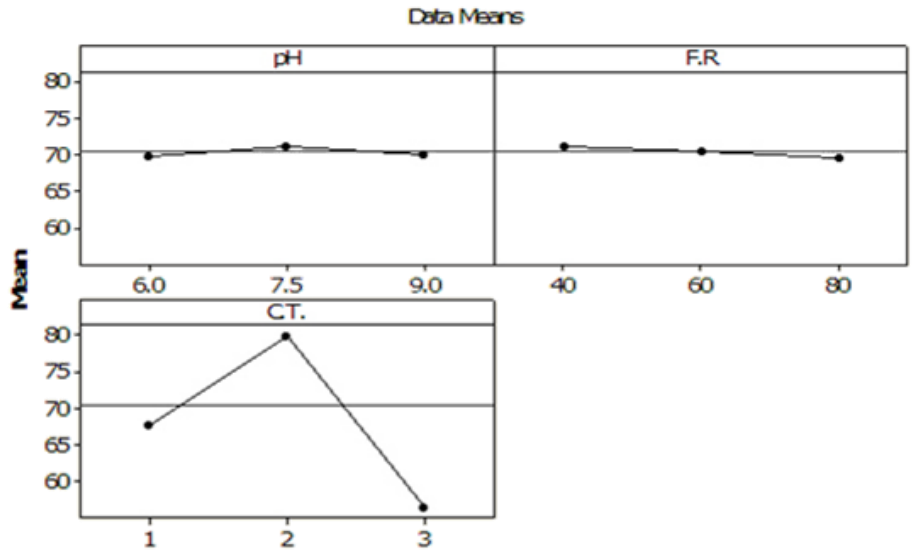


Fig.4.48 Main effects plot for COD removal in MBBR after ASPF process

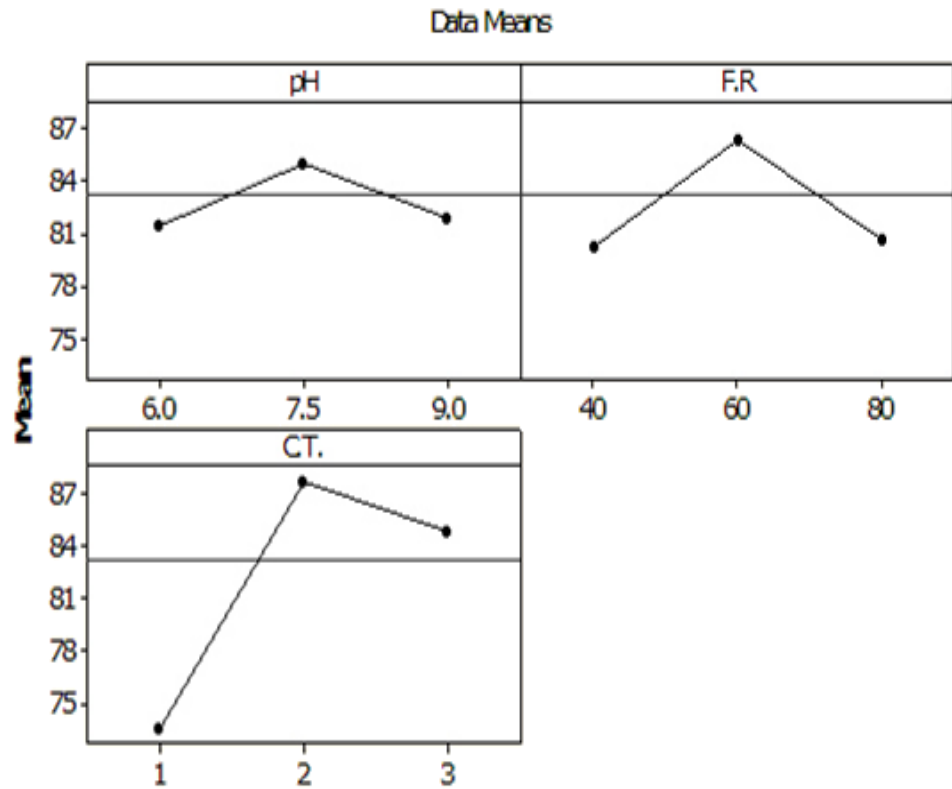


Fig.4.49 Main effects plot for color removal in MBBR after ASPF process

Main effects plot for BOD, COD and color removal has been given in figures 4.47, 4.48 and 4.49 respectively. The contact time is found to have more significance in degradation efficiency as discussed in section 4.19.1.

It has been found that after treatment through MBBR pretreated by ASPF process, the effluent COD is 172.5mg/l and BOD is 61.7mg/l. Hence, the effluent can be disposed as irrigation water. However, a modification is needed for the effluent to meet the standards for disposing into inland waters.

#### **4.20 MBBR induced with magnetic field after ASPF process**

The effect of magnetic field is studied by varying the exposure time and magnetic intensity and observing the %COD and BOD reduction. Table 4.32 and Fig.4.50 shows the variation of %COD removal for various exposure times by keeping the magnetic field intensity 5mT. After attaining a peak level of COD removal in 8 hours, it gets slightly reduced. The dropping of COD removal after peak may be due to the death of organisms which induces some amount of organic matter.

**Table 4.32 Variation of COD removal with exposure time for magnetic field induced MBBR after ASPF**

Exposure time (hrs)	0	4	8	12
%COD removal	82.4	83.1	85.8	85.6

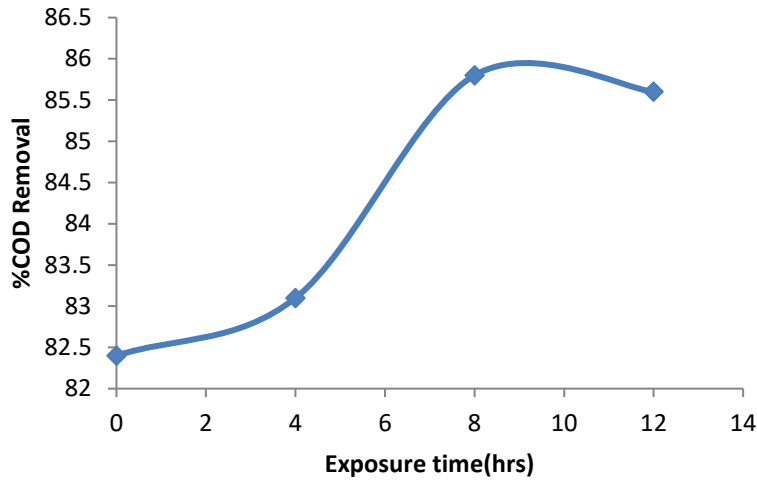


**Fig.4.50 COD removal versus exposure time in magnetic field induced MBBR after ASPF**

By keeping the exposure time as 8 hours, vary the magnetic field intensity and %BOD and %COD removal have been computed. The maximum BOD and COD removals are obtained as 86.5% and 90.2% respectively at magnetic field intensity 10mT as given by Table 4.33 and Fig.4.51.

**Table 4.33 Variation of COD and BOD removal with field intensity for magnetic field induced MBBR after ASPF**

Field intensity, mT	4	6	8	10	12	14
%COD removal	85.8	86.6	88.4	90.2	90.2	90.2
%BOD removal	74.5	76.1	83.8	86.8	86.8	86.8

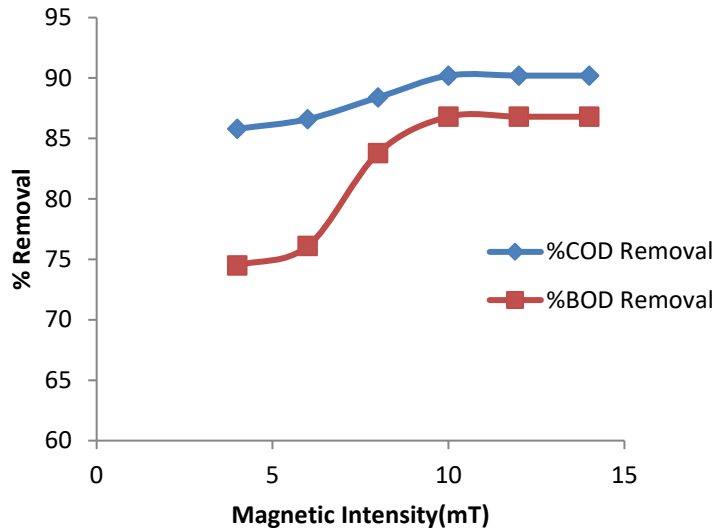


**Fig.4.51 %removals with field intensity in magnetic field induced MBBR after ASPF**

The percentage removals of COD and BOD increased as the magnetic field intensity increased up to 10 mT. The efficiency of azoarcus bacteria reaches maximum at 10 mT during an exposure time of 8 hours. The field intensity and exposure time for the integrated ASPF-MBBR treatment are lesser than those of the integrated HSPF-MBBR process. The decrease in these values may be due to the improvement in properties in the presence of nZVI. COD reduced to 96mg/l and BOD reduced to 28.3mg/L when MBBR exposed to a magnetic field intensity of 10mT during a time of 8 hours. Hence the effluent can be disposed into inland waters.

#### **4.21 Conductivity measurements**

Conductivity of the effluent after pretreatments and after MBBR with magnetic field have been found out and given in Table 4.34.

**Table 4.34 Conductivity measurements**

	Type of effluent	Conductivity, mS/cm
MBBR with HSPF	Raw waste	0.85
	After HSPF	0.97
	After MBBR	1.08
	After MBBR with magnetic field	1.52
MBBR with ASPF	Raw waste	0.85
	After ASPF	1.10
	After MBBR	1.19
	After MBBR with magnetic field	1.77

The conductivity of the effluent increased from 0.85ms/cm to 1.52 mS/cm in MBBR pre-treating by HSPF process and from 0.85 to 1.77 mS/cm in MBBR pre-treating by ASPF process, after inducing the magnetic field. In the absence of magnetic field, the value is only 1.08mS/cm and 1.19 mS/cm in MBBR after HSPF and ASPF process respectively. In the presence of magnetic field, the organic molecules in wastewater absorb energy and enter into an unstable excited state; this increased the chemical reaction rate which accelerated flocculation and improved the settling (Liu et al, 2011). Also, the biological organisms become more active in the presence of magnetic field. The higher conductivity, pH and osmotic pressure of magnetized water caused an increase in the permeability of cell membrane. This will improve the metabolic activities, mainly enzyme activity of bacteria. Again, the surface tension in water reduced due to the induction of magnetic field and it caused adsorption of paramagnetic oxygen from the atmosphere which increased the oxygen concentration in waste water and, thus the organic matter decomposition (Cheng et al, 2014). It can be seen that the conductivity is more for the effluent after ASPF process than that after HSPF process which may be due to the impact of nZVI. This is the cause of higher degradation rate for the effluent from MBBR pretreated by ASPF process.

## 4.22 Comparison of time, effluent BOD and COD after various treatment options

Reaction time required in various treatment options are given in Table 4.35 and Fig.4.52.

**Table 4.35 Reaction time required for various treatment options**

	Treatment options	Reaction time, days
I	Conventional MBBR	11
II	Modified MBBR	7
III	Modified MBBR after HSPF pretreatment	2.43
IV	Modified MBBR after ASPF pretreatment	1.98

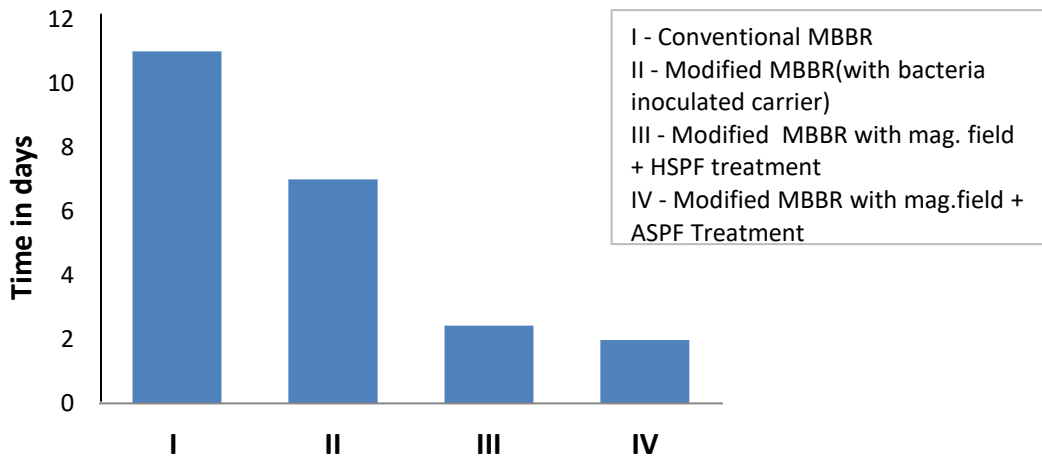


**Fig.4.52 Time versus Treatment Graph**

Reaction time required is in the decreasing order I>II>III>IV. Owing to the presence of bacteria inoculated carrier materials, magnetic field and nZVI, the reaction time can be

considerably reduced. BOD and COD of the effluent after each treatment are given in Tables 4.36 and 4.37 and figures 4.53 and 4.54. As per Fig.4.53, BOD is less than 30mg/l in the treatment options VI and IX in which pretreated effluent has been treated with modified MBBR induced with magnetic field, while it is less than 100mg/l in the treatment options II, III, V, VI, VIII and IX. As per Fig.4.54, COD is less than 250mg/l in the treatment options III, V, VI, VIII and IX. The effluent can be disposed as irrigation water as per E(P) rules after treatments III, V, VI, VIII and IX. The effluent can be disposed into inland water after treatments VI and IX.

**Table 4.36 Characteristics of Treated Effluent from MBBR with Magnetic Field pre-treating by HSPF**

Parameters	Raw effluent	After HSPF	After HSPF + MBBR	After HSPF + MBBR with magnetic field	Max. admissible concentration if discharged directly into	
					As per E(P) Rules 1984, IV(A)	
					Irrigation water	Inland waters
BOD(mg/l)	210	152	65	29.8	100	30
COD(mg/l)	980	381	197	128.4	-	250
pH	12	5	6.5	6.6	5.5-9	5.5-9
Alkalinity(mg/l)	1200	612	52	48	-	-
Chloride(mg/l)	180	120	20	19	1000	600
Hardness(mg/l)	64	50	22	20	-	-
Turbidity(NTU)	140	98	40	35	-	-
Sulphide(mg/l)	44	24	4	BDL	-	2

**Table 4.37 Characteristics of Treated Effluent from MBBR with Magnetic Field pre-treating by ASPF**

Parameters	Raw effluent	After ASPF	After ASPF + MBBR	After ASPF + MBBR with magnetic field	Max. admissible concentration if discharged directly into	
					As per E(P) Rules 1984, IV(A)	
					Irrigation water	Inland waters
BOD(mg/l)	210	151	61.7	28.3	100	30
COD(mg/l)	980	377	172.5	96	-	250
pH	12	5.5	6.5	6.6	5.5-9	5.5-9
Alkalinity(mg/l)	1200	606	50	44	-	-
Chloride(mg/l)	180	112	18	15	1000	600
Hardness(mg/l)	64	48	20	18	-	-
Turbidity(NTU)	140	88	44	32	-	-
Sulphide(mg/l)	44	19	2	2	-	2

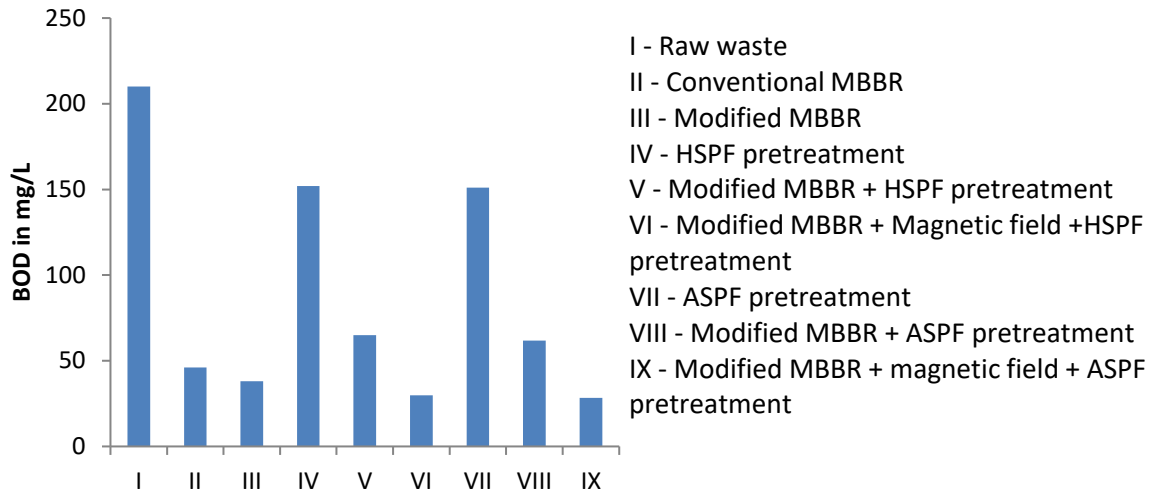


**Fig.4.53 BOD versus Treatment Graph**

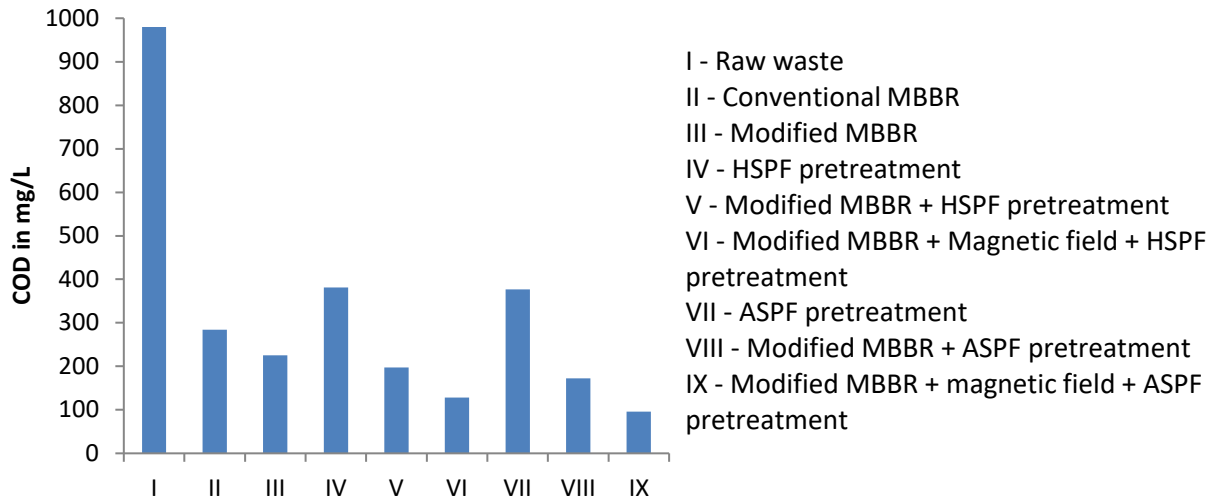


**Fig.4.54 COD versus Treatment Graph**

### 4.23 Cost analysis

Table 4.38 and 4.39 show the capital cost and operating cost of the integrated system (HSPF+MBBR with magnetic field), and Table 4.40 and 4.41 show that of the integrated system (ASPF+MBBR with magnetic field).

**Table 4.38 Capital cost of the Integrated system (HSPF+MBBR)**

	Unit	Rate (Rs/m <sup>3</sup> )	Amount	Life (yrs)	Annualized Capital Cost (Rs/yr)
HSPF	HSPF Reactor (9.1m <sup>3</sup> )	10,000	91,000	15	11,964
	Pumps	300	30,000	15	3,944
	Power supply unit	3,750	375,000	15	49,303
MBBR	MBBR Reactor(241m <sup>3</sup> )	12,000	618,000	50	62,331
	Carriers	600	60,000	5	15,828
	Copper wire	50	10,150	10	1,660
	Total Cost (Rs/yr)				145,030
	Total Cost (Rs/m <sup>3</sup> )				3.97

**Table 4.39 Operating cost of the Integrated system (HSPF+MBBR)**

	Operating cost (Rs./m <sup>3</sup> )			Operating cost, Rs./yr
	HSPF	Chemical cost	63.19	Rs./m <sup>3</sup>
Electricity Consumption		0.01	kWh/m <sup>3</sup>	
Electricity cost		0.055	Rs./m <sup>3</sup>	2007.5
MBBR	Electricity Consumption	0.13	kWh/m <sup>3</sup>	
	Electricity cost	0.715	Rs./m <sup>3</sup>	26097.5
	Sludge management cost	4	Rs./m <sup>3</sup>	14600
	Total cost (Rs/year)			2,480,540
	Total cost (Rs/m <sup>3</sup> )			68

Total cost of the Integrated system = Rs 71.97/m<sup>3</sup> (\$1.03/m<sup>3</sup>)

**Table 4.40 Capital cost of the Integrated system (ASPF+MBBR)**

	Unit	Rate (Rs/m <sup>3</sup> )	Amount	Life (yrs)	Annualized Capital Cost (Rs/yr)
ASPF	ASPF Reactor (7.14m <sup>3</sup> )	10,000	71,400	15	9,387
	Pumps	300	30,000	15	3,944
	Power supply unit	3,750	375,000	15	49,303
MBBR	MBBR Reactor (197m <sup>3</sup> )	12,000	552,000	50	55,674
	Carriers	600	60,000	5	15,828
	Copper wire	50	10,150	10	1,660
	Total Cost (Rs/yr)				135,796
	Total Cost (Rs/m <sup>3</sup> )				3.72

**Table 4.41 Operating cost of the Integrated system (ASPF+MBBR)**

	Operating cost (Rs./m <sup>3</sup> )			Operating cost, Rs./yr
	ASPF	Chemical cost	62.65	Rs./m <sup>3</sup>
Electricity Consumption		0.01	kWh/m <sup>3</sup>	
Electricity cost		0.055	Rs./m <sup>3</sup>	2007.5
MBBR	Electricity Consumption	0.18	kWh/m <sup>3</sup>	
	Electricity cost	0.99	Rs./m <sup>3</sup>	36135
	Sludge management cost	2.1	Rs./m <sup>3</sup>	76650
	Total cost(Rs/yr)			2,401,518
	Total cost (Rs/m <sup>3</sup> )			65.8

Total cost of the Integrated system = Rs 69.52/m<sup>3</sup> (\$0.99/m<sup>3</sup>)

Table 4.42 consolidated the cost analysis and corresponding graph is given in Fig.4.55.

**Table 4.42 Consolidated cost analysis**

	Treatment options	Annualized capital cost, Rs/m <sup>3</sup>	Operating cost, Rs/m <sup>3</sup>	Total cost, Rs/m <sup>3</sup>
I	MBBR with magnetic field after HSPF	3.97	68.00	71.97
II	MBBR with magnetic field after ASPF	3.72	65.80	69.52

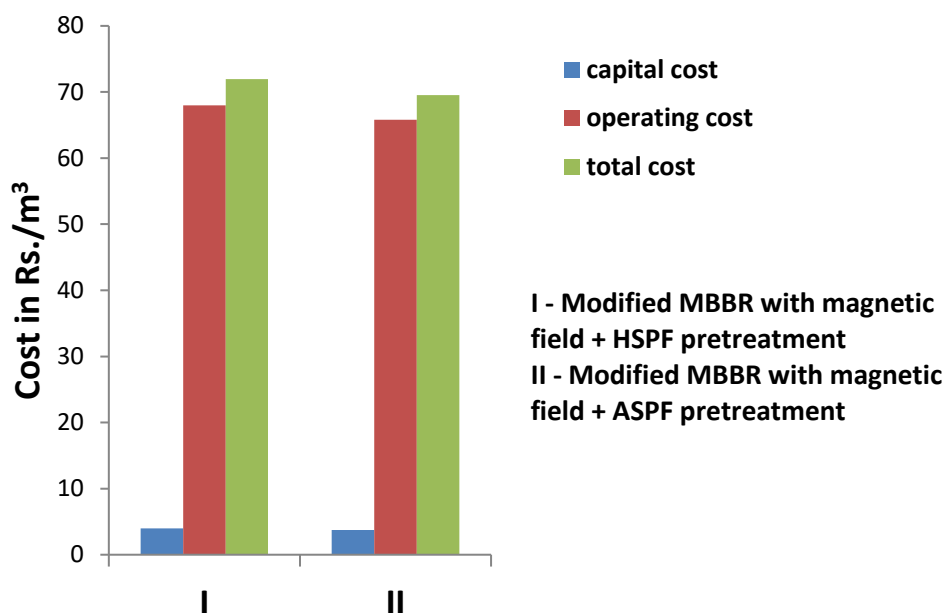


**Fig.4.55 Cost versus Treatment graph**

It can be seen that the annualized capital cost, operating cost and hence the total cost of the treatment is less for the integrated system with ASPF pretreatment. Annualized capital cost directly related to contact time and hence the volume required for the reactor, which increases the construction cost. As the contact time required in treatment II is less, the capital cost decreases. Operating cost is mainly due to the cost of chemicals which is small in treatment II. On comparing the costs of the treatments I and II, treatment II (MBBR induced with magnetic field after ASPF pre-treatment) incurred slightly less expense due to the use of nZVI.

# CHAPTER 5

## CONCLUSION

Textile industry discharges colored wastewaters containing synthetic dyes into water bodies which will adversely affect the aquatic environment. It is necessary to treat the wastewater before it is discharged. The conventional physicochemical and biological treatment methods are insufficient for textile wastewater treatment. The objective of this thesis is to propose an optimal integral treatment scheme minimizing the total treatment cost. The integral treatment consists of an advanced oxidation process as the pretreatment to enhance the biodegradability of the wastewater followed by a biological treatment.

The present investigation revealed that the textile effluent can be treated with MBBR with textile sludge inoculum without any pre-treatment. However, the contact time required is very large as 11days. The treatment has been undergone under pH 8 and filling ratio of carrier materials 70%. Maximum COD removal attained after the treatment is 71%, while it is 78% in the case of BOD removal. As the effluent COD and BOD are 284mg/l and 46mg/l respectively, the effluent meets the standards for disposing into irrigation water. However, it does not meet the standards of effluent for disposing into inland water bodies.

The dominant bacteria present in the textile sludge which has been isolated by serial plate dilution method and identified by 16S rRNA method was azoarcus bacteria. When azoarcus bacteria inoculated carrier materials are used in the MBBR, the contact time was reduced to 7 days attaining a COD removal of 77% and BOD removal 82%. Here also, though the effluent is ready for irrigation purpose as its COD and BOD are 225mg/l and 38mg/l respectively, it cannot be disposed into inland water bodies. The long treatment period is due to the small biodegradability index of textile effluent.

The nZVI produced from *Amaranthus Dubius* leaf extract is found to have average size in the range 2.5nm to 10nm and surface area 3.74m<sup>2</sup>/gram and can be used successfully in photo Fenton process.

Toxicity studies for the effluent after various AOPs, namely HPF, HSPF, APF and ASPF processes have been conducted and found that solar based processes have performed better in reducing toxicity, while it was slightly less in the processes containing nZVI.

The catalyst, biosynthesized nZVI exhibits excellent reusability. It can be used effectively up to third cycle without very much loss in efficiency and after that the degradation efficiency is found to reduce. The high removal efficiency and low levels of iron leaching (around 9%) suggests that nZVI synthesized from *Amaranthus Dubius* leaf is a highly efficient and cost effective catalyst for photo Fenton oxidation of textile effluent.

The kinetic coefficients  $k$  and  $K_s$  clearly define the enhanced biodegradability after HPF, HSPF, APF and ASPF processes. The  $k$  value is more for the effluent after HPF and APF processes than HSPF and ASPF processes, due to the increased biochemical degradation rate, which results in a low BI.

Gas chromatography results for the effluent after ASPF process prove that the presence of solar light and nZVI in Fenton process successfully reduce the carcinogenic and harmful compounds present in the textile effluent and enhanced the biodegradability.

HSPF and ASPF processes were found to increase the BI above 0.4,  $SVI < 100 \text{ mL/g}$ , reduce the toxicity and produce satisfactory sludge, and hence selected as pre-treatments to biological treatment. The optimum conditions for HSPF pre-treatments were pH 2.6,  $\text{Fe}^{2+}$  dosage 39.5mg/l,  $\text{H}_2\text{O}_2$  dosage 63mM, contact time 25minutes and  $30 \pm 2 \text{ W/m}^2$  solar light intensity. The optimum conditions for ASPF process were pH 2.6,  $\text{H}_2\text{O}_2$  dosage 62.6mM, nZVI dosage 38.7mg/l, contact time 15minutes and  $30 \pm 2 \text{ W/m}^2$  solar light intensity.

MBBR after HSPF gives 68.9% overall BOD removal, 79.9% COD removal & 91% color removal under optimum conditions pH 7.1, carrier materials filling ratio 62% and contact time 2.41days. The effluent BOD and COD are 65mg/l and 197mg/l respectively conforming to the standards of water for irrigation purpose, but cannot be disposed into inland water bodies. When MBBR has been modified by exposing to a magnetic field of 12mT at an exposure time of 12hours, BOD and COD reduced to 29.8mg/l and 128.4mg/l respectively and the effluent meets the standards of effluent disposed to inland water bodies.

Similarly, MBBR after ASPF ensures 70.6% BOD removal, 82.4% COD removal and 94% color removal under optimum conditions pH 7.5, carrier materials filling ratio 59% and contact time 1.97days. The effluent (BOD 61.7mg/l and COD 172.5mg/l) meets the standards of water for irrigation purposes, but cannot be disposed to inland water bodies. However, when modified MBBR induced with the magnetic field of 10mT at an exposure time of 8 hours has been used, it caused to reduce the BOD and COD to 28.3mg/l and 96mg/l respectively and the effluent meets the standards of water disposed to inland water bodies. Magnetic field increases conductivity which accelerated chemical reaction, flocculation, improved the settling and biodegradation rate.

Cost analysis has been done and found that MBBR after pretreatment by ASPF costs Rs.69.52/m<sup>3</sup> of effluent, while it is Rs.71.97/m<sup>3</sup> for MBBR after HSPF.

Hence, the integral treatments, magnetic field induced MBBR after ASPF pretreatment or HSPF pretreatment can be used efficiently in the textile effluent treatment, while the integral ASPF-MBBR treatment system is found to be slightly less expensive than the other integral HSPF-MBBR system.

## REFERENCES

- A.T. Nair, A. R. Makwana, M. M. Ahammed, (2014), The use of response surface methodology for modelling and analysis of water and wastewater treatment process: A review, *Water Science Technology*, 69.3, 464-478.
- Abdallaa K. Z. and Hammam G., (2014), Correlation between biochemical oxygen demand and chemical oxygen demand for various wastewater treatment plants in Egypt to obtain the biodegradability indices, *International Journal of Sciences: Basic and Applied Research*, 13(1), 42-48.
- Abdul Aziz, A. R., Asghar, A., Ashri wan Daud, W. M., (2014), Comparison of different oxidizing agents for textile wastewater treatment, *Journal of Seçuk University Natural and Applied Science*, 968-984.
- Abdul Majeed A., Alwan H., Baki I., Abtan F. and Sultan H., (2012), Wastewater treatment in Baghdad city using moving bed biofilm reactor (MBBR) technology, *Engineering and technology journal*, 30(9), 1550-1561.
- Abdulgader M, Jimmy Yu Q., Zinatizadeh A. A., Williams P, Rahimi Z, (2020), Application of response surface methodology (RSM) for process analysis and optimization of milk processing wastewater treatment using multi-stage flexible fiber biofilm reactor, *Environmental Chemical Engineering*, 8(3), 103792.
- Accinelli C., Sacca M.L., Mencarelli M. and Vicari A., (2012), Application of bioplastic moving bed biofilm carriers for the removal of synthetic pollutants from wastewater, *Journal of Bioresource Technology*, 180-186.
- Adriana M., Marco S., Claudio D. and Giovanni B., (2014), Textile Wastewater Treatment: Aerobic Granular Sludge Vs Activated Sludge Systems, *Journal of Water Research*, 7(5), 371-376.
- Ahmadi M., Rahmani K., Rahmani A. & Rahmani H., (2017), Removal of benzotriazole by Photo-Fenton like process using nano zero-valent iron: response surface methodology with a Box-Behnken design, *Polish Journal of Chemical Technology*, 19(1), 104-112.
- Ahmed R. Mobarki, Ebrahiem E. Ebrahiem, Mohammedanoor N & Al-Maghrabi, (2013), Removal of organic pollutants from industrial wastewater by applying photo-Fenton oxidation technology, *Arabian journal of chemistry*, 541, 85-91.
- Ai Ni Soon, Hameed B.H., (2011), Heterogeneous catalytic treatment of synthetic dyes in aqueous media using Fenton and photo-assisted Fenton process, *Desalination*, 269(1-3), 1-16.
- Al-Degs Y, Khraisheh M.A.M., Allen S.J., Ahmad M.N., (2000), Effect of carbon surface chemistry on the removal of reactive dyes from textile effluent, *Water Research*, 34(3), 927-935.

- Aleem M., Cao J., Li C., Rashid H., Wu Y., Nawaz M.I., Abbas M. & Akram M. W., (2020), Coagulation and adsorption based environmental impact assessment and textile effluent treatment, *Water, Air & Soil Pollution*, 231(45).
- Al-Momani F., Touraud E., Degorce Dumas J. R., Roussy J., & Thomas O., (2002), Biodegradability Enhancement of Textile Dyes and Textile Wastewater by UV Photolysis, *Journal of Photochemistry & Photobiology A*, 153, 191-197.
- Alorkpa E.J., Boadi N.O., Badu M. Saah, S.A., (2016), Phytochemical screening, antimicrobial and antioxidant properties of assorted carica papaya leaves in Ghana, *Journal of Medicinal Plants Studies*, 4(6), 193-198.
- Alunaimi M. M., Rauf M. A., Ashraf S. S., (2008), A comparative study of Natural Red decoloration by photo Fenton and photo catalytic processes, *Dyes & Pigments*, 7, 332-337.
- Andleeb S., Atiq N., Ali M., Ur-Rehman A. Hameed S., (2010), Biodegradation of Anthraquinone Dye by *Aspergillus Niger* Sa1 in Self Designed Fluidized Bed Bioreactor, *Iranian Journal of Environmental Health Science and Engineering*, 7(5), 371-376.
- APHA, (1998), Standard Methods for the Examination of Water and Wastewater, 20th edition, Clesceri L.S., Greenberg A.E. and Eaton A.D. (eds.) American Water Works Association, Water Environment Federation, Published by APHA, Washington, D.C., USA.
- APHA, (2005), American Public Health Association. Standard methods for examination of water including bottom sediments and sludges. Standard Methods. Edn. 19:874.
- Aquino J. M., Rocha-Filho R. C., Ruotolo L. A., Bocchi N., & Biaggio S. R., (2014), Electrochemical degradation of a real textile wastewater using PbO<sub>2</sub> and DSA anodes. *Chemical Engineering Journal*, 251, 138-145.
- Arslan-Alaton I. and Gurses F., (2004), Photo-Fenton and photo-Fenton-like oxidation of Procaine Penicillin G formulation effluent, *Journal of Photochemistry & Photobiology A: Chemistry*, 165, 165-175.
- Arun Prasad A.S., Bhaskara Rao K.V., (2010), Physico chemical characterization of textile effluent and screening for dye decolorizing bacteria, *Global Journal of Biotechnology and Biochemistry*, 5(2), 80-86.
- Baban A., Yediler A., Lienert D., Kemerdere N., Kettrup A., (2003), Ozonation of high strength segregated effluents from a woollen textile dyeing and finishing plant, *Dyes and Pigments*, 58 (2). 93-98.
- Babu B.R., Parande A.K., Raghu S., Kumar T.P., (2007), Textile technology-cotton textile processing: waste generation and effluent treatment, *Journal of Cotton Science*, 11, 141-153.
- Babuponnusami A. & Muthukumar K., (2014), A review on Fenton and improvements to the Fenton process for wastewater treatment, *Journal of Environmental Chemical engineering*, 2(1), 557-562.

- Baker J.S. and Judd S.J., (1996), Magnetic amelioration of scale formation, *Water Research*, 30 (2), 247–260.
- Bao T., Jin J., Dantie M. M., Wu K., Ming Yu Z., Wang L., Chen J., Zhang Y., Frost R. L., (2019), Green synthesis and application of nano zero-valent iron/ rectorite composite material for P-chlorophenol degradation via heterogeneous Fenton reaction, *Journal of Saudi Chemical Society*, 23(7), 864-878.
- Baouab M.H.V., Gauthier R., Gauthier H., Rammah M.E.B., (2001), Cationized sawdust as ion exchanger for anionic residual dyes, *Journal of Applied Polymer Science*, 82, 31–37
- Bartosz S., Jaroslaw G. & Jan S., (2017), Sludge Volume Index (SVI) Modelling: Data Mining Approach, *Proceedings of 38<sup>th</sup> International Conference on Information Systems Architecture and Technology–ISAT*.
- Bauer R., Waldner G., Fallmann H., Hager S., Klare M., Krutzler T., Malato S. and Maletzky P., (1999), The photo-Fenton reaction and the TiO<sub>2</sub>/UV process for wastewater treatment – novel developments, *Catalysis Today*, 53, 131-144.
- Bayramoglu M., Eyvaz M. & Kobya M., (2007), Treatment of the textile wastewater by electro coagulation: Economical evaluation, *Chemical Engineering Journal*, 128(2-3), 155-161.
- Bazrafshan E., Mahvi A.H. & Zazouli M.A., (2014), Textile wastewater treatment by electro coagulation process using aluminium electrodes, *Iranian Journal of Health Sciences*, 2(1), 16-29.
- Bezerra, M. A., Santelli, R. E., Oliveiraa, E. P., Villar, L. S. & Escalera, L. A., (2008), Response surface methodology (RSM) as a tool for optimization in analytical chemistry, *Talanta*, 76, 965–977.
- Bhatmagar A., Minicha A. K., (2008), Conventional and non-conventional adsorbents for removal of pollutants from water: A review, *Indian Journal of Chemical Technology*, 15, 101-106.
- Bilinska L.L., Gmurek M. & Ledakowicz S., (2016), “Comparison Between Industrial and Simulated Textile Wastewater Treatment By Advanced Oxidation Processes- Biodegradability, Toxicity and Cost Assessment”, *Chemical Engineering Journal*, 306, 550-559.
- Bishop D.F., Stern G., Fleischmann M. and Marshall L.S., (1968), Hydrogen peroxide catalytic oxidation of refractory organics in municipal waste waters, *Indian Engineering Chemistry Process Design & Development*, 7, 110-117.
- Bisschops I. & Spanjers H., (2003), Literature Review on Textile Wastewater Characterization, *Environmental Technology*, 24, 1399-1411.
- Bo F., Liao X., Liang R. and Ding L., (2010), COD removal from expanded granular sludge bed effluent using a moving bed biofilm reactor and their microbial community analysis, *World Journal of Microbiology & Biotechnology*, 27, 915-923.

- Borade A.S., Babasaheb N.K., Rajkumar V.S., (2011), A phyto-pharmacological review on *Lawsoniainermis* (Linn.), *International Journal of Pharmacy & Life Sciences*, 2(1), 536-541.
- Borja J.Q., Ngo M.A.S., Cyrill C., Saranglao, Tiongo R.P.M., Roque E.C and Dugos N.P., (2015), Synthesis of green zero-valent iron using polyphenols from dried green tea extract, *Journal of Engineering Science and Technology*, 10, 22-31.
- Borkar R., Gulhane M. and Kotangale A. (2013), Moving Bed Biofilm Reactor – A New Perspective in Wastewater Treatment, *IOSR Journal Of Environmental Science, Toxicology and Food Technology*, 6(6), 15-21.
- Box G. E. P. & Behnken D. W., (1960), Some new three level designs for the study of quantitative variables, *Technometrics*, 2, 455–475.
- Box G. E. P. & Wilson K. B., (1951), The exploration and exploitation of response surfaces: some general considerations and examples, *Biometrics*, 10, 16–60.
- Cai R., Yang H., He J. and Zhu W., (2009), The effects of magnetic fields on water molecular hydrogen bonds, *Journal of Molecular Structure*, 938 (1–3), 15–19.
- Cappuccino G.J. & Sherman N., (1992), *Microbiology: A Laboratory Manual*, Pearson Education Publication, Edition 7.
- Carlesso F., Zin G., Souza S. G., Oliveira J. V., (2015), Magnetic field on fouling control of ultrafiltration membranes applied in treatment of a synthetic textile effluent, *Environmental Technology*, 37(8), 1-8.
- Carmen S., Luis M. and Rui A., (2014), Synthetic Textile Dyeing Wastewater Treatment by Integration of Advanced Oxidation and Biological Processes –Performance Analysis with Cost Reduction, *Journal of Environmental Chemical Engineering*, 2, 1027–1039.
- Castro A., Nogueira M.V., Lopes I., Santos T.R., Pereira R., (2019), Evaluation of the Potential Toxicity of Effluents from the Textile Industry before and after Treatment, *Applied Sciences*.
- Chan W.T. & Koe L.C.C., (1991), A Knowledge Based Framework for the Diagnosis of Sludge Bulking in the Activated Sludge Process, *Water Science Technology*, 23(4-6), 847-855
- Chang J.S., Chou C., Lin Y., Ho J., Hu T.L., (2001), Kinetic Characteristics of Bacterial Azo Dye Decolorization by *Pseudomonas luteola*, *Water Research*, 35, 2041.11
- Chatzisyneon E., Xekoukoulotakis N.P., Coz A., Kalogerakis N., Mantzavinos D., (2006), Electrochemical treatment of textile dyes and dyehouse effluents, *Journal of Hazardous Materials*, 137(2), 998-1007.
- Chen K.C., Huang W.T., Wu J.Y., Houg J.Y., (1999), Microbial Decolorization of Azo Dye by *Proteus mirabilis*. *Indian Journal of Microbiology & Biotechnology*, 23, 686.12.
- Chen P.J., Su C.H., Tseng C.Y., Tan S.W. & Cheng C., (2011), “Toxicity Assessment of nano scale Zero Valent Iron and its Oxidation Products in Medaka (*Oryzias Latipes*) Fish”, *Marine Pollution Bulletin*, 63(5-12), 339-346.

- Cheng Y., Fan W. & Guo L., (2014), Coking wastewater treatment using magnetic porous ceramsite carrier, *Separation & Purification Technology*, 130, 167-172.
- Chhabra M., Mishra S. & Sreekrishnan T.R., (2015), Combination of chemical and enzymatic treatment for efficient decolorization/degradation of textile effluent: High operational stability of the continuous process, *Journal of Biochemical Engineering*, 93, 17–24.
- Chhatwani P., (2011). Amazing uses of magnetised water. *Health and Fitness Article*.  
<http://EzineArticles.com/?expert=PremChhatwani>
- Chinta S., VijayKumar S., (2013), Technical facts and figures of reactive dyes used in textiles, *Indian Journal of Engineering and Materials Sciences*, 4(3), 308-12.
- Choudhury A.K.R., (2018), Ecofriendly Dyes & Dyeing, *Advanced Materials, Technologies & Environmental Applications*, 2(1), 145-176.
- Ciardelli G., Ranieri N., (2001), The treatment and reuse of wastewater in the textile industry by means of ozonation and electroflocculation, *Water Research*, 35, 567–572.
- Claudia S.G., Guadalupe P., Werner L. and Sabine R., (2001), An Advanced Molecular Strategy to Identify Bacterial Communities, *Journal of Microbiological Methods*, 45, 77-87.
- Colic, M. and Morse D., (1999), The elusive mechanism of the magnetic ‘memory’ of water, *Colloid Surface, A.*, 154(1–2), 167–174.
- Collivignarelli M.C., Pedrazzani R., Sorlini S and Abba A., (2017), H<sub>2</sub>O<sub>2</sub> based oxidation processes for the treatment of real high strength aqueous wastes, *Sustainability*, 244, 1-14.
- Cotoruelo, M.L., Marques, M.D. and Rodriguez, J.J., (2007), Adsorption of aromatic compounds on activated carbons from lignin: Equilibrium and thermodynamic study, *Industrial & Engineering Chemistry Research*, 46, 4982-4990.
- Cuzzola A., Bernini M. & Salvadori P., (2002), A preliminary study on iron species as heterogeneous catalysts for the degradation of linear alkylbenzenesulphonic acids by H<sub>2</sub>O<sub>2</sub>, *Applied Catalysis B: Environmental*, 36(3), 231-237.
- Darvishmotevalli M., Zarei A., Moradnia M., Noorisepehr M., Mohammadi H., (2019), Optimization of saline wastewater treatment using electro chemical oxidation process: prediction by RSM method, *MethodsX*, 6, 1101-1113.
- Davis L., Ford P., (1992), *Toxicity reduction evaluation and control*, Technomic Publishing Company Inc.
- DiasFernando F.S., Filho C., (2009), Degradation of reactive black 5 dye in a photo-Fenton reactor with neural network modelling, *Dyes and pigments*, 56, 108-113.
- Dick R. I., Vesilind P. A., (1969), The sludge volume index: What is it?, *Water Pollution Control Federation*, 41(7), 1285-1291.
- Dincer A.R., Gunes Y. & Karakaya N., (2007), Coal based bottom ash waste material as adsorbent for removal of textile dye stuffs from aqueous solution, *Journal of Hazardous Materials*, 141(3), 529-535.

- Dong B., Chen H., Yang Y., He Q. & Dai X., (2014), Treatment of printing and dyeing wastewater using MBBR followed by membrane separation process, *Desalination & Water Treatment*, 52, 4562-4567.
- Duarte F., Morais V., Hodar M., Madeira L. M., (2013), Treatment of textile effluents by the heterogeneous Fenton process in a continuous Packed Bed Reactor using Fe/activated carbon as catalyst, *Chemical Engineering Journal*, 232, 34-41.
- Duc D. S., (2013), Degradation of Reactive Blue 181 Dye by Heterogeneous Fenton Technique Using Modified Fly Ash, *Asian Journal of Chemistry*, 25, 4083-4086.
- Dulman V. & Cucu-Man S.S., (2009), Sorption of some textile dyes by beech wood sawdust, *Journal of Hazardous Materials*, 162(2-3), 1457-1464.
- Ebrahiem E. E., Al-Maghrabi M.N., Mobarki A.R., (2017), Removal of organic pollutants from industrial wastewater by applying photo-Fenton oxidation technology, *Arabian Journal of Chemistry*, 10(2), 1674-1679.
- Eletta O.A.A., Mustapha S.I., Ajayi O.A. & Ahmed A.T., (2018), Optimization of dye removal from textile wastewater using activated carbon from saw wood, *Nigerian Journal of Technological Development*, 15(1), 26-32.
- Ellouze E., Tahri N., Amar R., Ben, (2012), Enhancement of textile wastewater treatment process using Nanofiltration, *Desalination*, 286, 16–23.
- El-Sayed, E.M., Elkady, M.F., El-Latif, Abd M.M., (2017), Biosynthesis and characterization of zerovalent iron nanoparticles and its application in azo dye degradation, *Indian journal of chemical technology*, 24, 541-547.
- El-Temsah Y.S., Sevcu A., Bobcikova K., Cernik M. & Joneš E.J., DDT Degradation Efficiency and Ecotoxicological Effects of 2 types of nano sized Zero Valent Iron in Water and Soil, *Chemosphere*, 144, 2016; 2221-2228.
- Eremektar, G., Selcuk, H., Meric, S., (2007), Investigation of the relation between COD fractions and the toxicity in a textile finishing industry wastewater: Effect of preozonation, *Desalination*, 211, 314–320.
- Ertugay N & Acar F.N., (2013), Sonocatalytic degradation of Direct Blue 71 azo dye at the presence of zero valent iron (ZVI), *Desalination and Water Treatment*, 51(40-42), 7570-7576.
- Esplugas S. and Ollis D.F., (1997), Economic aspects of integrated (chemical + biological) processes for water treatment, *Journal of Advanced Oxidation Technology*, 1, 197-202.
- Fajardo C., Saccà M.L., Martinez-Gomariz M., Costa G., Nande M. & Martin M., (2013), Transcriptional and proteomic stress responses of a soil bacterium *Bacillus cereus* to nanosized zero-valent iron (nZVI) particles, *Chemosphere*, 93, 1077–1083.
- Farshchi H.K., Azizi M., Jaafari M.R., Nemati S.H. & Fotovat A., (2018), Green synthesis of iron nanoparticles by Rosemary extract and cytotoxicity effect evaluation on cancer cell lines, *Biocatalysis & Agricultural biotechnology*, 16, 54-62

- Fathi A., Mohamed T., Claude G., Maurin G., and Mohamed B.A., (2006), Effect of a magnetic water treatment on homogeneous and heterogeneous precipitation of calcium carbonate, *Water Research*, 40 (10), 1941–1950.
- Faunce A. & Cabell S., (1890), Electric means for preventing boiler incrustation (U.S. Patent No. 438579).
- Faust B. & Hoigné J., (1990), Photolysis of hydroxy-complexes as sources of OH• radicals in clouds, fog and rain, *Atmos. Environ.*, 24A, 79-89.
- Fenton, H.J.H., (1894), Oxidation of tartaric acid in presence of iron, *Journal of the Chemical Society, Transactions*, 65, 899-910.
- Francisco E., Ribeiro S., Aline M., Carlos A. and Marco P., (2014), Application of ElectroFenton Process as Alternative for Degradation of Novacron Blue Dye, *Journal of Environmental Chemical Engineering*, 2, 875–880.
- Garg P. & Sardana S., (2016), Pharmacological and therapeutic effects of oicum sanctum, *European Journal of Pharmaceutical and Medical Research*, 3(8), 637-640.
- Garrido R. & Theng B., (2010), Clays and Oxide Minerals as Catalysts and Nano-Catalysts in Fenton-Like Reactions : A Review, *Journal of Applied Clay Science*, 47, 182–192
- Gautam S., Ahmad S., Dhingra A. & Fatima, Z., (2017), Cost-effective treatment technology for small size sewage treatment plants in India, *Journal of Scientific & Industrial Research*, 76. 249-254.
- Gayathri V. & Kiruba D., (2014), Preliminary Phytochemical Analysis of Leaf Powder Extracts of *Psidium guajava* L., *International Journal of Pharmacognosy and Phytochemical Research*, 6(2), 332-334.
- Geng S., Fu W., Chen W., Zhang S., Gao Q., Wang J. & Ge X., (2020), Effect of an external magnetic field on microbial functional genes and metabolism of activated sludge based on metagenomic sequencing, *Scientific Reports*, 10, 8818.
- Gernjak W., Krutzler T., Glaser A., Malato S., Cáceres J., Bauer R. & FernándezAlba A.R., (2003), Photo-Fenton treatment of water containing natural phenolic pollutants, *Chemosphere*, 50, 71-78.
- Gernjak W., Maldonado M.I., Malato S., Cáceres J., Krutzler T., Glaser A. & Bauer R., (2004), Pilot-Plant Treatment of Olive Mill Wastewater (OMW) by Solar TiO<sub>2</sub> Photocatalysis and Solar Photo-Fenton, *Solar Energy*, 77, 567-572.
- Ghafari S., Aziz H.A., Hasnain M.I. & Zinatizadeh A.K., (2009), Application of response surface methodology (RSM) to optimize coagulation flocculation treatment of leachate using poly aluminum chloride (PAC) and alum, *Journal of Hazardous Materials*, 163, 650–656.
- Ghaly A.E., Ananthashankar R., Alhattab M. & Ramakrishnan V.V., (2014), Production, characterization and Treatment of textile effluent: A critical review, *Journal of Chemical Engg & Process Technology*, 5(182), 1-19.
- Gogate P.R. & Pandit A.B., (2004), A review of imperative technologies for wastewater treatment II: Hybrid methods, *Advances in Environmental Research*, 8(3-4), 553-597.

- Golob V., Vinder A. & Simonic M., (2005), Efficiency of the coagulation/flocculation method for the treatment of dye bath effluents, *Dyes & Pigments*, 67(2), 93-97.
- Gonçalves J.R., (2016), The Soil and Groundwater Remediation with Zero Valent Iron Nanoparticles, *Advances in Transportation Geotechnics 3*, The 3rd International Conference on Transportation Geotechnics, 143, 1268-1275.
- Gutierrez-Mata A.G., Velazquez-Martinez S., Alvarez-Gallegos A., Ahmadi M., Hernandez-Perez J.A., Ghanbari F. and Silva-Martinez S., (2017), Recent Overview of Solar Photocatalysis and Solar Photo-Fenton Processes for Wastewater Treatment, *International Journal of Photo energy*.
- Hait S. & Mazumder D., (2008), scope of improvement of treatment capacity of activated sludge process by hybrid modification, *Journal of Environmental Engineering and Science*, 7(2), 147-158.
- Harshiny M., Iswarya C.N. & Matheswaran M., (2015), Biogenic synthesis of Iron Nanoparticles using *Amaranthus dubius* leaves extract as reducing agents, *Powder Technology*, 286, 744-749.
- Hassan H. & Hameed B.H., (2011), Fe-clay as Effective heterogeneous Fenton catalyst for the Decolorization of Reactive Blue 4, *Chemical Engineering Journal*, 171, 912-918.
- Hassan M.M. & Carr C.M., (2018), A critical review on recent advancements of the removal of reactive dyes from dyehouse effluent by ion-exchange adsorbents, *Chemosphere*, 209(1), 201-219.
- Hincapié M., Maldonado M.I., Oller I., Gernjak W., Sánchez-Pérez J. A., Ballesteros M. M. & Malato S., (2005), Solar photocatalytic degradation and detoxification of EU priority substances, *Catalysis Today*, 101, 203-210.
- Hoag G.E., Collins J.B., Holcomb J.L., Hoag J.R., Nadagouda M.N. & Varma R.S., (2009), Degradation of bromothymol blue by greener nZVI synthesized using tea polyphenols, *Journal of Material Chemistry*, 19(45), 8671-77.
- Hosseini K., Alavi M. & Hashemib S., (2011), Post-Treatment of Anaerobically Degraded Azo Dye Acid Red 18 using Aerobic Moving Bed Biofilm Process: Enhanced Removal of Aromatic Amines, *Journal of Hazardous Materials*, 19, 147– 154.
- Hu Q.H., Qiao S.Z., Haghseresht F., Wilson M.A. & Lu G.Q., (2006), Adsorption study for removal of basic red dye using bentonite, *Industrial & Engineering Chemistry Research*, 45, 733-738.
- Hunger K., (2003), *Industrial dyes: Chemistry, properties and applications*. Weinheim: Willey-VCH.
- Imran M., Crowley D. E., Khalid A., Hussain S., Mumtaz M.W. & Arshad M., (2015), Microbial biotechnology for decolorization of textile wastewaters, *Reviews in Environmental Science and Biotechnology*, 14(1), 73-92.
- Irina-Isabella S. & Romen B., (2009), Wastewater Characteristics In Textile Finishing Mills, *Journal of Environmental Engg. & Management*, 19(5), 257-265.

- Islam M.R.&Mostafa M.G., (2019), Textile Dyeing Effluents and environment concerns: A review, *Journal of Environmental Science and Natural Resources*, 11(1-2), 131-144.
- Jafaria N., Soudib M.R.&Kasra-Kermanshahi R., (2014), Biodegradation Perspectives of Azo Dyes by Yeasts, *Microbiology*, 8, 484–97.
- Jahid M.M., Habib S.M., Parvin F., Rahman M., Saadat A. & Mubarak A., (2013), Removal of industrial dye effluent (Drimarene yellow) by renewable natural resources, *American Academic & Scholarly Research Journal*, 5(2).
- Jeyasundari J., Praba P.S., Jacob Y.B.A., Vasantha V.S. &Shanmugaiah V., (2017), Green Synthesis and Characterization of Zero Valent Iron Nanoparticles from the Leaf Extract of PsidiumGuajava Plant and their Antibacterial Activity, *Chemical Science Review and Letters*, 6(22), 1244-1252.
- Ji Y., Wang Y., Sun J., Yan T., Li J., Zhao T., Yin X. & Sun C., (2010), Enhancement of biological treatment of wastewater by magnetic field, *Bioresource Technology*, 101(22), 8535-8540.
- Jordão C., Puppim R. &BroegaA.C., (2018), Solutions notes on clean textile waste, *International Conference on innovation, engineering and entrepreneurship*, 682-689.
- Kalyani D.C., Telke A.A., Dhanve R.S. &Jadhav J.P., (2008), Ecofriendly Biodegradation and Detoxification of Reactive Red 2 Textile Dye by Newly Isolated *Pseudomonas* sp. *SUKI*, *Journal of Hazardous Materials*, 163, 735.13
- Kang Y.W. & Hwang K.Y., (2000),Effect of reaction condition on the oxidation efficiency in the Fenton process, *Water Research*, 34(10), 2786-2790.
- KannadasanT. M., Thirumarimurugan K.S., Sowmya K., Sukanya M.& Vijayashanthi, (2013), Dye industry effluent treatment using cactus (*Opuntia*) and water hyacinth (*Eichhornia crassipes*), *IOSRJournal of Environmental Science Toxicology & Food Technology*, 3 (4), 41-43.
- Kermani M. & Bina B., (2009), Biological Phosphorus and Nitrogen Removal from Wastewater using Moving Bed Biofilm Process, *Iranian Journal of Biotechnology*, 7(1), 120-130.
- Khan R., Bhawana P. &Fulekar M.H., (2013), Microbial decolorization and degradation of synthetic dyes: A review, *Rev Environ Sci Bio/Technol.*,75–97.5
- Khan, S.& Malik, A., (2018), Toxicity evaluation of textile effluents and role of native soil bacterium in biodegradation of a textile dye, *International Journal of Environmental Science and Pollution Research*, 25(5), 4446-4458.
- Khandegar V. &Saroja A.K., (2013), Electrocoagulation for the treatment of textile industry effluent – a review, *Journal of Environmental Management*, 128, 949–963.
- Khuri A.I. & Cornell J.A.,(1996), *Response Surface, Design and Analyses*. 2nd edn, Marcel Dekker Inc., New York, USA.
- Kim Y., Hai-Uk N., Jong-Hyun L. & Tae-Joo P,(2004), Fenton Oxidation Process Control using Oxidation-reduction Potential Measurement for Pigment Wastewater Treatment, *Korean Journal of Chemical Engineering*, 21(4), 801-805.

- Koch M., Yediler A., Lienert D., Insel G. & Kettrup M., (2002), A ozonation of hydrolyzed azo dye reactive yellow 84 (CI), *Chemosphere*, 46, 109–113.
- Kris O'Dowd & Suresh C. Pillai, (2020), Photo-Fenton disinfection at near neutral pH: Process, parameter optimization and recent advances, *Journal of Environmental Chemical Engineering*, 8, 104063.
- Krutzler T., Fallmann H., Maletzky P., Bauer R., Malato S. & Blanco J., (1999), Solar driven degradation of 4-chlorophenol, *Catalysis Today*, 54, 321-327.
- Kumar R., Singh R.D. & Sharma K.D., (2005), Water Resources of India, *Current Science India*, 89, 794-811.
- L.A.V.de Luna, T.H.G.Silva, R.F.P.Nogueira, F.Kummrow, & G.A.Umbuzeiro, Aquatic Toxicity of Dyes Before and After Photo Fenton Treatment, *Journal of Hazardous Materials*, 276, 2014; 332-338.
- Lafi R., Gzara L., Lajimi R.H. & Hafiani A., (2018), Treatment of textile wastewater by a hybrid ultrafiltration/ electro dialysis process, *Chemical Engineering & Processing*, 132, 105-113.
- Lai T.M., Shin J.H. & Hur J., (2011), Estimating the biodegradability of treated sewage samples using Synchronous Fluorescence Spectra, *Sensors*, 11, 7382-7394.
- Lau W.J. & Ismail A.F., (2009), Polymeric nanofiltration membranes for textile wastewater treatment: Preparation, performance evaluation, transport modelling and fouling control: a review, *Desalination*, 245(1-3), 321-348.
- Łebkowska M., Rutkowska-Narozniak A., Pajor E. & Pochanke, Z., (2011), Effect of a static magnetic field on formaldehyde biodegradation in wastewater by activated sludge, *Bioresource Technology*, 102 (19), 8777–8782.
- Ledakowicz S., Bilinska L. & Zylla R., (2012), Application of Fenton's reagent in the textile wastewater treatment under industrial conditions, *Ecological & Chemical Engineering*, 19(2), 163-174.
- Lee C., Kim J.Y., Lee W.I., Nelson K.L., Yoon J. & Sedlak D.L., (2008), Bactericidal Effect of Zero-Valent Iron Nanoparticles on *Escherichia coli*, *Environmental Science Technology*, 42, 4927–4933.
- Lellis B., Polonio C.Z.F., Pamphile J.A. & Polonio J.C., (2019), Effects of textile dyes on health and the environment and bioremediation potential of living organisms, *Biotechnology Research & Innovation*, 3, 275-290.
- Lin S.H. & Lin C.M., (1993), Treatment of textile waste effluents by ozonation and chemical coagulation, *Water Research*, 27(12), 1743-1748.
- Lin S.H. & Peng C.F., (2008), Treatment of textile wastewater by Fenton's reagent, *Environmental Science & Engineering*, 89-98.
- Lipczynska-Kochany E., (1992), Degradation of Nitrobenzene and Nitrophenols by Means of AOP's in Homogenous Phase: Photolysis in the Presence of Hydrogenperoxide versus the Fenton Reaction, *Chemosphere*, 24, 1369-1380.

- Liu B., Baoyu G., Xing X., Wei H., Qinyan Y., Yan W., Ying S., (2011), The combined use of magnetic field and iron-based complex in advanced treatment of pulp and paper wastewater, *Chemical Engineering Journal*, 178, 232–238.
- Liu M., Lu Z., Chen Z. & Gao C., (2011), Comparison of reverse osmosis and nano filtration membranes in the treatment of biologically treated textile effluent for water reuse, *Desalination*, 281(1), 372-378.
- Liu S., Yang F., Meng F., Chen H. & Gong Z., (2008), Enhanced anammox consortium activity for nitrogen removal: Impacts of static magnetic field, *Journal of Biotechnology*, 138(3-4), 96-100.
- Lowry G.V. & Casman E.A., (2009), Nanomaterial Transport, Transformation, and Fate in the Environment, *Nanomaterials: Risks and Benefits*, 125–137.
- Luo F., Chen Z., Megharaj M. & Naidu R., (2014), Biomolecules in grape leaf extract involved in one-step synthesis of iron-based nanoparticles, *RSC Advances*, 96, 53467-53474
- Machado S., Pinto S.L., Grosso, J.P., H.P.A. Nouws, Albergaria, J.T. & Delerue-Matos C., (2013), Green production of Zerovalent iron nano particles using tree leaf extracts, *Science of the Total Environment*, 445-446, 1-8
- Mahdieh R., Seyed A.M., Fei Y. & Joydeep D., (2021), Nano Zero valent iron on activated carbon cloth support as Fenton-like catalyst for efficient color and COD removal from melanoidin wastewater, *Chemosphere*, 263.
- Mahmood Q. P., Zheng E., Islam Y., Hayat M.J., Hassan G. Jilani, R. & Jin C., (2005), Lab scale studies on water hyacinth (*Eichhornia crassipes* Mart. Solms) for biotreatment of textile wastewater, *Caspian Journal of Environmental Science*, 3 (2), 83-88.
- Makgato S.S. & Chirwa E.M.N., (2010), Performance Evaluation of AOP/Biological Hybrid System for Treatment of Recalcitrant Organic Compounds, *International Journal of Chemical Engineering*, 1-10.
- Malaeb L. & Ayoub G.M., (2011), Reverse osmosis technology for water treatment: state of the art review, *Desalination*, 267, 1-8.
- Malato S., Blanco J., Vidal A., Alarcón D., Maldonado M. I., Cáceres J. & Gernjak W., (2003), Applied studies in solar photocatalytic detoxification: an overview, *Solar Energy*, 75, 329-336.
- Manenti D.R., Soares P.A. & Módenes A.N., Insights into solar photo-Fenton process using iron(III)–organic ligand complexes applied to real textile wastewater treatment, *Chemical Engineering Journal*, 266, 2015; 203–212.
- Mariana N., Yediler A., Siminiceanu I. & Kettrup A., (2003), Oxidation of commercial reactive azo dye aqueous solutions by the photo-Fenton and Fenton-like processes, *Journal of Photochemistry and Photobiology A: Chemistry*, 161, 87–93.
- Masciangioli T. & Shang W.X., (2003), Environmental technology at nanoscale, *Environmental Science Technology*, 37(5), 102-108.

- Massart D. L., Vandeginste B.G.M., Buydens L.M.C., De Jong S., Lewi P.J. & Smeyers-Verbeke J., (1998), Handbook of chemometrics and qualimetrics: part A. In: Data Handling in Science and Technology, 20A, Elsevier, The Netherlands.
- Mazumder D., (2011), Process evaluation and treatability study of wastewater in a textile dyeing industry, International Journal Of Energy And Environment, 2(6), 1053-1066.
- Meibodi M.E., Parsaeian M.R. & Banaei M., (2013), Ozonation and electron beam irradiation of dyes mixture, Ozone: Science & Engineering, 35(1), 49-54.
- Meric S., Kaptan D. & Olmez T., (2004), Color and COD removal from wastewater containing Reactive Black 5 using Fenton's oxidation process, Chemosphere, 54(3), 435-441.
- Metcalf & Eddy Inc. (2003), Wastewater Engineering : Treatment, Disposal and Reuse., Tata Mc. Graw Hill Publishing Company, New Delhi, 4th edition.
- Miranzadeh M.B., Zarjam R., Dehghani R., Haghghi M., Badi H.Z., Marzaleh M.A. & Tehrani A., (2016), Comparison of Fenton and Photo-Fenton Processes for Removal of Linear Alkyle Benzene Sulfonate (Las) from Aqueous Solutions, Polish Journal of Environmental Studies, 25(4), 1639-1648.
- Mirbagheri S. and Charkhestani A., (2015), Pilot-scale treatment of textile wastewater by combined biological-adsorption process, Desalination and water treatment, 57(20), 9082-9092.
- Moghaddam S.S., Moghaddam M.R.A. & Arami M., (2010), Coagulation/flocculation process for dye removal using sludge from water treatment plant: Optimization through response surface methodology, Journal of Hazardous Materials, 175(1-3), 651-657.
- Mohammed R.R., Ketabchi M.R. & McKay G., (2014), Combined magnetic field and adsorption process for treatment of biologically treated palm oil mill effluent (POME), Chemical Engineering Journal, 243, 31-42.
- Montgomery, D.C., (2010), Design and Analysis of Experiments, 7th edn, Wiley India Pvt. Ltd, New Delhi.
- Mosaddeghi M.R., Shariati F.P., Yazdi S.A.V. & Bidhendi G.N., (2020), Application of response surface methodology (RSM) for optimizing coagulation process of paper recycling wastewater using *Ocimum basilicum*, Environmental Technology, 41(1), 100-108.
- Mountassir Y., Benyaich A., Rezrazi, M., Berçot, P. & Gebrati L., (2013), Wastewater effluent characteristics from Moroccan textile industry, Water Science Technology, 67, 2791-2799.
- Murdani, Jaktar, Ekawati D., Nadira R. & Darmadi D., (2018), Application of response surface methodology (RSM) for wastewater of hospital by using electro coagulation, IOP Conference series Materials Science and Engineering, 345(1), 012011.
- Myers R.H., Khuri A.I. & Carter W.H.Jr., (1989), Response surface Methodology: 1966-1988, Technometrics, 31(2), 137-153.

- Myers R.H., Montgomery D.C. & Anderson-Cook C.M.,(2009), *Response Surface Methodology: Process and Product Optimization Using Designed Experiments*, 2nd edn, John Wiley & Sons, New York.
- Nadagouda M.N., Castle A.B., Murdock R.C., Hussain S.M. &Varma R.S., (2010), In vitro biocompatibility of nZVI particles synthesized using tea polyphenols, *Green Chemistry*, 12(1), 114-135.
- Naseem T. &Farrukh M.A., (2015), Antibacterial activity of green synthesis of iron nanoparticles using Lawsoniainermis and Gardenia jasminoides leaves extract, *Journal of Chemistry*, 1-7.
- Nawaz M.S. & Ahsan M., (2014), Comparison of physic-chemical, advanced oxidation and biological techniques for the textile wastewater treatment”, *Alexandria Engineering Journal*, 53(3), 717–722
- Newman M.C., (2015), *Fundamentals of ecotoxicology: The science of pollution*, Boca Raton: CRC Press.
- Nilesh T.P. &Chaudhari S., (2007), Degradation of azo dyes by sequential Fenton’s oxidation and aerobic biological treatment, *Dyes and Pigment*, 69, 698–705.
- Niraimathee V.A., Subha V., Ernest Ravindran R.S. &Renganathan S., (2016), Green synthesis of iron oxide nanoparticles from Mimosa pudica root extract, *International Journal of Environment and Sustainable Development*, 15(3), 227-240.
- Niu C., Liang W., RenH.,Geng J., Ding L. &Xu K., (2014), Enhancement of activated sludge activity by 10–50 mT static magnetic field intensity at low temperature, *Bioresource Technology*, 15, 48–54
- NiyasAhamed I., Anbu S., Vikraman G., Nasreen S., Muthukumari M. &Munishkumar M., (2016), Synthesis of NZVI for environmental remediation, *Life Science Archives*, 2(3), 549-554.
- NoopurAmeta, Pinki B.P., Jyoti S., Sanyogita S. &Sudhish Kumar, (2012), Copper modified iron oxide as heterogeneous photo-Fenton reagent for degradation of coomasi brilliant blue R-250, *International Journal of Chemistry*, 151 A,943- 948.
- Ogugbue C.J. &Sawidis T., (2011), Bioremediation and Detoxification of Synthetic Wastewater Containing Triarylmethane Dyes by Aeromonashydrophila Isolated from Industrial Effluent, *Biotechnology Research International*, 1-11.
- Oliveira R., Almedia F., Santos L. & Madeira M., (2006), Experimental Design of 2,4-Dichlorophenol Oxidation by Fenton’s Reaction, *Journal of Environmental Engineering and Management*, 45(4), 1266-1276.
- Olya M.E., Kasiri M.B., Aleboyeh H. & Salary A., (2008), Application of response surface methodology to optimize C.I.Acid Orange 7 Azo dye mineralization by UV/H<sub>2</sub>O<sub>2</sub> process, *Journal of Advanced Oxidation Technologies*, 11(3), 561-567.
- Onal E.S., Yatkin T., Aslanov T., Ergut E. &Ozer A., (2019), Biosynthesis & characterization of iron nanoparticles for effective adsorption of Cr(VI), *International Journal of chemical Engineering*.

- Orts F., Del Río A.I., Molina J., Bonastre J. & Cases F., (2018), Electrochemical treatment of real textile wastewater: TrichromyProcion HEXL®, *Journal of Electroanalytical Chemistry*, 808, 387-394.
- Ozakia H. & Lib H., (2002), Rejection of organic compounds by ultra-low pressure reverse osmosis membrane, *Water Research*, 36, 123-130.
- Ozkan Z.Y., Cakirgoz M., Kaymak E.S. & Erdim E., (2017), Rapid decolorization of textile wastewater by green synthesized nanoparticles, *Water science and technology*, 77, 511-517.
- Paździor K., Wrebiak J., Klepacz-Smółka A., Gmurek M., Bilinska L. & Kos L., (2017), Influence of ozonation and biodegradation on toxicity of industrial textile wastewater, *Journal of Environmental Management*, 195, 166-173.
- Palanivelan R., Rajkumar S., Jayanthi P. and Ayyasamy P.M., (2013), Potential process implicated in bioremediation of textile effluents: A review, *Advances in applied science research*, 1, 131-145.
- Papadopoulos A.E., Fatta D. & Loizidou M., (2007), Development and optimization of dark Fenton oxidation for the treatment of textile wastewaters with high organic load, *Water Resources*, 36, 558-563.
- Papavinasam S., (2014), *Corrosion control in the oil and gas industry*, Gulf Professional Publishing, 841-918.
- Park H., Sanghwa O., Bade R. and Won S., (2011), Application of Fungal Moving-Bed Biofilm Reactors (MBBRs) and Chemical Coagulation for Dyeing Wastewater Treatment, *KSCE Journal of Civil Engineering*, 15(3), 453-461.
- Patel H. & Vashi R.T., (2015), *Characterization and treatment of textile wastewater*, BH Publications, 111-125.
- Patel H. & Vashi R.T., (2010), Treatment of textile wastewater by adsorption and coagulation, *Journal of Chemistry*, 7(4), 1468-1476.
- Patil A.D. & Raut P.D., (2014), Treatment of textile wastewater by Fenton's process as an advanced oxidation process, *IOSR Journal of Environmental Science, Toxicology & Food Technology*, 8(10), ver.III, 29-32.
- Pattanayak M. & Nayak P.L., (2013), Green Synthesis and Characterization of Zero Valent Iron Nanoparticles from the leaf Extract of *Azadirachta indica* (Neem), *World Journal of Nano Science and Technology*, 2, 6-9.
- Paul S., Chavan S. & Khambe S., (2012), Studies on Characterization of Textile Industrial Waste Water in Solapur City, *International Journal of Chemical Science*, 10(2), 635-642.
- Pawar V. & Gawande S., (2015), An overview of the Fenton Process for Industrial Wastewater, *Journal of Mechanical and Civil Engineering*, 127-136.
- Peralta-Zamora P., Kunz A., Gomez de Morales S., Pelegrini R., Moleiro P.C., Reyes J. & Duran N., (1999), Degradation of reactive dyes I. A comparative study of ozonation, enzymatic and photochemical processes, *Chemosphere*, 38(4), 835-52.

- Pérez-Estrada L., Maldonado M.I., Gernjak W., Agüera A., Fernández-Alba A.R., Ballesteros M.M. & Malato S., (2005), Decomposition of diclofenac by solar driven photocatalysis at pilot-plant scale, *Catalysis Today*, 101, 219-226.
- Phenrat T., Saleh N., Sirk K., Tilton R.D. & Lowry G.V., (2007), Aggregation and Sedimentation of Aqueous Nanoscale Zerovalent Iron Dispersions, *Environmental Science Technology*, 41, 284–290.
- Philips J. & Sanny J., (2008), The Biot-Savart law: From infinitesimal to infinite, *The Physics Teacher*, 46(1), 44-47.
- Pignatello J.J., (1992), Dark and Photoassisted Fe<sup>3+</sup>Catalyzed Degradation of Chlorophenoxy Herbicides by Hydrogen Peroxide, *Environmental Science Technology*, 26, 944-951.
- Prashanth G.K. & Krishnaiah G.M., (2014), Chemical composition of the leaves of *Azadirachta Indica* Linn (Neem), *International journal of advancement in engineering technology, management and applied sciences*, 1(5), 21-31.
- Primo O., Rivero M.J. & Ortiz I., (2008), Photo-Fenton process as an efficient alternative to the treatment of landfill leachates, *Journal of Hazardous Materials*, 153, 834-842.
- Punzi M, Nilsson F. & Anbalagan A., (2015), Combined anaerobic-ozonation process for treatment of textile wastewater: removal of acute toxicity and mutagenicity, *Journal of Hazardous Materials*, 292, 52–60.
- Rahman F.B.A. & Akter M., (2016), Removal of dyes from textile wastewater by adsorption using shrimp shell, *International Journal of Waste Resources*, 6.3.
- Rahman M.A., Ahmed T., Salehin I.N. & Hossain M.D., (2017), Color removal from textile wastewater using date seed activated carbon, *Bangladesh Journal of Scientific & Industrial Research*, 52(1), 31-42.
- Rahman M.M., Bari Q.H. & Yousuf M.A., (2011), Treatment of textile wastewater with activated carbon produced from rice husk, *Journal of Engineering Science*, 2, 73-79.
- Rahmani A.R., Zarrabi M., Samarghandi M.R., Afkhami A. & Ghaffari H.R. (2010), Degradation of Azo Dye Reactive Black 5 and Acid Orange 7 by Fenton-Like Mechanism, *Iranian Journal of Chemical Engineering*, 7(1), 87-94.
- Rajeshwari S.C., Agnes Mariya D. & Venckatesh R., (2011), Isolation, characterization and growth kinetics of bacteria metabolizing textile effluent, *Journal of Bioscience & Technology*, 2(4), 324-330.
- Ramesh Babu R., Parande A.K. & Raghu S, (2007), Textile technology: Cotton Textile Processing: Waste Generation and Effluent Treatment, *Journal of Cotton Science*, 2, 141-153.
- Rao V.V.B. & Rao S.R.M., (2006), Adsorption studies on treatment of textile dyeing industrial effluent by flyash, *Chemical Engineering Journal*, 116(1), 77-84.
- Ravichandran V. & Amarnath D., (2012), Performance Evaluation of Moving Bed Bio-Film Reactor Technology for Treatment of Domestic Waste Water in Industrial Area at MEPZ

- (Madras Exports Processing Zone), Tambaram, Chennai, India, *Elixir International Journal*, 2, 11741-11744.
- Rikta S.Y, Alam M., Hossain K.F.B. &Tareq S.M., (2015), Photodegradation of textile effluent using solar radiation, *International Journal of Environmental Protection & Policy*, 3(2-1), 14-18.
- Robinson T., McMullan G. &Marchant M., (2001), Remediation of dyes in textile effluent: A critical review on current treatment technologies with a proposed alternative, *Bioresource Technology*, 77(3), 247-55.
- Rosli M.R., Zulhaimi H.I., Ibrahim S.K.M., Gopinath S.C.B., Kasim K.F., Akmal H.M., Nuradibah M.A. & Sam T.S., (2018), Photosynthesis of iron nanoparticle from *A.Bilimbi Linn*, *IOP Conf. series: Materials science &Engg*, 318.
- Ruppert G., Bauer R. &Heisler G., (1993), The Photo-Fenton Reaction - an Effective Photochemical Wastewater Treatment Process, *Journal of Photochemistry & Photobiology A: Chem.*, 73, 75-78.
- Sabur M.A., Khan A.A. &Safiullah S., (2012),Treatment of textile wastewater by coagulation precipitation Method, *Journal of Scientific Research*, 4(3), 623-633.
- Saif S., Tahir A. & Chen Y., (2016), Green synthesis of iron nanoparticles and their environmental applications and implications, *Nanomaterials*, 209, 1-26
- Sala M. & Gutierrez-Bouzan M., (2012), Electrochemical techniques in textile processes and wastewater treatment, *International Journal of Photoenergy*, 1-12.
- Sandhya S., (2010), Biodegradation of azo dyes under anaerobic condition: Role of azoreductase. In H. A. Erkurt (Ed.), *Biodegradation of azo dyes. The handbook of environmental chemistry*, 9, Berlin, Heidelberg: Springer, 39-57.
- Santos S.C.R. &Boaventura R.A.R., (2015), Treatment of a simulated textile wastewater in a sequencing batch reactor with addition of a low-cost adsorbent, *Journal of Hazardous Materials*, 291, 74-82.
- Sarabia L. A. & Ortiz M. C., (2009) Response surface methodology. In: *Comprehensive Chemometrics: Chemical and Biochemical Data Analysis*, 1, Elsevier, The Netherlands, 345–390.
- Saratale R.G., Saratale G.D., Chang J.S. &Govindwar S.P., (2011), Bacterial decolorization and degradation of azo dyes: A review, *Journal of Taiwan Inst Chemical Engineering*, 7, 138–57.
- Sarria V., Deront M., Péringer P. &Pulgarín C., (2003), Degradation of biorecalcitrant dye precursor present in industrial wastewater by a new integrated iron(III) photoassisted-biological treatment, *Applied Catalysis B: Environmental*, 40, 231-246.
- Sarria V., Parra S., Adler N., Péringer P., Benitez N. &Pulgarin C., (2002), Recent developments in the coupling of photoassisted and aerobic biological processes for the treatment of biorecalcitrant compounds, *Catalysis Today*, 76, 301-315.
- Schrack B, Hydutsky B.W., Blough J.L. &Mallouk T.E., (2004), Delivery vehicle for zero valent metal nanoparticles in soil and ground water, *Chemical Materials*,16, 2187-2193.

- Selcuk, (2005), Decolonization and detoxification of textile wastewater by ozonation and coagulation processes, *Dyes and Pigments*, 64, 217-222.
- Selvakumar S., Manivasagam R. & Chinnappan K., (2012), Biodegradation and decolourization of textile dye wastewater using *Ganoderma Lucidum*, *3Biotech*, 3(1), 71-79
- Senthilkumar K., Chitradevi V., Mothil S. & Naveenkumar M., (2018), Adsorption studies on treatment of textile wastewater using low-cost adsorbent, *Desalination & Water Treatment*, 123, 90-100.
- Sevcu A., El-Temsah S., Joner E.J. & Cerník M., (2011), "Oxidative Stress Induced in Microorganisms by Zero-valent Iron Nanoparticles", *Microbes Environ.*, 26, 271-281.
- Shahwan T., Abu Sirriah S., Nairat M., Boyaci E., Eroglu A.E., Scott T.B. & Hallam K.R., (2011), Green synthesis of iron nanoparticles and their application as a fenton-like catalyst for the degradation of cationic and anionic dyes, *Chemical Engineering Journal*, 172, 258-266.
- Shaikh M.A., (2009), Water conservation in textile industry, *PTJ*, 48-51.
- Sharma B., Dangi A. K. & Shukla P., (2018), Contemporary enzyme based technologies for bioremediation: A review, *Journal of Environmental Management*, 210, 10-22.
- Sharma K.P., Sharma S., Sharma S., Singh P.K., Kumar S., Grover R. & Sharma P.K., (2007), A comparative study on characterization of textile wastewaters (untreated and treated) toxicity by chemical and biological tests, *Chemosphere*, 69, 48-54.
- Shepard D.P., Edling B. & Reimers R., (1995), Magnetic water treatment, *Golf Course Management*, 63(3), 55-58.
- Shin D.H., Shin W.S., Kim Y.H., Myung H.H. & Choi S.J., (2006), Application of a combined process of MBBR and chemical coagulation for dyeing wastewater, *Water Science & Technology*, 54(9), 181-189.
- Shojaei S., Khammarnia S., Saeed S. & Sasani M., (2017), Removal of Reactive Red 198 by Nanoparticle Zero Valent Iron in the Presence of Hydrogen Peroxide, *Journal of Water & Environmental Nanotechnology*, 2(2), 129-135
- Siddique K., Rizwan M., Shahid M.J., Ali S., Ahmad R. & Rizwi H., (2017), Textile wastewater treatment options: A critical review, *Enhancing clean up of Environmental Pollutants*, Springer International Publishing AG, 183-207.
- Singh L. & Singh V.P., (2015), Textile Dyes Degradation: A Microbial Approach for Biodegradation of Pollutants. In *Microbial Degradation of Synthetic dyes in Waste waters*, Environmental Science and Engineering. Springer International Publishing; Switzerland; 2015.6
- Singh S., Singh C. & Mukherjee S., (2010), Impact of land-use and land-cover change on groundwater quality in the Lower Shiwalik hills: A remote sensing and GIS based approach, *Open Geosciences*, 2(2), 124-131.
- Sirianuntapiboon S. & Saengow W., (2004), Removal of vat dyes from textile wastewater using biosludge, *Water Quality Research Journal Canada*, 39(3), 276-284.

- Smelcerovic M., Dordevic D., Novakovic M. & Mizdrakovic M., (2010), Decolourization of a textile vat dye by adsorption on waste ash, *Journal of Serbian Chemical Society*, 75(6), 855-872.
- Sosamony K.J. & Soloman P.A., (2018), Treatment of pretreated textile wastewater using modified MBBR, *International Journal of Engineering and Technology*, 7(3.8), 106-110.
- Srinivasa Rao M. & Omprakash Sahu, (2013), Study of electromagnetic waves on industrial wastewater, *Physics and Materials Chemistry*, 1, 34-40.
- Stefaniuk M., Oleszczuk P. & Ok Y.S., (2015), Review on nanozerovalent iron (nZVI): From synthesis to environmental applications, *Chemical Engineering Journal*, 287, 618-632
- Sugasini A., Rajagopal K. & Banu N., (2014), A study on biosorption potential of *Aspergillus* sp. of tannery effluent, *Advances in Bioscience & Biotechnology*, 5(10), 1-9.
- Suhas K., Shivtej B., Muruganandham T., Sanjay P.G., Byong-Hun J., Senthil Kumar, (2019), Combined biological and advanced oxidation process for decolorization of textile dye, *SN Applied Sciences*, 1(97).
- Sun Y. & Pignatello J.J., (1993), Photochemical reactions involved in the total mineralization of 2,4-D by  $\text{Fe}^{3+}/\text{H}_2\text{O}_2/\text{UV}$ , *Environmental Science Technology*, 27, 304-310.
- Sun Y.P., Li X.Q., Zhang W.X. & Wang H.P., (2007), A method for the preparation of stable dispersion of zero-valent iron nanoparticles, *Colloids and Surfaces A: Physicochemical Engineering Aspects*, 308, 60-66.
- Sunardi, Ashadi, Rahardjo, S.B. and Inayati, (2017), Ecofriendly synthesis of nano zero valent iron from banana peel extract, *Journal of Physics*, 795, 1-5
- Sundararaman T.R., (2009), Decolorization and COD removal of reactive yellow 16 by Fenton oxidation and comparison of dye removal with photo Fenton and sono Fenton process, *Modern applied science*. 3(8), 15-22.
- Suresh S., (2014), Treatment of textile dye containing effluents, *Current Environmental Engineering*, 1(2), 1-24.
- Szczés A., Chibowski E., Holysz L. & Rafalski P., (2011), Effects of static magnetic field on water at kinetic condition, *Chemical Engineering Process*, 50(1), 124-127.
- Tetteh E.K. & Rathilal S., (2020), Application of magnetized nano-material for textile effluent remediation using response surface methodology, *Materials today: Proceedings*, 1-8.
- Thakur C, Srivastava V.C. & Mall I.D., (2009), Electrochemical treatment of a distillery wastewater: parametric and residue disposal study, *Chemical Engineering Journal*, 148(2-3), 496-505.
- Tigini V., Giansanti P., Mangiavillano A., Pannocchia A. & Varese G.C., (2011), Evaluation of toxicity, genotoxicity and environmental risk of simulated textile and tannery wastewaters with a battery of biotests, *Ecotoxicology & Environmental Safety*, 74, 866-873.
- Tomska A. & Wolny L., (2008), Enhancement of biological wastewater treatment by magnetic field exposure, *Desalination*, 222, 368-373.

- Torrades F., Saiz S. & García-Hortal J.A., (2011), Using central composite experimental design to optimize the degradation of black liquor by Fenton reagent, *Desalination*, 268(1–3), 97–102.
- Tratnyek P.G. & Johnson R.L., (2006), Nanotechnologies for environmental cleanup, *Nano Today*, 1, 44–48.
- Turakhia B., Turakhia P. & Shah P., (2018), Green synthesis of zero valent iron nanoparticles from spinaciaoleracea (spinach) and its application in waste water treatment, *Jaetsd Journal For Advanced Research In Applied Sciences*, 5, 46-50.
- Tusseau-Vuillemin M.H., Dispan J., Mouchel J.M. & Servais P., (2003), Biodegradable fraction of organic carbon estimated under oxic and anoxic conditions, *Water Research*, 37, 2242-2247.
- Uday U.S.P., Bandhyopadhyay T.K. & Bhunia B., (2016), Bioremediation and detoxification technology for treatment of dyes from textile effluent, *Textile wastewater treatment*, E. Perrin Akçakoca Kumbasar and Ayşegül Ekmekçi Körlü, IntechOpen, DOI: 10.5772/62309.
- Uzal N., Yilmaz L. & Yetis U., (2009), Nanofiltration and reverse osmosis for reuse of indigo dye rinsing waters, *Separation Science and Technology*, 45(3).
- Vemeiren T., (1958), Magnetic treatment of liquids for scale and corrosion prevention, *Corrosion Technology*, 5, 215–219.
- Verma A.K., Dash R.R. & Bhunia P., (2012), A review on chemical coagulation/flocculation technologies for removal of colour from textile wastewaters, *Journal of Environmental Management*, 93, 154–168
- Verma Y., (2008), Acute toxicity assessment of textile dyes and textile and dye industrial effluents using *Daphnia magna* bioassay, *Toxicology & Industrial Health*, 24, 491–500.
- Victoria M., Tuttolomondo G., Solange A. & Federico D., (2014), Removal of azo Dyes from water by Sol–Gel immobilized *Pseudomonas* Sp., *Journal of Environmental Chemical Engineering*, 2(11), 12-21.
- Vilaseca M., Gutierrez M.C., Grimau V.L. & Crespi M., (2010), Biological treatment of a textile effluent after electrochemical oxidation of reactive dyes, *Water Environment Research*, 82(2), 176-82.
- Vogelpohl A. & Kim S.M., (2004), Advanced oxidation processes (AOPs) in wastewater treatment, *Journal of Industrial & Engineering Chemistry*, 10(1), 33-40.
- Wang C. & Yin Y., (2012), Preparation, characterization and application of ultra-fine modified pigment in textile dyeing, *Eco-friendly Textile Dyeing and Finishing*. DOI:10.5772/53489.
- Wang X.H., Diao M.H., Yang Y., Shi Y.J., Gao M.M. & Wang S.G., (2012), Enhanced aerobic nitrifying granulation by static magnetic field, *Bioresource Technology*, 110, 105–110.
- Water & wastewater treatment opportunity in India: An overview, Avlon Global Research, Mumbai, India, 2011. <http://www.tamas.gov.il/NR/.....-160811.pdf> (DOA 10-10-2015)

- Willen B.M., (1995), Effect of different parameters on settling properties of activated sludge, Rapport.
- Wookeun B., Dukkyu H. &Fenghao C., (2014), Microbial Evaluation for biodegradability of recalcitrant organic in textile wastewater using an immobilized-cell activated sludge, *KSCE Journal of Civil Engineering*, 18(4), .964-970.
- Wuhrmann K., Mechsner K. &Kappeler T., (1980), Investigations on rate determining factors in the microbial reduction of azo dyes, *European Journal of Applied Microbiology & Biotechnology*, 9, 325–38.10
- Xiao-Bao, (2016), Advanced treatment of textile dyeing wastewater through the combination of moving bed bioreactors and ozonation, *Separation Science & Technology*, 51(9).
- Yadollahpour A., Rashid S., Ghotbeddin Z., Jalilifar M. &Rezaee Z., (2014), Electromagnetic fields for the treatments of wastewater: A review of applications and future opportunities, *Journal of Pure and Applied Microbiology*, 8(5), 3711-3719.
- Yang X., Lopez-Grimau V., Vilaseca M. &Crespi M., (2020), Treatment of textile wastewater by CAS, MBR and MBBR: A comparative study from technical, economical and environmental perspectives, *Water*, 12,1306, 1-17.
- Yavuz H. &Celebi S.S., (2004), Influence of magnetic field on the kinetics of activated sludge, *Environmental Technology*, 25(1), 7-13.
- Zaharia C. &Suteu D., (2013), Coal fly ash as adsorptive material for treatment of a real textile effluent: operating parameters and treatment efficiency, *Environmental Science and Pollution Research* **20**, 2226–2235.
- Zaidi N.S., Johan S. , Khalida M. & Mika S., (2014), Magnetic field application and its potential in water and wastewater treatment systems, *Separation & Purification Reviews*,43, 206–240.
- Zarghi M.H., Jaafazadeh N., Roudbari A. &Zahedi A., (2020), Application of surface response method (RSM) to optimize ammonia-nitrogen removal from fresh leachate using combination of ultra-sound and ultra-violet, *Water Science Technology*, 81(2), 358-366.
- Zepp R.G., Faust B.C. &Hoigné J. (1992), Hydroxyl radical formation in aqueous reactions (pH 3-8) of iron(II) with hydrogen peroxide: The photo-Fenton reaction, *Environmental Science & Technology*, 26, 313-319.
- Zhao Y., Xi B. , Li Y. , Wang M., Zhu Z., Xia X., Lie-yu Z., Lijun W.&Zhaokun L., (2012), Removal of phosphate from wastewater by using open gradient superconducting magnetic separation as pretreatment for high gradient superconducting magnetic separation, *Separation and Purification Technology* 86, 255-261.
- <https://www.ibef.org/industry/textiles.aspx>
- <https://www.mordointelligence.com/industry-reports-global-textile-industry>
- [https://en.wikipedia.org/wiki/Sludge\\_volume\\_index](https://en.wikipedia.org/wiki/Sludge_volume_index)

# PUBLICATIONS

- K.J.Sosamony & P.A.Soloman, (2020) “Comparison in performance of magnetic field induced MBBR coupled with AOPs for textile effluent treatment with cost estimation” *Environmental Quality Management*,(SCI), 30:145-157. <https://doi.org/10.1002/tqem.21722>.
- K.J.Sosamony, P.A.Solomon, (2018), “Treatment of Pretreated textile wastewater using modified MBBR” *International Journal of Engineering & Technology*, (Scopus), 7(3.8), 106-110. DOI: [10.14419/ijet.v7i3.8.16843](https://doi.org/10.14419/ijet.v7i3.8.16843).
- K.J.Sosamony & P.A Soloman, (2021), “Treatment of Textile Effluent using Solar Photo Fenton Process with Biosynthesized nZVI” *International Journal of Environmental Engineering*, 1(1):1. DOI: 10.1504/IJEE.2021.10035539. (Scopus)
- K.J.Sosamony & P.A.Soloman, (2020), “Treatment of ASPF pretreated Textile Effluent using MBBR induced with magnetic field” Proceedings of the 10<sup>th</sup> International Conference on Science & Innovative Engineering, Chennai, India

## APPENDIX 1

### Characteristics of wastewater samples collected at various days

	Unit	04.11.2016	11.11.2016	18.11.2016	28.11.2016	02.12.2016	08.12.2016	15.12.2016
BOD	mg/l	215	205	226	194	227	193	228
COD	mg/l	905	1055	904	1056	903	1057	902
pH	-	11.1	12.9	11	13	10.9	13.1	10.8
Turbidity	NTU	58	70	57	71	56	72	55
Sulphide	mg/l	39	49	38	50	37	51	36
Chloride	mg/l	165	195	164	196	163	197	162
Conductivity	mS/cm	0.8	0.9	0.89	0.81	0.88	0.82	0.87
Hardness	mg/l	131	149	130	150	129	151	128
Alkalinity	mg/l	1090	1310	1089	1311	1088	1312	1087

## APPENDIX 1 -----Contd.

### Characteristics of wastewater samples collected at various days

	Unit	22.12.2016	30.12.2016	05.01.2017	11.01.2017	17.01.2017	23.01.2017	28.01.2017
BOD	mg/l	192	229	191	230	190	231	189
COD	mg/l	1058	901	1059	900	1060	919	1041
pH	-	13.2	10.7	13.3	11.6	12.4	11.5	12.5
Turbidity	NTU	73	54	74	53	75	52	76
Sulphide	mg/l	52	35	53	42	46	33	55
Chloride	mg/l	198	161	199	160	200	159	201
Conductivity	mS/cm	0.83	0.88	0.82	0.85	0.85	0.84	0.86
Hardness	mg/l	152	127	153	126	154	125	155
Alkalinity	mg/l	1313	1086	1314	1085	1315	1084	1315

**APPENDIX 1 -----Contd.**

**Characteristics of wastewater samples collected at various days**

	Unit	04.02.2017	11.02.2017	18.02.2017	26.02.2017	03.03.2017	10.03.2017	18.03.2017
BOD	mg/l	222	198	223	197	234	186	235
COD	mg/l	918	1042	917	1043	896	1064	920
pH	-	11.4	12.6	11.3	12.7	11.4	12.6	11.1
Turbidity	NTU	63	65	62	66	68	60	63
Sulphide	mg/l	44	44	43	45	40	48	39
Chloride	mg/l	158	202	157	203	170	190	170
Conductivity	mS/cm	0.83	0.87	0.82	0.88	0.81	0.89	0.70
Hardness	mg/l	124	156	138	142	142	138	136
Alkalinity	mg/l	1083	1317	1082	1318	1082	1319	1080

**APPENDIX 1 -----Contd.**

**Characteristics of wastewater samples collected at various days**

	Unit	25.03.2017	02.04.2017	10.04.2017	17.04.2017	24.04.2017	01-05-2017	08.05.2017
BOD	mg/l	185	226	194	227	193	228	192
COD	mg/l	1040	914	1046	893	1067	892	1068
pH	-	12.9	11	13	11.9	12.1	11.8	12.2
Turbidity	NTU	65	67	61	66	62	65	63
Sulphide	mg/l	49	38	50	37	51	46	42
Chloride	mg/l	190	176	184	173	187	177	183
Conductivity	mS/cm	1	0.79	0.91	0.78	0.92	0.87	0.82
Hardness	mg/l	144	135	145	129	151	138	142
Alkalinity	mg/l	1320	1079	1321	1078	1322	1087	1313

**APPENDIX 1 -----Contd.**

**Characteristics of wastewater samples collected at various days**

	Unit	15.05.2017	22.05.2017	30.05.2017	18.06.2017	Mean	SD
BOD	mg/l	229	191	230	190	210	18.38653
COD	mg/l	916	1054	905	1045	980	75.18794
pH	-	10.7	13.3	10.6	13.4	12	0.925621
Turbidity	NTU	59	69	58	70	64	6.681703
Sulphide	mg/l	45	43	39	49	44	5.886014
Chloride	mg/l	171	189	170	190	180	15.58328
Conductivity	mS/cm	0.86	0.83	0.75	0.94	0.85	0.05693
Hardness	mg/l	137	143	136	144	140	9.807831
Alkalinity	mg/l	1176	1224	1175	1225	1200	110.4478